

SYNTHESIS AND CHARACTERIZATION OF TRANSITION METAL COMPLEXES FOR NONLINEAR OPTICAL ACTIVITY

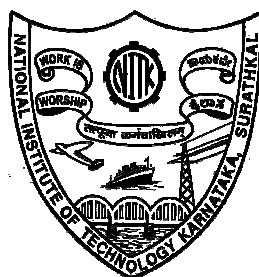
Thesis

**Submitted in partial fulfilment of the requirements for the degree of
DOCTOR OF PHILOSOPHY**

by

SAMPATH KUMAR H. C.

(Registration No: 081010CY08P04)



**DEPARTMENT OF CHEMISTRY
NATIONAL INSTITUTE OF TECHNOLOGY KARNATAKA,
SURATHKAL, MANGALORE-575025**

November, 2013

DECLARATION

by the Ph.D. Research Scholar

I hereby *declare* that the Research Thesis entitled “**Synthesis and characterization of transition metal complexes for nonlinear optical activity**” which is being submitted to the *National Institute of Technology Karnataka, Surathkal* in partial fulfilment of the requirements for the award of the Degree of *Doctor of Philosophy in Chemistry* is a *bonafide report of the research work carried out by me*. The material contained in this Research Thesis has not been submitted to any University or Institution for the award of any degree.

Sampath Kumar H. C.

(Reg. No: 081010CY08P04)

Department of Chemistry

Place: NITK, Surathkal

Date:28/11/2013

CERTIFICATE

This is to *certify* that the Research Thesis entitled “**Synthesis and characterization of transition metal complexes for nonlinear optical activity**” submitted by **Sampath Kumar H. C.** (Register Number: **081010CY08P04**) as the record of the research work carried out by him, is *accepted as the Research Thesis submission* in partial fulfilment of the requirements for the award of degree of **Doctor of Philosophy**.

Dr. B. Ramachandra Bhat

Research Guide

Date:

Chariman-DRPC

Date:

Dedicated to

My Parents

ACKNOWLEDGEMENTS

It gives me immense pleasure to express my heartfelt gratitude to my research guide Prof. B. Ramachandra Bhat. I am very much grateful for his invaluable suggestions, generous advice, criticism and trust throughout the present investigation. It was refreshing to work for and with a professional of such a high calibre. Without his guidance and extreme patience, I never would have been able to complete such a demanding task.

Besides my mentor, I would like to thank the rest of my RPAC committee members: Prof. S. M. Kulkarni, Department of Mechanical Engineering and Dr. H. S. Nagaraja, Department of Physics, for spending their valuable time in evaluating my progress and providing thoughtful suggestions.

I sincerely thank the former Heads of the Department, Prof. A. Nithyanand Shetty and Prof. A. Vasudeva Adhikari as well as the present Head of the Department, Dr. A. Chitharanjan Hegde for providing me with the laboratory facilities. I sincerely acknowledge Dr. D. Krishna Bhat, Dr. Arun M. Isloor, Dr. D. Uday Kumar and Dr. Darshak R. Trivedi for their continuous encouragement and co-operation.

I will not be doing justice without mentioning my gratitude to Dr. Reji Philip, Dr. Suchand Sandeep, Smijesh, Muhamed Shafi and Kishore of Raman Research Institute Bangalore for helping me with nonlinear optical studies. The enthusiasm and energy of this group has greatly influenced me. Their assistance and intellectual suggestions, has played a major role in completion of this research. A special thanks to Dr. John Kiran, and Mr. Manjunath K.B., for helping me to understand the subject better.

I would like to mention a word of gratitude to my friends Dr. Nonappa, Dr. Ganesh Rai, Dr. Ramesh G.K. Dr. Chaithanya Jain, Dr. Venkatesh Hatwar, Dr. Vinyaka Sankolli, Dr. Anusha, Dr. Ravi, Gayathri and Rachitha for their help through out my research work.

My special thanks to my teachers Mr. Madhusudan, PGT Biology, JNV Balehonnure and Mr. Keshav Hegde, Lecturer, S.D.M. College and my friends Dr. Pramod Hegde and Dr. Manjunath for motivating me to take up the research work.

I am very thankful to my fellow researchers for helping me in various stages of this research work. A special thanks to Dr. Dileep, Dr. Ravindra, Dr. Ramasubramanian, Dr. Rudresh, Mrs. Sandya Rani, Mr. Aravinda, Mrs. Aparna, Ms. Pooja and Mr. Raghavendra Prasad for their good support and cooperation.

I am grateful to the non-teaching staff, Mr. Ashok, Mrs. Kasthuri, Mr. Prashanth, Mr. Pradeep, Mr. Harish, Ms. Shilpa Kunder, Ms. Swarna, Mrs. Sharmila, Mrs. Deepa and Mrs. Usha who were prompt enough to lend me a helping hand at times of need.

I would like to thank my friends from JNVCKM Alumni association, Votrasi Imaging and JCI Surathkal for all their support and co-operation.

The time spent at NITK was dominated by happy moments. Thanks to all the scholar friends for making my research days at NITK a fun-filled and memorable one. Whether it was for long discussions, for clearing of my doubts, for exchanging knowledge, for lending glasswares/chemicals or even for sharing of joy and sorrow, they were always there for me. I whole heartedly thank each one of them and wish them success in their research work and all future endeavours.

My thanks are due to all the authorities of Mangalore Refinery and Petrochemical Ltd. for permitting me to carry out the research activities and also to all my MRPL Laboratory colleagues for their encouragement and support.

I would like to thank my wife Dr. Aarti for standing beside me throughout my research work. She has been my inspiration and motivation to improve my knowledge. I also thank my little kid Aastha, for making me smile always. Hope that one day she can read my thesis and understand how she was the reason of my happiness in this difficult situation

Nothing can be achieved without the blessings of elders. I like to thank each and every member of my family whose good wishes worked like a guiding lamp on the road leading to my goal.

Finally, I would like to thank all those who, either by their thoughts or deeds, have directly or indirectly contributed for the completion of this research work.

Thank you.

Sampath Kumar H. C.

ABSTRACT

Transition metal complexes have become an integral part of nonlinear optics. The design of technologically useful metal complexes poses a continuous challenge for inorganic chemists. Keeping this in view, the present thesis addresses three major areas. First, to design and develop transition metal complexes using ligands with extensive π -conjugation. Second, to synthesize and characterize all the complexes by established techniques like Elemental analysis, FT-IR spectroscopy, UV-Vis spectroscopy, Single crystal XRD and NMR spectroscopy. Lastly, to evaluate the nonlinear optical activity of the complexes using techniques like Z-scan technique and Optical Kerr Gate method and thereby establishing a relationship between the complex structure and optical nonlinearity. All the complexes exhibited third-order optical nonlinearity. The Fe(II), Ni(II) and Zn(II) complexes of 1,2-diaminobenzene and 2-hydroxynaphthaldehyde and Co(II), Ni(II) and Zn(II) complexes of 3,4-diaminobenzophenone and 2-hydroxynaphthaldehyde displayed a two-photon absorption. On the other hand, Ni(II), Cu(II) and Zn(II) complexes of Schiff base ligands of dimethylamino benzaldehyde and thiosemicarbazide and Cu(I) complex with 1,10-phenanthroline and triphenylphosphine exhibited three-photon absorption mechanism. The ionic liquid tagged Schiff base metal complex also revealed effective two photon absorption with good third-order optical response. The nonlinear optical study on the complexes revealed encouraging results which can act as a base for any further improvement and their usage as optical limiters.

Keywords: Coordination complexes, Schiff base complexes, nonlinear optics, third-order nonlinearity, Z-scan technique.

CONTENTS

CHAPTER 1

INTRODUCTION

1.1. INTRODUCTION TO COORDINATION COMPLEXES.....	1
1.2. NONLINEAR OPTICS.....	2
1.2.1. Theory of nonlinear optics.....	3
1.2.2. Nonlinear optical materials.....	4
1.2.3. Requirements for materials to exhibit NLO response.....	5
1.3. NONLINEAR OPTICAL PROCESSES.....	6
1.3.1. Second Harmonic Generation (SHG).....	7
1.3.2. Sum and Difference Frequency Generation.....	7
1.3.3. Two photon absorption (2PA) process.....	8
1.3.4. Three photon absorption (3PA) process.....	9
1.3.5. Excited State Absorption (ESA).....	9
1.3.6. Saturable Absorption.....	11
1.4. THIRD ORDER OPTICAL NONLINEARITY.....	12
1.5. CO-ORDINATION COMPLEXES AS NLO MATERIALS.....	12
1.6. EXPERIMENTAL TECHNIQUES.....	14
1.6.1. Kurtz powder test.....	15
1.6.2. Z-scan method.....	16
1.6.3. Degenerate Four-Wave Mixing (DFWM).....	19
1.6.4. Hyper-Rayleigh Scattering (HRS).....	21
1.6.5. Optical Kerr Gate.....	22

CHAPTER 2

LITERATURE SURVEY AND OBJECTIVES OF THE WORK

2.1. A BRIEF REVIEW ON THE LITERATURE.....	25
2.2. SCOPE AND OBJECTIVES OF THE WORK.....	35

CHAPTER 3

SYNTHESIS, CHARACTERIZATION AND NONLINEAR OPTICAL STUDIES OF Fe(II), Ni(II) AND Zn(II) SCHIFF-BASE COMPLEXES

3.1. INTRODUCTION.....	39
3.2. EXPERIMENTAL.....	41
3.2.1. Materials.....	41
3.2.2. Physical measurements.....	41
3.2.3. Z-scan measurement	42
3.3. SYNTHESIS OF METAL COMPLEXES.....	43
3.3.1. Synthesis of ligand (L1).....	43
3.3.2. Synthesis of iron complex (C1).....	43
3.3.3. Synthesis of nickel complex (C2).....	44
3.3.4. Synthesis of zinc complex (C3).....	45
3.4. RESULTS AND DISCUSSION.....	46
3.4.1. FT-IR spectra.....	47
3.4.2. ¹ H-NMR spectra.....	50
3.4.3. Thermogravimetric analysis.....	52
3.4.4. UV-Visible spectra.....	53
3.5. NONLINEAR OPTICAL MEASUREMENTS.....	54

CHAPTER 4

SYNTHESIS, CHARACTERIZATION AND THIRD-ORDER NONLINEAR OPTICAL STUDIES OF Co(II), Ni(II) AND Zn(II) – 3,4-DIAMINOBENZOPHENONE SCHIFF BASE COMPLEXES

4.1. INTRODUCTION.....	59
4.2. EXPERIMENTAL.....	60
4.2.1. Materials.....	60
4.2.2. Physical measurements.....	60

4.3. SYNTHESIS OF METAL COMPLEXES.....	61
4.3.1. Synthesis of ligand (L2).....	60
4.3.2. Synthesis of cobalt complex (C4).....	62
4.3.3. Synthesis of nickel complex (C5).....	63
4.3.4. Synthesis of zinc complex (C6).....	64
4.4. RESULTS AND DISCUSSION.....	65
4.4.1. FT-IR spectra.....	66
4.4.2. ¹ H-NMR spectra.....	68
4.4.3. UV-Visible spectra.....	71
4.5. NONLINEAR OPTICAL MEASUREMENTS.....	72
CHAPTER 5	
SYNTHESIS, CHARACTERIZATION AND NONLINEAR OPTICAL STUDIES	
OF THIOSEMICARBAZIDE COMPLEXES OF Ni(II), Cu(II) AND Zn(II)	
5.1. INTRODUCTION.....	79
5.2. EXPERIMENTAL.....	80
5.2.1. Materials.....	80
5.2.2. Physical measurements.....	80
5.3. SYNTHESIS OF METAL COMPLEXES.....	81
5.3.1. Synthesis of ligand (L3).....	81
5.3.2. Synthesis of nickel complex (C7).....	82
5.3.3. Synthesis of copper complex (C8).....	83
5.3.4. Synthesis of zinc complex (C9).....	84
5.4. RESULTS AND DISCUSSION	85
5.4.1. FT-IR spectra.....	86
5.4.2. ¹ H-NMR spectra.....	88
5.4.3. UV-Visible spectra.....	91
5.5. NONLINEAR OPTICAL MEASUREMENTS.....	91

CHAPTER 6

THIRD-ORDER NONLINEAR OPTICAL STUDY OF COPPER COMPLEXES USING Z-SCAN TECHNIQUE

6.1. INTRODUCTION.....	97
6.2. EXPERIMENTAL.....	99
6.2.1. Materials.....	99
6.2.2. Physical measurements.....	99
6.3. SYNTHESIS OF METAL COMPLEXES.....	101
6.3.1. Synthesis of CuCl(Phen)PPh ₃ (C10).....	101
6.3.2. Synthesis of CuBr(Phen)PPh ₃ (C11).....	102
6.3.3. Synthesis of CuI(Phen)PPh ₃ (C12).....	102
6.4. RESULTS AND DISCUSSION.....	103
6.4.1. FT-IR spectra.....	104
6.4.2. NMR spectra.....	105
6.4.3. Single crystal XRD.....	107
6.4.4. UV-Visible spectra.....	112
6.5. NONLINEAR OPTICAL MEASUREMENTS.....	112
6.5.1. NLO measurement in solution state.....	112
6.5.1.1. Sample preparation.....	112
6.5.1.2. Z-scan measurement.....	113
6.5.2. NLO measurement using composite film.....	115
6.5.2.1. Composite film preparation.....	115
6.5.2.2. NLO measurement.....	116
6.5.2.3. Optical Kerr Gate measurement	119

CHAPTER 7

NONLINEAR OPTICAL STUDIES OF IONIC LIQUID TAGGED Ni(II) SCHIFF BASE COMPLEXES

7.1. INTRODUCTION.....	123
------------------------	-----

7.2. EXPERIMENTAL.....	124
7.2.1. Materials.....	124
7.2.2. Physical measurements.....	124
7.3. SYNTHESIS OF METAL COMPLEXES.....	125
7.3.1. Synthesis of ligand (L4).....	125
7.3.2. Synthesis of ligand (L5).....	126
7.3.3. Synthesis of complex (C13).....	127
7.3.4. Synthesis of complex (C14).....	128
7.4. RESULTS AND DISCUSSION	129
7.4.1. FT-IR spectra.....	130
7.4.2. ¹ H-NMR spectra.....	133
7.4.3. UV-Visible spectra.....	136
7.5. NONLINEAR OPTICAL MEASUREMENT.....	136
CHAPTER 8	
SUMMARY AND CONCLUSIONS	
8.1. SUMMARY AND CONCLUSIONS.....	141
8.2. SCOPE FOR FUTURE WORK.....	144
REFERENCES.....	147
LIST OF PUBLICATIONS	173
CURRICULUM VITAE.....	175

LIST OF ABBREVIATIONS AND SYMBOLS

NLO	Nonlinear optics
α	Linear polarizability
$\chi^{(1)}$	First order susceptibility
$\chi^{(2)}$	Second order susceptibility
$\chi^{(3)}$	Third order susceptibility
β	First hyperpolarizability
γ	Second hyperpolarizability
SHG	Second Harmonic Generation
2PA	Two photon absorption
3PA	Three photon absorption
ESA	Excited State Absorption
RSA	Reverse Saturable Absorption
MLCT	Metal to ligand charge transitions
LMCT	Ligand to metal charge transitions
DFWM	Degenerate four-wave mixing
HRS	Hyper-Rayleigh scattering
FT-IR	Fourier Transform Infra red Spectroscopy
NMR	Nuclear Magnetic Resonance
DMF	Dimethyl formamide
DMSO	Dimethyl sulfoxide

LIST OF FIGURES

Fig. no.	Caption	Page no.
Fig. 1.1	Schematic representation of “push-pull” chromophores	6
Fig. 1.2	Geometry of second harmonic generation	7
Fig. 1.3	Geometry of sum frequency generation	8
Fig. 1.4	Geometry of difference frequency generation	8
Fig. 1.5	(a) Two photon Absorption (2PA) and (b) Three photon Absorption (3PA) processes	9
Fig. 1.6	Energy level diagram showing 2PA, 3PA, ESA and ISC	10
Fig. 1.7	Experimental arrangement of Kurtz powder technique	16
Fig. 1.8	Schematic representation of Z-scan	17
Fig. 1.9	Typical open aperture Z-scan transmittance curves for a cubic nonlinearity	18
Fig. 1.10	Typical closed Z-scan transmittance curves for a cubic nonlinearity	19
Fig. 1.11	DFWM set-up in BOXCAR configuration, $4(k_4)$ is the signal	20
Fig. 1.12	DFWM signal versus Probe	20
Fig. 1.13	Schematic experimental set up for SHG efficiency measurements	22
Fig. 1.14	Schematic diagram of optical Kerr gate experiment	23
Fig. 2.1	Chemical structure of [Fe(salen)(pyridyl)X]	25

Fig. 2.2	Chemical structure of $[\text{Fe}(\text{PM-L})_2(\text{NCS})_2]$	27
Fig. 2.3	Chemical structure of Ni(II) complexes of pyrrole 2-aldehyde and substituted diamine	28
Fig. 2.4	Chemical structure of boronates (R = p-tolylsulfonyl, SC_8H_{17} , $\text{SO}_2\text{C}_8\text{H}_{17}$)	29
Fig. 2.5	Chemical structure of boron complexes	30
Fig. 2.6	Chemical structure of coumarin derived Zn(II) complexes	31
Fig. 2.7	Schematic illustration of $[\text{BMI}]\text{BF}_4$ and $[\text{BMI}]\text{PF}_6$ ionic liquid structures (X = BF_4 , PF_6)	31
Fig. 2.8	Chemical structure of 2-aminothiazole and 3-formylchromone metal complexes	32
Fig. 2.9	Chemical structure of 4-((E)-(4-chlorophenyl)diazenyl)-2-hydroxybenzylideneamino)-1,5-dimethyl-2-phenyl-1H-pyrazol-3(2H)-one	33
Fig. 2.10	Chemical structure of mixed ligand Ni(II) complexes	34
Fig. 2.11	Chemical structure of $[\text{PdLPPH}_3]$ (L=N-(2-pyridyl)-N-(salicylidene)hydrazine)	34
Fig. 3.1	IR spectrum of L1	48
Fig. 3.2	IR spectrum of C1	48
Fig. 3.3	IR spectrum of C2	49
Fig. 3.4	IR spectrum of C3	49
Fig. 3.5	$^1\text{H-NMR}$ spectrum of L1	51
Fig. 3.6	$^1\text{H-NMR}$ spectrum of C2	51

Fig. 3.7	Thermal analysis of C1	52
Fig. 3.8	Linear absorption spectra of ligand L1 and complexes C1-C3	53
Fig. 3.9	Spatial profile of the Nd:YAG laser beam used for the Z-scan experiment, measured using the knife-edge technique. The solid line is a Gaussian fit to the measured data	54
Fig. 3.10	Nonlinear transmission curve of C1 . Inset shows the open aperture Z-scan curve. Linear transmission of the sample (corresponding to $T(\text{norm.}) = 1$) is 75%. Circles are data points while solid curves are numerical fits using equation 3.1	55
Fig. 3.11	Nonlinear transmission curve of C2 . Inset shows the open aperture Z-scan curve. Linear transmission of the sample (corresponding to $T(\text{norm.}) = 1$) is 60%. Circles are data points while solid curves are numerical fits using equation 3.1	55
Fig. 3.12	Nonlinear transmission curve of C3 . Inset shows the open aperture Z-scan curve. Linear transmission of the sample (corresponding to $T(\text{norm.}) = 1$) is 70%. Circles are data points while solid curves are numerical fits using equation 3.1	56
Fig. 4.1	IR spectrum of L2	67
Fig. 4.2	IR spectrum of C4	67
Fig. 4.3	IR spectrum of C5	68
Fig. 4.4	IR spectrum of C6	68
Fig. 4.5	$^1\text{H-NMR}$ spectrum of L2	69
Fig. 4.6	$^1\text{H-NMR}$ spectrum of C4	70
Fig. 4.7	$^1\text{H-NMR}$ spectrum of C5	70

Fig. 4.8	¹ H-NMR spectrum of C6	71
Fig. 4.9	Linear absorption spectra of ligand L2 and complexes C4-C6	72
Fig. 4.10	(a) Open aperture Z-scan curve. Linear transmission of the sample (corresponding to T (norm.) = 1) is 60%. Circles are data points while solid curves are numerical fits using equation 4.1. (b) Nonlinear transmission curve of C4	74
Fig. 4.11	(a) Open aperture Z-scan curve. Linear transmission of the sample (corresponding to T (norm.) = 1) is 64%. Circles are data points while solid curves are numerical fits using equation 4.1. (b) Nonlinear transmission curve of C5	74
Fig. 4.12	(a) Open aperture Z-scan curve. Linear transmission of the sample (corresponding to T (norm.) = 1) is 68%. Circles are data points while solid curves are numerical fits using equation 4.1. (b) Nonlinear transmission curve of C6	75
Fig. 4.13	Five level energy diagram showing nonlinear absorption mechanisms	77
Fig. 5.1	IR spectrum of L3	86
Fig. 5.2	IR spectrum of C7	87
Fig. 5.3	IR spectrum of C8	87
Fig. 5.4	IR spectrum of C9	88
Fig. 5.5	¹ H-NMR spectrum of L3	89
Fig. 5.6	¹ H-NMR spectrum of C7	89
Fig. 5.7	¹ H-NMR spectrum of C8	90
Fig. 5.8	¹ H-NMR spectrum of C9	90

Fig. 5.9	Linear absorption spectra of ligand L3 and complexes C7-C9	91
Fig. 5.10	(a) Open aperture Z-scan curve. Circles are data points while solid curve is a numerical fit for three-photon absorption. (b) Nonlinear transmission in C7	92
Fig. 5.11	(a) Open aperture Z-scan curve. Circles are data points while solid curve is a numerical fit for three-photon absorption. (b) Nonlinear transmission in C8	93
Fig. 5.12	(a) Open aperture Z-scan curve. Circles are data points while solid curve is a numerical fit for three-photon absorption. (b) Nonlinear transmission in C9	93
Fig. 5.13	Energy level diagram showing three photon absorption	94
Fig. 6.1	IR spectrum of C10	104
Fig. 6.2	IR spectrum of C11	105
Fig. 6.3	IR spectrum of C12	105
Fig. 6.4	¹ H-NMR spectrum of C10	106
Fig. 6.5	¹ H-NMR spectrum of C11	106
Fig. 6.6	¹ H-NMR spectrum of C12	107
Fig. 6.7a	Single crystal XRD structure of C10 with solvent (CH ₂ Cl ₂) of crystallization	108
Fig. 6.7b	View of complex C10 . Displacement ellipsoids are shown at the 50% probability level. Hydrogen atoms are of arbitrary size	109
Fig. 6.8a	Powder XRD of C10 in powder form	111
Fig. 6.8b	Powder XRD of single crystal of C10	111

Fig. 6.9	Linear absorption spectra of complexes C10-C12	112
Fig. 6.10	Nonlinear transmission curve of C10 . Inset shows the open aperture Z-scan curve. Linear transmission of the sample (corresponding to $T(\text{norm.}) = 1$) is 65%. Circles are data points while solid curves are numerical fits using equation 6.1.	114
Fig. 6.11	Nonlinear transmission curve of C11 . Inset shows the open aperture Z-scan curve. Linear transmission of the sample (corresponding to $T(\text{norm.}) = 1$) is 62%. Circles are data points while solid curves are numerical fits using equation 6.1.	114
Fig. 6.12	Nonlinear transmission curve of C12 . Inset shows the open aperture Z-scan curve. Linear transmission of the sample (corresponding to $T(\text{norm.}) = 1$) is 65%. Circles are data points while solid curves are numerical fits using equation 6.1.	115
Fig. 6.13	Open aperture Z-scan results at 800 nm. The data corresponding to the input intensity 8.7 GWcm^{-2} are fitted with equation (6.2), assuming 3PA	117
Fig. 6.14	3PA result for the compound in PMMA film at 1250 nm. The solid line is a theoretical data fit of the experimental	119
Fig. 6.15	Optical Kerr effect (OKE) signal from the coordination compound/PMMA film at 800nm. The nonlinear response is faster than or comparable to the laser pulse width (90 fs). The reference OKE signal of CS_2 is shown as an inset	120
Fig. 7.1	IR spectrum of L4	131
Fig. 7.2	IR spectrum of L5	132
Fig. 7.3	IR spectrum of C13	132

Fig. 7.4	IR spectrum of C14	133
Fig. 7.5	¹ H-NMR spectrum of L4	134
Fig. 7.6	¹ H-NMR spectrum of L5	134
Fig. 7.7	¹ H-NMR spectrum of C13	135
Fig. 7.8	¹ H-NMR spectrum of C14	135
Fig. 7.9	Linear absorption spectra of ligands (L4- L5) and complexes (C13-C14)	136
Fig. 7.10	Fig. 7.10(a) Open aperture Z-scan curve for complex Linear transmission of the sample (corresponding to T (norm.) = 1) is 66%. Circles are data points while solid curves are numerical fits using equation 7.1. . (b) Nonlinear transmission curve of C13	138
Fig. 7.11	Fig. 7.11 (a) Open aperture z-scan curve for complex. Linear transmission of the sample (corresponding to T (norm.) = 1) is 66%. Circles are data points while solid curves are numerical fits using equation 7.1. (b) Nonlinear transmission curve of C14	138

LIST OF SCHEMES

Scheme no.	Caption	Page no.
Scheme 1.1	General procedure for the synthesis of Schiff base	13
Scheme 3.1	Synthetic scheme for L1	43
Scheme 3.2	Synthetic scheme for C1	44
Scheme 3.3	Synthetic scheme for C2	45
Scheme 3.4	Synthetic scheme for C3	46
Scheme 4.1	Synthetic scheme for L2	62
Scheme 4.2	Synthetic scheme for C4	63
Scheme 4.3	Synthetic scheme for C5	64
Scheme 4.4	Synthetic scheme for C6	65
Scheme 5.1	Synthetic scheme for L3	82
Scheme 5.2	Synthetic scheme for C7	83
Scheme 5.3	Synthetic scheme for C8	84
Scheme 5.4	Synthetic scheme for C9	85
Scheme 6.1	Synthetic scheme for C10	101
Scheme 6.2	Synthetic scheme for C11	102
Scheme 6.3	Synthetic scheme for C12	103
Scheme 7.1	Synthetic scheme for L4	126
Scheme 7.2	Synthetic scheme for L5	127

Scheme 7.3	Synthetic scheme for C13	128
Scheme 7.4	Synthetic scheme for C14	129

LIST OF TABLES

Table no.	Caption	Page no.
Table 3.1	Analytical data of Schiff base complexes	46
Table 3.2	Infrared spectral data (cm^{-1}) for ligand and its Schiff base complexes	47
Table 3.3	^1H -NMR spectral details of ligands and complexes	50
Table 3.4	2PA coefficient β of Schiff base complexes	58
Table 4.1	Analytical data of Schiff base complexes	65
Table 4.2	Infrared spectral data (cm^{-1}) for ligand and its Schiff base complexes	66
Table 4.3	2PA coefficient β of Schiff base complexes	78
Table 5.1	Analytical data of Schiff base complexes	85
Table 5.2	Infrared spectral data (cm^{-1}) for ligand and its complexes (C7-C9)	88
Table 5.3	Three photon coefficient γ of thiosemicarbazide complexes	96
Table 6.1	Analytical and electronic spectral data of complexes C10-C12	103
Table 6.2	Infrared spectral data (cm^{-1}) for complexes C10-C12	104
Table 6.3	^1H -NMR and ^{31}P -NMR spectral details of complexes	107
Table 6.4	Selected geometric parameters (\AA , $^\circ$)	109
Table 6.5	Crystallographic data and structure refinement summary for C10	110

Table 6.6	Three photon coefficient γ of copper complexes	113
Table 7.1	Analytical data of Schiff base complexes	130
Table 7.2	Infrared spectral data (cm^{-1}) for ligands and complexes (C13-C14)	131
Table 7.3	2PA coefficient β of Schiff base complexes	139

CHAPTER 1

INTRODUCTION

Abstract

This chapter speaks about the origin and introduction to co-ordination compounds. It also introduces the basics of nonlinear optics highlighting the nonlinear optical processes and the common experimental techniques employed.

1.1 INTRODUCTION TO COORDINATION COMPOUNDS

Alfred Werner's coordination theory in 1893 was the first attempt to explain the bonding in coordination complexes. This theory was put forward before the electron had been discovered by J.J. Thompson in 1896. This theory and his painstaking work over the next twenty years won Sir Alfred Werner the Nobel Prize for Chemistry in 1913. With the proposal of various theories like Valence Bond Theory, Crystal Field Theory and Molecular Orbital Theory, the elucidation of geometry and nature of bonding in the complexes received a theoretical foundation. Since then, the field of coordination chemistry has been widely explored. The number and complexity of the coordination compounds still continue to grow. In fact, a survey on the literature in inorganic chemistry reveals that more than 70% of the published articles deal with coordination compounds. With the variety of the coordination compounds being discovered and their stereochemistry being solved, the applications of these compounds have also widened. Moreover, the importance of coordination complexes in our day to day life is increasing due to its interesting electrical, optical and magnetic properties.

For better functioning of the complexes, the choice of the ligand is very significant. Ligands generally bond to the central metal ion through sulfur, nitrogen

and/or oxygen atom present in its structure. The denticity and structure of the ligand plays a crucial role in determining the stereochemistry of the complex. Depending upon the usage of the complexes in medicines, sensors, optics, etc., the structure of the coordination compound is designed by carefully choosing the central metal ion and ligand.

1.2 NONLINEAR OPTICS

Nonlinear optics (NLO) is the study of interaction of light with matter. It is the branch of optics that describes the behavior of light in nonlinear media, that is, media in which the dielectric polarization P responds nonlinearly to the electric field E of the light. This nonlinearity is typically only observed at very high light intensities such as lasers.

The nonlinear interaction of light with matter is the basis of photonics. In linear interactions of light with matter the relative change of intensity is not a function of intensity, i.e., interactions like dispersion, refraction, reflection, absorption and diffraction are observable in the linear range. But all these linear interactions may become nonlinear if the intensity is high enough and behave as a nonlinear function of the applied light. Hence, in nonlinear optics the intensity of light is of significance.

Photons are the quantum units of light similar to electrons and carry a certain amount of energy which can be used for a wide variety of applications. The electromagnetic field of photons oscillates much faster than is possible for electrons. Also unlike in electronics, in photonic circuits, there is no magnetic and electrical interference making it more compatible.

Potentially many kinds of gases, liquids and solids are useful for nonlinear optical applications based on nonlinear absorption and emission. Organic and inorganic systems are used as nonlinear absorbers for optical switching and mode locking in laser oscillators. Basically, in a photonic circuit, a photon is used to acquire, store, process and transmit information. Light can be switched from one channel to another at certain

junction points. The materials which manipulate the light at these junction points are known as nonlinear optical materials and these materials are gaining importance in optical switching, storage and new display technologies. These applications demand better knowledge about the nonlinear optical process.

1.2.1 Theory of Nonlinear Optics

According to the classical theory of Raman Effect, when a molecule in an electric field (E) interacts with a material, there is an instantaneous displacement of the electron density away from the nucleus. This displacement of the electron density results in an induced electric dipole moment (P) and the molecule is said to be polarized. The size of the induced dipole moment depends both on the magnitude of the applied electric field and on the ease with which the molecule can be polarized. At molecular level, this can be expressed as follows.

$$P = \alpha E \quad \dots\dots\dots (1.1)$$

where α is linear polarizability.

At molecular level,

$$P = \chi^{(1)} E \quad \dots\dots\dots (1.2)$$

where $\chi^{(1)}$ is polarizability of the material.

For such a relation, the plot of polarization as a function of applied electric field is a straight line whose slope is linear polarizability of the medium. Before the advent of lasers, it was assumed that the optical parameters are independent of the intensity of the incident light. However, the discovery of lasers (Maiman 1960) brought a new dimension in the field of optics. The word LASER is an abbreviation for Light Amplification by Stimulated Emission of Radiation. Lasers are high intensity light sources which are characteristically different from ordinary light sources. Laser light possesses unique features like coherence, collimation and a narrow spectral width and

can focus at a possible minimum space. A laser can generate a high electric field which can affect the atomic electric fields of the medium and thereby affect the optical properties of the medium. This interaction leads to a generation of new electromagnetic fields altered in phase, frequency and amplitude, giving rise to nonlinear optical (NLO) phenomena. Actually the polarization of a medium is given by

$$P = \chi^{(1)}E + \chi^{(2)}E^2 + \chi^{(3)}E^3 + \dots \quad \dots\dots\dots (1.3)$$

where $\chi^{(2)}$ and $\chi^{(3)}$ represent second and third order susceptibilities of the medium respectively.

At molecular level, eq. (1.3) is expressed as

$$P = \sum \alpha_{ij}E + \sum \beta_{ijk}E^2 + \sum \gamma_{ijkl}E^3 + \dots \quad \dots\dots\dots (1.4)$$

where β_{ijk} and γ_{ijkl} are first and second hyperpolarizabilities and i, j, k, l correspond to molecular coordinates.

For small fields $\chi^{(2)}$ and $\chi^{(3)}$ can be neglected, so that the induced polarization is proportional to the strength of the applied field. However, for an intense electric field such as laser pulse, $\chi^{(2)}$ and $\chi^{(3)}$ become significant.

1.2.2 Nonlinear optical materials

The foremost criteria for a material to exhibit second order nonlinearity is a requirement of noncentrosymmetry in the material structure. This can be illustrated by considering an electric field incident on a centrosymmetric medium. The resultant second order polarization for this medium will be βE^2 . However, since the medium is centrosymmetric, it must possess an inversion symmetry, i.e., $-\beta E^2$. This holds good only when the polarization field is zero, indicating $\beta = 0$ for centrosymmetric media. Generally inorganic crystals like potassium dihydrogen phosphate (KDP), β -barium borate (BBO) and lithium niobate (LOB) are examples for noncentrosymmetric materials frequently used for their second order nonlinearity. These crystals exhibit β value in the

order of $1-100 \times 10^{-9}$ esu, arising from the electron polarizability due to the crystal band structure and asymmetry associated with the crystal structure.

Contrary to the situation found for second order optical nonlinearities, there is no such requirement that the material must be noncentrosymmetric to exhibit third order optical nonlinearity. Here, the polarization field produced by the molecule will be γE^2 and $-\gamma E^2$, thus giving rise to second order hyperpolarizability term (γ) as the first non-zero nonlinear term in centrosymmetric media. Compared to second order nonlinear materials, less no of materials have been studied for their third order nonlinear properties. This is mainly due to the lack of a detailed understanding of the effect of molecular structure on the third order NLO response. Generally conjugated organic polymers exhibit large third order nonlinear coefficients due to highly polarizable electronic networks in their delocalized π -systems.

1.2.3 Requirements for materials to exhibit NLO response

Most molecules that possess large β values contain an electron donor group (D) connected to an electron acceptor group (A) by a π -conjugated polarizable bridge as shown in Fig. 1.1. The linear optical properties of such dipolar, polarizable (D- π -A) molecules are characterized by low-energy, $D \rightarrow A$ intramolecular charge-transfer (ICT) excitations. It has been discovered that octupolar molecules which possess zero ground state dipole moments can also show large β values (Zyss and Ledoux 1994). For a centrosymmetric molecule, β is necessarily equal to 0, but no symmetry restrictions exist for γ . Although the primary requirement for large γ values is simply an extensive π -conjugated system, factors such as molecular asymmetry and 2-D conjugation are also important for enhancing cubic NLO responses (Tykwinski et al. 1998).

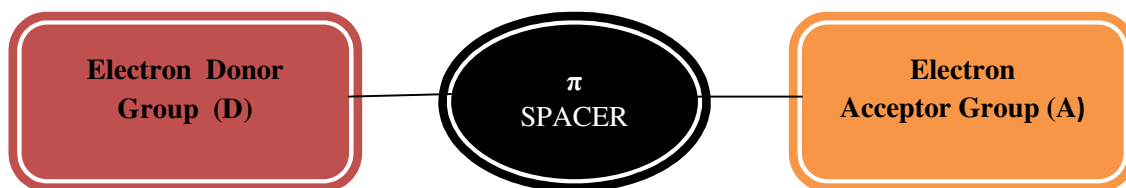


Fig. 1.1 Schematic representation of “push-pull” chromophores

For a bulk material, the extent of potentially useful NLO activity depends not only on molecular structure, but also on the macroscopic ordering of the component molecules, i.e., the crystal-packing arrangement or the ordering within a thin-film or other material. At the microscopic level, a nonzero $\chi^{(2)}$ value can only be exhibited by a noncentrosymmetric material, but no special symmetry requirements apply to $\chi^{(3)}$. The creation of materials for quadratic NLO effects is hence especially challenging because it necessitates both the molecular engineering of suitable structures and their incorporation into appropriate bulk arrangements. While modern synthetic chemistry allows a high degree of control over molecular structures, current ability to predetermine macroscopic structures (e.g. by crystal engineering) is rather limited. By contrast, although the design criteria for $\chi^{(3)}$ materials are not well defined, all substances exhibit some degree of cubic NLO activity. The challenge in this area is hence primarily to prepare molecules with NLO responses sufficiently large for practical applications (Tykwinski et al. 1998).

1.3 NONLINEAR OPTICAL PROCESSES

Nonlinear absorption is the change in transmittance of a material as a function of intensity or fluence. With an increase in the input intensity, the probability of absorbing more than one photon enhances. Few of the main phenomena responsible for nonlinear absorption are described below.

1.3.1 Second Harmonic Generation (SHG)

In second harmonic generation, two photons of frequency ω are destroyed and a photon of frequency of 2ω is simultaneously created in a single quantum-mechanical process (Fig. 1.2). Under proper experimental conditions, the process of second harmonic generation can be so efficient that nearly all the power in the incident beam at frequency ω is converted to radiation at the second harmonic frequency 2ω . One common use of SHG is to convert the output of a fixed frequency laser to a different spectral region. For example, the Nd:YAG laser operates in the near infrared at a wavelength of $1.06\ \mu\text{m}$. SHG is routinely used to convert the wavelength of the radiation to $0.53\ \mu\text{m}$, in the middle of the visible spectrum.

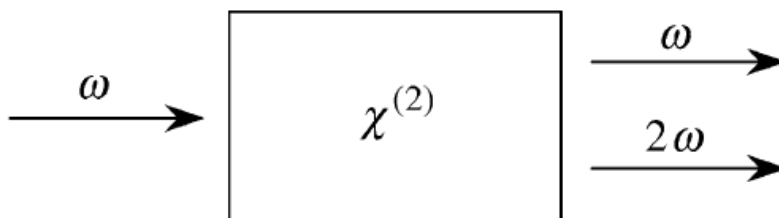


Fig. 1.2 Geometry of second harmonic generation

1.3.2 Sum and Difference Frequency Generation

The process of sum frequency generation is analogous to second harmonic generation, except that in sum frequency generation the two input waves are at different frequencies (Fig. 1.3). One application of sum frequency generation is to produce tunable radiation in the ultraviolet spectral region by choosing one of the input waves to

the output of the fixed-frequency visible laser and the other to be the output of a frequency-tunable visible laser.

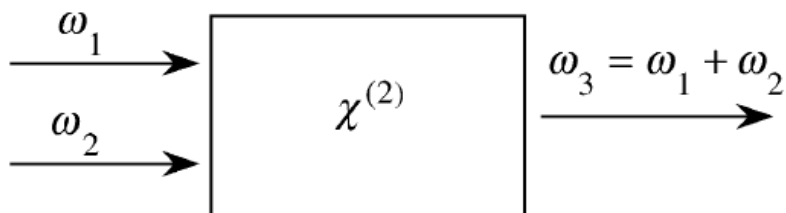


Fig. 1.3 Geometry of sum frequency generation

In case of difference frequency generation, the frequency of the generated wave is the difference of those of the applied fields (Fig. 1.4). It can be used to produce tunable infrared radiation by mixing the output of a frequency-tunable visible laser with that of a fixed-frequency visible laser. Here, the lower frequency input field is amplified. Hence this process is also known as optical parametric amplification.

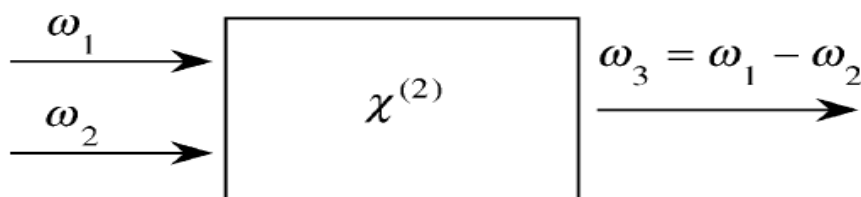


Fig. 1.4 Geometry of difference frequency generation

1.3.3 Two photon Absorption (2PA) process

Two photon absorption is the process by which the energy gap between two real states is bridged by the simultaneous absorption of two photons, not necessarily at the same frequency (Fig. 1.5a). The energy difference between the two states is equal to the sum of energies of the two photons. Initially, a photon oscillating at frequency $h\nu$ is absorbed to make the transition to reach a virtual state. In the next step, another photon of same energy is absorbed from the virtual state to jump in to the real excited state. In both cases, the virtual state is not real, i.e., the system must absorb the two photons simultaneously.

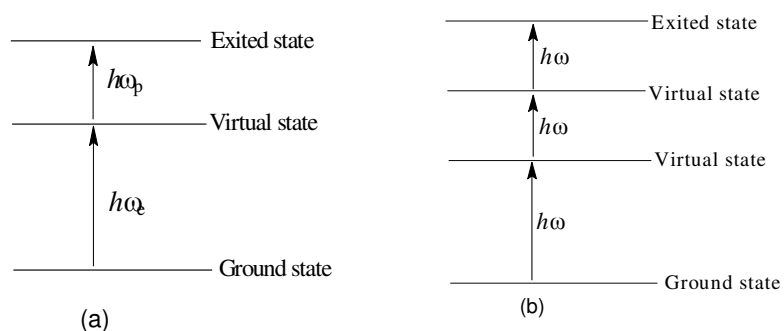


Fig. 1.5 (a) Two photon Absorption (2PA) and **(b)** Three photon Absorption (3PA) processes

1.3.4 Three photon Absorption (3PA) process

Three photon absorption (3PA) is the process which involves the simultaneous absorption of three photons from the ground state of a system to a higher energy state (Fig. 1.5b). With an increase in the input energy, the number of photon absorbed increases resulting in multi-photon absorption.

1.3.5 Excited State Absorption (ESA)

When the incident intensity is well above the saturation intensity, then the excited state becomes significantly populated. The excited electrons can rapidly make a transition to one of the higher states before it eventually transits back to the ground state. In such kind of process, there are a large number of higher energy states whose energy difference is in near resonance with the incident photon energy.

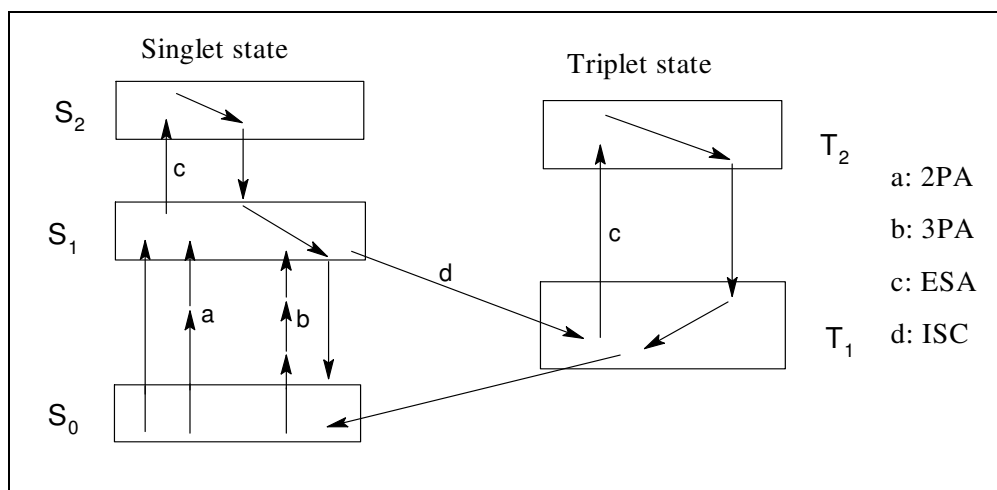


Fig. 1.6 Energy level diagram showing 2PA, 3PA, ESA and ISC

The mechanism of various types of absorption processes is represented in Fig. 1.6. The diagram shows different energy levels of a molecule, the singlet ground state S_0 , the excited singlet states S_1 and S_2 , as well as triplet excited states T_1 and T_2 . It also displays the different transitions between the energy levels. The transition from the ground S_0 to a higher singlet state by the absorption of a single photon gives rise to linear absorption. When the photons of same or different energy are simultaneously absorbed from the ground to higher excited state (S_0 to S_1), it is denoted as two photon absorption (2PA), which occurs at high light intensities. When the excited state absorption (ESA)

occurs, molecules are excited from an already excited state to a higher excited state (S_1 to S_2 and/or T_1 to T_2). For this to happen the population of the excited states (S_1 and/or T_1) needs to be high so that the probability of photon absorption from that state is high. Therefore high intensity light is needed to pump up the molecules to the excited states before a substantial amount of ESA starts to take place. Also, it is important that life times of excited states are long enough so that a population of excited states can be obtained. The life times of the triplet states are longer than the singlet states and therefore ESA could be enhanced if the molecules could undergo intersystem crossing (ISC) to the triplet states. More ISC could be achieved by including heavy atoms which introduces a strong spin orbit coupling between the states. If more absorption occurs from the excited state than from the ground state, it is usually referred to as reverse saturable absorption (RSA).

1.3.6 Saturable Absorption

Many materials have the property that their absorption coefficient decreases when measured using high laser intensity. When the absorption cross section of the excited state is smaller than that of ground state, the transmission of the system will be increased once the system is highly excited. This process is called as saturable absorption. Certain nonlinear optical systems can possess more than one output state for a given input state. The measured absorption coefficient (α) depends on the intensity (I) of the incident laser light by the following expression

$$\alpha = \frac{\alpha_0}{1 + I / I_s} \dots\dots\dots (1.5)$$

where α_0 is low-intensity absorption co-efficient and I_s is saturation intensity. One consequence of saturable absorption is optical bistability. Optical bistability refers to the situation in which two different output intensities are possible for a given input intensity.

The principle of optical bistability is generally used in optical switches for optical communications or optical data processing.

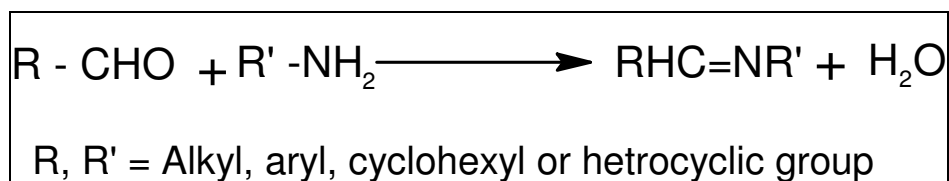
1.4 THIRD ORDER OPTICAL NONLINEARITY

Optical nonlinearity of the third order is a universal property, found in any material regardless of its spatial symmetry. This nonlinearity is the lowest order nonlinearity for a broad class of centrosymmetric materials, where all the even-order nonlinear susceptibilities are identically equal to zero for symmetry reasons. Third-order nonlinear processes include a vast variety of four-wave mixing processes, which are extensively used for frequency conversion of laser radiation and as powerful methods of nonlinear spectroscopy. Frequency degenerate and Kerr-effect phenomena constitute another important class of third order nonlinear processes. These effects are used for optical compressors, mode-locked femtosecond lasers and numerous photonic devices, where one laser pulse is used to switch, modulate or gate another laser pulse.

1.5 COORDINATION COMPLEXES AS NLO MATERIALS

Nonlinear optical responses of coordination complexes have attracted much attention because of their advantages such as coordination geometry, low-lying intense metal to ligand charge transitions (MLCT) or ligand to metal charge transitions (LMCT), variable oxidation states and thermal stability which tune the NLO performance. The metal center may act as donor or acceptor, giving rise to electron asymmetry and hence possess optical nonlinearity. Coordination complexes also have high environmental stability as well as considerable NLO response and thus become an important choice for NLO materials. Thus compared to organic molecules, metal complexes can offer greater scope for the creation of multifunctional materials.

While designing coordination complex for NLO applicability, the choice of ligand is crucial as the ligands environment plays an essential role in determining the type of nonlinear behavior in the complex. An overview of the literature shows that metal complexes having Schiff base ligands have the potential to exhibit large NLO activity. Basically, compounds containing an azomethine group (-CH=N-), are known as Schiff bases (Etthing 1840, Schiff 1869). Schiff base is named after its discoverer, German chemist Hugo Schiff (1834-1915) and is also known as imine, anils, enamines, etc. Schiff bases are versatile ligands which are synthesized from the condensation of primary amines and aldehydes or ketones ($RCH=NR'$, where R and R' represents alkyl and/or aryl substituents) (Scheme 1.1).



Scheme 1.1. General procedure for the synthesis of Schiff base

Schiff bases have an excellent chelating ability towards a large number of metal ions. This is mainly due to the lone pair of electrons on the sp^2 hybridized orbital of nitrogen atom of azomethine group. The chelation can be further improved by substituting with groups containing one or more donor atoms like oxygen and sulfur in the vicinity of azomethine group. Thus, depending on the substituent groups, Schiff base can behave as a monodentate, bidentate or even tridentate ligand. This flexibility in the denticity of the ligand combined with the ease of its preparation makes this ligand capable of forming stable complexes with many transition metal ions.

The interest in Schiff bases was initially due to its excellent catalytic activity. Several review works can be found on the contribution of Schiff base metal complexes as

catalyst in the field of coordination chemistry (Nishinaga et al. 1989, Chakraborty et al. 1994). With the advent of science, they also found applications in biological field as they displayed good antimicrobial (Saxena and Shrivastava 1987, Bhardwaj and Singh 1994, Dholakiya and Patel 2002, Sari et al. 2003, Singh et al. 2006), antifungal (Singh et al. 1999, Ramesh and Sivagamsundari 2003) and antiviral activities and they are even found to be good anticarcinogens and antitumour compounds (Singh et al. 1996, Chohan and Sherazi 1999, Jayabalakrishanan and Natarajan 1999, Jeewoth et al. 2000). Emphasis is now placed not only on the catalytic and biological activities of these Schiff base complexes, but even on their optical applications.

Along with the chelating ability of the ligands, an extensive π -electron conjugation also aids the optical nonlinearity. Such kind of conjugation system is generally provided by organic moieties like alkynyl group (Powell et al. 2004, Dalton et al. 2007), bipyridine derivatives (Sakaguchi et al. 1991), arenes (Ray et al. 2010), triphenylphosphine (Thangadurai et al. 2010) and so on. This kind of conjugation acts as a bridge between the donor and acceptor groups for an easy electrical communication. Also, the extension or reduction of the electron system brings about a change in the electron density which may subsequently lead to an efficient optical switching (Sun et al. 2011).

In order to extend the conjugation, charged molecules like ionic liquids can be tagged to the ligand group. Ionic liquids are generally organic in nature and exist in liquid state even at room temperature. These ionic liquids can also be added as solvent during the synthesis of the ligands or complexes. By varying the anionic and cationic components of ionic liquid, it is possible to tailor the desired properties. Hence in recent times, ionic liquids have gained importance to enhance optical properties of the coordination complex. Also in the past couple of years, optical potential of room temperature ionic liquids based in imidazolium cations has been recognized. However, very few reports on its physicochemical and optical applications have been reported (Souza et al. 2008, Calixto et al. 2009)

1.6 EXPERIMENTAL TECHNIQUES

The initial stages in the development of novel molecular NLO materials are the synthesis of molecules with large β and/or γ values and their incorporation into materials with substantial $\chi^{(2)}$ and/or $\chi^{(3)}$ coefficients. Although many additional factors must be considered for practical device applications (e.g. thermal and photochemical stability, processability, etc.) the NLO properties of molecules and molecular materials can be adequately described here by reference to values of β , γ , $\chi^{(2)}$ and $\chi^{(3)}$. Several methods have been developed to measure these parameters. Few of the important experimental techniques have been described below.

1.6.1 Kurtz powder test

For studies of quadratic NLO properties, $\chi^{(2)}$ values are obtained from solid-state SHG measurements, and Kurtz powder test is often used to screen materials for activity (Kurtz and Perry 1968). This technique most often involves collection of 532 nm second harmonic (SH) light produced following irradiation with a near-infrared 1064 nm Nd³⁺:YAG laser. The SHG efficiencies may be quoted with respect to quartz, ADP, KDP, urea or other reference samples. Urea is the most commonly used standard for organic compounds, the relative 1064 nm SHG activities are: quartz (0.0025); ADP \approx KDP (ca. 0.04); LiNbO₃ (1.5). Different laser fundamentals (e.g. 1907 nm) may be used with materials which absorb strongly around 532 nm. However, Kurtz powder test is only semi quantitative, the results being affected by various factors including particle sizes. Furthermore, a lack of SHG often merely indicates the adoption of a centrosymmetric crystal structure by a molecule which may nevertheless on its own possess a significant β value. Powder SHG testing is hence not useful for establishing structure-activity correlations (SACs).

The schematic diagram of Kurtz powder technique is shown in Fig. 1.7. In this technique the sample is prepared by sandwiching the graded crystalline powder with average particle size of about 90 μm between two quartz slides using copper spacers of 0.4 mm thickness. The powdered sample (S) is illuminated using a Q-switched Nd:YAG laser emitting 1.06 μm 40 ns laser pulses with spot radius of 1 mm. The energy meter D1 serves as a reference to monitor the fluctuation in the input pulse. Filter F1 that transmits the fundamental laser emission is used to cut off the fundamental laser radiation and to pass the generated second harmonic. The second harmonic signal generated in the sample is collected by the lens and detected by the cathode ray oscilloscope (CRO) coupled with the photo multiplier tube D2.

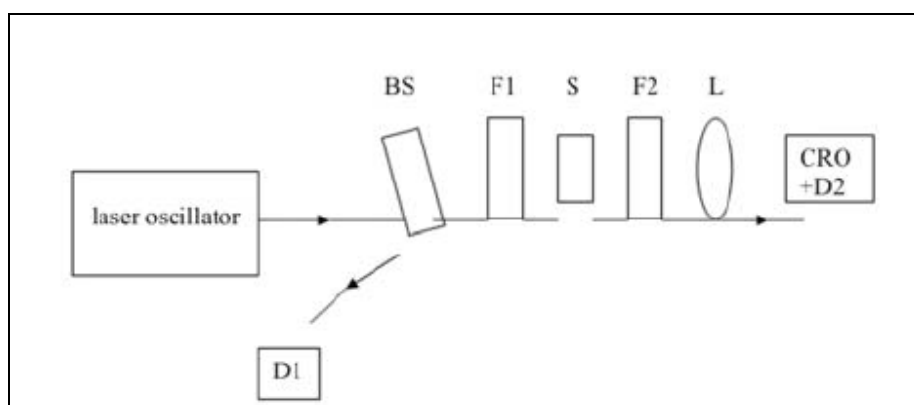


Fig. 1.7 Experimental arrangement of Kurtz powder technique

1.6.2 Z-Scan method

The Z-scan technique provides a highly sensitive and straightforward method for determining the nonlinear refractive index (n_2) and nonlinear absorption coefficient (β) of nonlinear materials. Both the sign and the magnitude of the real and the imaginary part of the third order susceptibility can be deduced by this method. The typical Z-scan experimental setup is shown in Fig. 1.8. In this technique, a polarized Gaussian laser

beam, propagating in the Z-direction, is focused to a narrow waist. In a typical configuration, the sample is moved along the propagation axis of the laser beam (Z-axis) near the focal position. Gaussian laser beam is used for molecular excitation and its propagation direction is taken as the Z-axis. The beam is focused using a convex lens, the focal point is taken as $Z = 0$. The experiment is done by moving the sample in the beam path and measuring the corresponding transmission at different positions with respect to the focus (different values of Z). When the sample is far from the focus and closer to the lens, the energy density is low and the transmittance characteristics are linear. As the sample is moved closer to the focus, the energy density increases inducing optical nonlinearity which decreases the transmittance. The laser beam will have maximum energy density at the focus, and the transmittance is observed to be minima at the focus. As the sample is moved further towards the detector end, the energy density decreases which leads to increased transmittance. When the sample is far from the focus and near to the detector end, the energy density is low and the transmittance again becomes independent of light intensity. Energy density will symmetrically reduce on either side of $Z=0$, i.e. for the positive and negative values of Z. Thus the sample sees different laser intensity at each Z position. The typical open aperture Z-scan curve is shown in Fig. 1.9. In the open aperture configuration the detected transmittance will only be sensitive to nonlinear absorption since the entire beam enters the detector at all times. On the other hand, in a closed aperture configuration an aperture is introduced in front of the detector and the detected transmittance will be sensitive to nonlinear refraction. From the corresponding transmission values, the nonlinear absorption β and nonlinear refraction coefficient (η_2) of the sample can be calculated following the Sheik-Bahae formalism (Bahae et al. 1990).

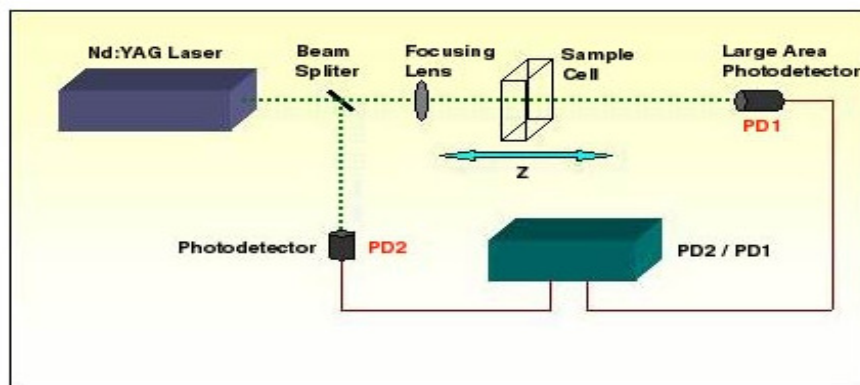


Fig. 1.8 Schematic representation of Z-scan

For instance, when a thin sample of a material with a negative nonlinear refraction being translated along the Z -axis, the situation can be regarded as treating the sample as a thin lens of variable focal length due to the change in the refractive index at each position. When the sample is far from the focus and closer to the lens, the irradiance is low and the transmittance characteristics are linear. Hence the transmittance through the aperture is fairly constant in this region. As the sample is moved closer to the focus, the irradiance increases which induces a negative lensing effect. A negative lens before the focus tends to collimate the beam. This causes beam narrowing leading to an increase in the measured transmittance at the aperture. A negative lens after the focus tends to diverge the beam resulting in the decrease of transmittance. As the sample is moved far away from the focus, the transmittance again becomes linear in Z direction as the irradiance becomes low. Thus the curve for transmittance versus Z has a peak followed by a valley for a material with negative refractive nonlinearity. The curve for a positive refractive nonlinearity will give rise to the opposite effect, i.e. a valley followed by a peak shown in Fig. 1.10. Z-scan technique has the advantage of being a simple technique; it is fairly sensitive and provides quick results.

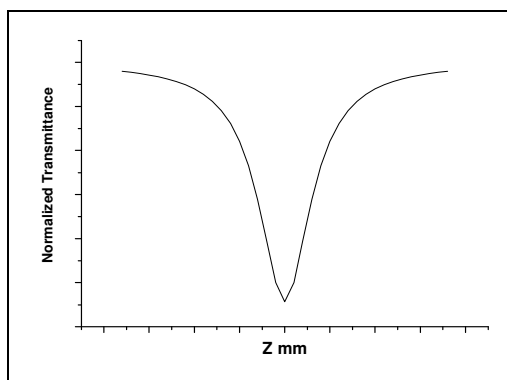


Fig. 1.9 Typical open aperture Z-scan transmittance curves for a cubic nonlinearity

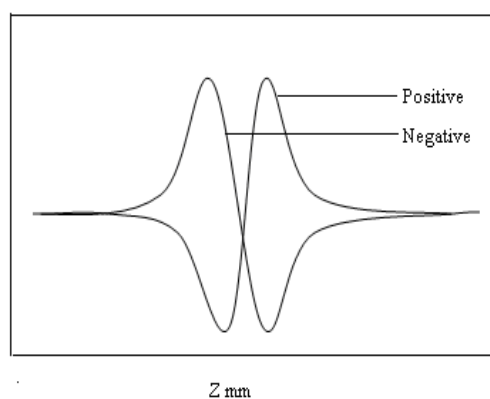


Fig. 1.10 Typical closed aperture Z-scan transmittance curves for a cubic nonlinearity

1.6.3 Degenerate Four-Wave Mixing (DFWM)

The interaction of four electromagnetic waves in a nonlinear optical medium via third-order nonlinearity is termed as four wave mixing. When all the waves have the same frequency, it is called degenerate four-wave mixing (DFWM). This is a popular method for characterizing third-order nonlinear materials and has been used extensively. There are different geometries like phase conjugate geometry, BOXCARS geometry etc., in which a four-wave mixing experiment can be set up. A typical BOXCARS geometry (Sutherland 2003 and Santhosh et al. 2009), where a laser beam is split into three beams

and the beams are aligned such that they form spots on the three corners of a square in the input plane, is shown in Fig. 1.11. The diametrically opposite beams are the pump beams, and have the same intensity. The third beam is the probe, which is adjusted to have an intensity of about 20% of the pump beam. These three beams will interact nonlinearly when focused on to a sample. The resultant DFWM signal can be detected at the fourth corner of a square in the output plane which is generated due to the phase-matched interaction $k_4 = k_3 - k_2 + k_1$. The signal is measured using a high sensitive silicon detector. The strength of this signal beam is proportional to the effective $\chi^{(3)}$. This technique has several advantages. The signal beam is readily distinguishable from the other interacting beams. Under proper experimental conditions, the detected signal has a characteristic dependence on the laser intensity ($I^e \propto I^3$). Typical variation of the DFWM signal as function of the pump intensity is shown in Fig. 1.12.

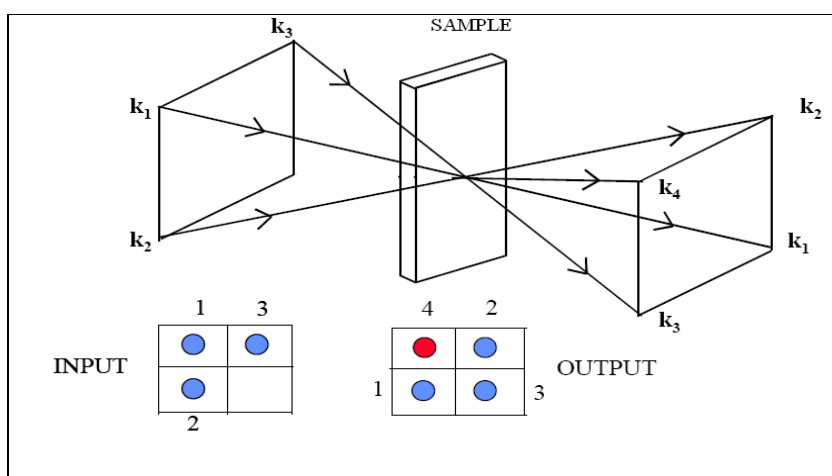


Fig. 1.11 DFWM set-up in BOXCAR configuration, 4(k_4) is the signal

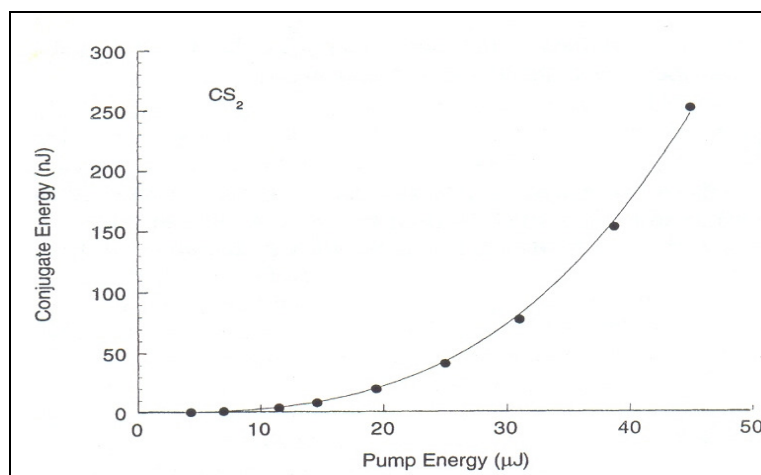


Fig. 1.12 DFWM signal versus Probe

1.6.4 Hyper-Rayleigh scattering (HRS)

Since the early 1990s the versatile hyper-Rayleigh scattering (HRS) technique has also become widely available (Terhune et al.1965). This approach depends on the fact that microscopic anisotropy within a solution of molecules with quadratic NLO activity can produce incoherent SH scattering which can be analyzed to afford different directional components of β . The HRS technique has certain advantages over Electric field induced second harmonic generation (EFISHG); e.g., it does not require knowledge of molecular dipole moments (μ) and is applicable to charged and octupolar compounds which are not amenable to EFISHG study. Although a lack of discrimination between HRS and multi-photon fluorescence can complicate the derivation of reliable β values for certain compounds, this potential problem can be circumvented (Olbrechts et al. 1998).

The results from EFISHG or HRS experiments can be corrected for resonance enhancement by using a simple theoretical two-state model (TSM) given by equation (1.6) and equation (1.7) (Oudar and Chemla 1977, Oudar 1977), which is reasonably valid for dipolar molecules in which β is primarily associated with a single ICT excitation.

$$\beta = \beta_0 \frac{E_{\max}^2}{[1 - (2E_f)^2 (E_{\max}^2)^{-1}] [(E_{\max})^2 - E_f^2]} \quad \dots\dots\dots (1.6)$$

$$\beta_0 = \frac{3\Delta\mu_{12}(\mu_{12})^2}{2(E_{\max})^2} \quad \dots\dots\dots (1.7)$$

where E_f is the fundamental laser energy, E_{\max} is the energy of maximal absorption, $\Delta\mu_{12}$ is the dipole moment change for ICT excitation, and μ_{12} is the transition dipole moment. The application of equation 1.6 to β values measured with a 1064 nm laser (β_{1064}), or at any other chosen wavelength, affords β_0 , the static or zero-frequency first hyperpolarizability, which provides an estimate of the ‘intrinsic’ molecular hyperpolarizability, in the absence of any resonance effects. For octupolar chromophores, a related three-state model can be used (Joffre et al. 1992). The complications of resonance enhancement are often minimized in EFISHG studies by using a 1907 nm laser, but HRS is not well suited to working at such low wavelengths because the SH scattering effect becomes very weak. However, a 1907 nm HRS technique was developed in the late 1990s. β_0 values are particularly useful when considering potential practical applications of molecular quadratic NLO materials which necessitate operation at ‘off-resonance’ wavelengths, generally in the NIR region ca. 1000-1500 nm. Schematic experimental set up for SHG efficiency measurements is shown in Fig. 1.13.

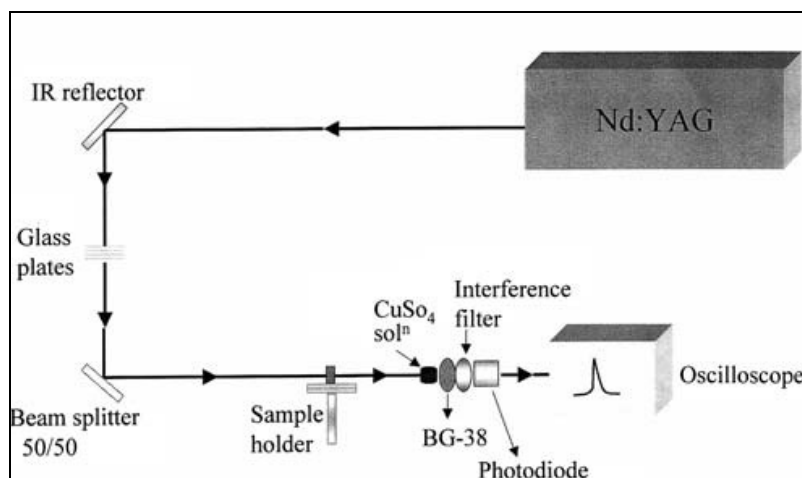


Fig. 1.13 Schematic experimental set up for SHG efficiency measurements

1.6.5 Optical Kerr Gate

A variety of two-beam experiments have been devised to measure NLO properties, the principle being that a high-intensity beam (the pump) causes a change in the optical properties of a material and the change is then (usually after a variable delay) detected by the second beam (the probe). The pump and probe beams can be at different frequencies (for nondegenerate nonlinear effect studies) or at the same frequency similar to the DFWM experiment. The simplest modification of a pump-probe experiment can be used to determine nonlinear absorption which can be related to the imaginary part. Another modification is called the Optical Kerr Gate (OKG). In the OKG experiment (Fig. 1.14) the pump is linearly polarized and its action on the material induces optical birefringence that is a change in the refractive index for directions parallel to the polarization and perpendicular to it.

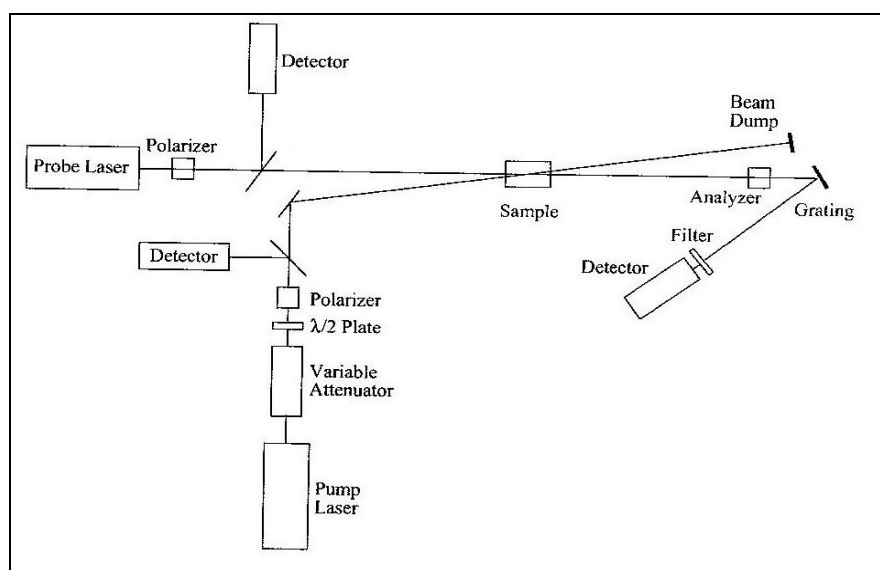


Fig. 1.14 Schematic diagram of optical Kerr gate experiment

Thus several methods have been developed to characterize the newly synthesized nonlinear optical materials, each method having its own advantages and disadvantages. Depending upon the material and the property desired, a particular measurement technique is chosen. As an example, if a material should be usable for second-harmonic generation, it should belong to a non-centrosymmetric group. Thus a test for this should be possible at a very early stage; the powder technique may be used for this purpose.

CHAPTER 2

LITERATURE SURVEY AND OBJECTIVES OF THE WORK

Abstract

In the last three decades, several reports on the preparation of coordination compounds suitable for NLO applications have been published. This chapter presents a brief survey on the literature regarding design and synthesis of coordination complexes and their significance in nonlinear optics. The chapter concludes with the outline of the present work highlighting the main objectives.

2.1 A BRIEF REVIEW ON THE LITERATURE

Since the invention of laser in 1960, there has been enormous increase in the applications of this newly available light source and its amazing properties and there is no end to this development in the near future. Generally, the basic necessity for a material to show NLO behavior is the existence of strong intramolecular charge transfer excitations in a non-centrosymmetric molecular environment. This can be achieved by considering a polarizable molecular system (eg. π -conjugation) having an asymmetric charge distribution due to the presence of donor and/or acceptor substituent groups. Besides the traditional donor-acceptor (“push-pull”) organic chromophores, coordination complexes with their unique characteristics such as various redox properties and diverse geometries, have given a new dimension to this field.

The study of NLO properties of coordination compounds was first reported in the mid-1980s. Report in 1987 that *cis*-1-ferrocenyl-2-(4-nitrophenyl)ethylene exhibited an SHG efficiency 62 times that of urea (Green et al. 1987) has motivated many organometallic chemists to enter this field. Until early 1990s the main strategy was to

design metal-organic NLO chromophores by simply substituting organic donors with metal centers. But later, inorganic complexes, where the d-electrons are more strongly held by the metal ion, have shown enhanced optical nonlinearities. Since then, many reports on the nonlinear properties and applications of these complexes have been published (Di Bellat et al. 1994, Dhenaut et al. 1995, Coe et al. 1999, Chao et al. 1999, Di Bella and Fragala 2000, Di Bella et al. 2004).

The first report of NLO metal complex of the tetradentate salen ligand was that of Chiang and co-workers (1991) where the metal-salen core was used to enhance the NLO response of the substituted pyridine ligand. The report by Di Bella et al. (1994) on various Ni(salen) derivatives with different NLO responses opened interesting perspectives for metal complexes. The second-order NLO properties of iron (III) complexes $[\text{Fe}(\text{salen})(\text{pyridyl})\text{X}]$, where $\text{X} = \text{F}, \text{Cl}, \text{Br}, \text{I}, \text{N}_3, \text{NCS}$ (Fig. 2.1) was studied by Chiang and his group (1996). While halide and thiocyanate complexes exhibited weak SHG intensities, azide complexes exhibited high SHG efficiency twice that of urea. The nonlinearity in this complex was attributed to be originating from charge-transfer transitions in both salen ligand and pyridyl-Fe π system.

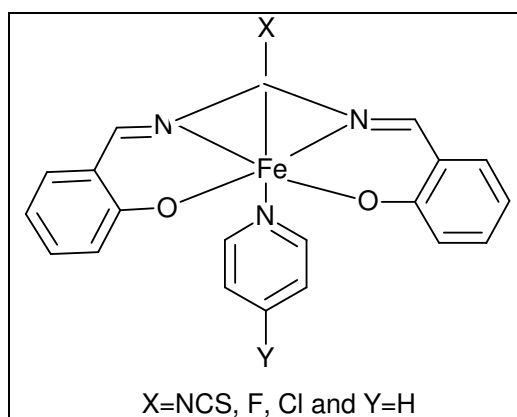


Fig. 2.1 Chemical structure of $[\text{Fe}(\text{salen})(\text{pyridyl})\text{X}]$

Di Bella in collaboration with Lacroix (Di Bella et al. 1995, Lacroix et al. 1996, Di Bella et al. 1997, Lenoble et al. 1998, Di Bella and Fragala 2000) have carried out a number of second-order NLO studies on bis(salicylaldehydiminato)metal Schiff base complexes. Bis(salicylaldehydiminato) Ni(II) Schiff base complexes have proved to be a new class of efficient NLO materials by showing low-energy charge transfer (CT) transitions.

Later Averseng et al. (1999) reported the electronic and second-order NLO properties of a new bis(salicylaldehydiminato) Ni(II) Schiff base complexes. These complexes showed modest NLO response compared to organic chromophores. The role of different metal ions in the enhancement of NLO response has also been well studied. NLO properties of a series of coordination compounds, $[M(\text{PM-L})_2(\text{NCS})_2]$, with large aromatic ligands PM-L and divalent metal ion ($M = \text{Mn}, \text{Fe}, \text{Co}, \text{Ni}$ and Zn) (Fig. 2.2) have been measured by HRS technique (Gaudry et al. 2000). The molecular hyperpolarizability value increased from Ni(II) complex (two unpaired electrons) to Mn(II) complex (five unpaired electrons).

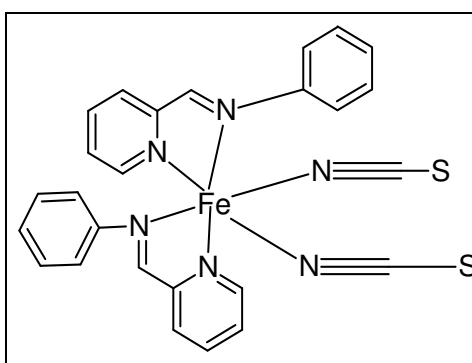


Fig. 2.2 Chemical structure of $[\text{Fe}(\text{PM-L})_2(\text{NCS})_2]$

Zinc halide complexes like ZnL_2X_2 ($\text{X} = \text{Cl}, \text{Br}, \text{I}$) with 4-methoxybenzaldehyde thiosemicarbazone exhibited SHG efficiency 10 times higher than that of urea (Tian et al.

2002). The relationship between the molecular structures and nonlinear optical properties were studied based on theoretical calculations and experimental methods.

The nonlinearity of substituted complexes is dominated by the nature and position of substituent on the aromatic ring. Also a review on the principle classes of NLO materials illustrates the implication of metal complexes in terms of their oxidation state, configuration and spin state, in the enhancement of nonlinear behavior (Di Bella 2001). The hyperpolarizability of Co(II), Cu(II) and Ni(II) complexes with 4-(diethylamino) salicylaldehyde and 4-nitroaniline studied by using second harmonic technique showed good NLO response (Lacroix et al. 2004, Costes et al. 2005). The crystal structure established a centrosymmetric molecular structure for Cu(II) and Ni(II) complexes whereas a pseudo-tetrahedral molecular structure was established for the Co(II) complex. The quadratic hyperpolarizabilities of the ligand and Co(II) complex were measured by EFISH technique and was found to be 66 and $110 \times 10^{-30} \text{ esu}^{-1}$ respectively, thereby displaying a large NLO response. The second-order nonlinear optical properties of a novel class of materials based on planar Ni(II) complexes of pyrrole 2-aldehyde and substituted diamine (Di Bella et al. 2004) have been reported (Fig. 2.3). Here, the tetra coordinated Ni(II) showed second-order optical nonlinearity 1.2 times greater than that of urea involving a significant octupolar contribution to the optical nonlinearity.

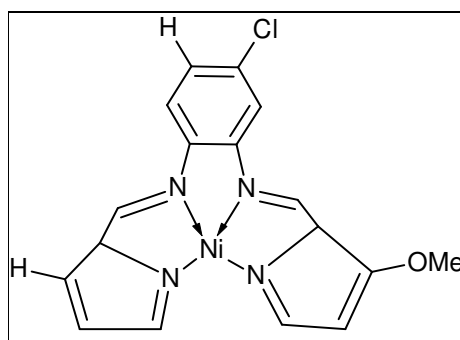


Fig. 2.3 Chemical structure of Ni(II) complexes of pyrrole 2-aldehyde and substituted diamine

During the same time, Sheikhshoaie and co-workers (2004) investigated two new monoazo Schiff base ligands 5-[(4-methylphenyl)azo]-N-(2-hydroxyphenyl) and 5-[(4-methylphenyl)azo]-N-(2-hydroxyphenyl)salicylaldimine for their nonlinear optical properties. They attributed the presence of NO₂ group for the enhancement in NLO response.

Other than transition metals, complexes of other metals like tin and boron have also been reported to exhibit good NLO response. Diorganotin compounds obtained by the reaction of methoxysalicylaldehyde or 4-diethylaminosalicylaldehyde, 2-amino-5-nitrophenol and dibutyltin or diphenyltin oxide revealed 1.5 times enhancement in hyperpolarizabilities with a change from boron to tin (Reyes et al. 2004). The boronates (Fig. 2.4) synthesized by the condensation of salicylaldehydes and 2-amino-5-nitrophenol and 1-naphthyl boronic acid or 2-naphthyl boronic acid or o-tolylboronic acid were characterized for their second-order (by EFISH technique) and third-order (by THG Maker Fringe technique) nonlinear behavior (Munoz et al. 2008). The nonlinearity was attributed to the different conformations of the aryl moieties around the boron-nitrogen bond which could potentially modulate the electronic properties on the boron compounds.

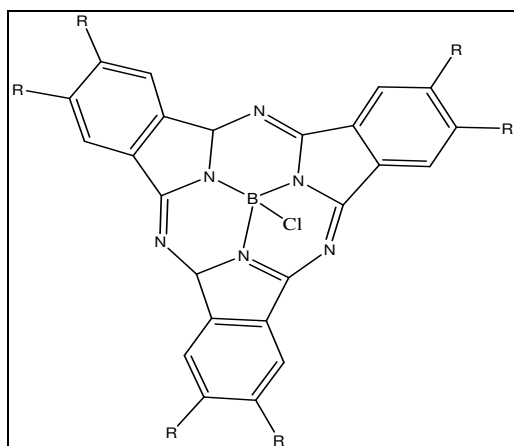


Fig. 2.4 Chemical structure of boronates (R = p-tolylsulfonyl, SC₈H₁₇, SO₂C₈H₁₇)

Recently boron complexes obtained by the reaction of bidentate ligands and diphenylboronic acid (Fig. 2.5) showed a cubic nonlinear optical susceptibility using THG Makers and Fringe technique (Rodriguez et al. 2012). The decrease in NLO response from ligands to boron complexes was attributed to structural conformation or deformation of electronic π -system. The electronic and structural features of the synthesized borinates may prove useful for new strategies in the design of novel NLO dyes.

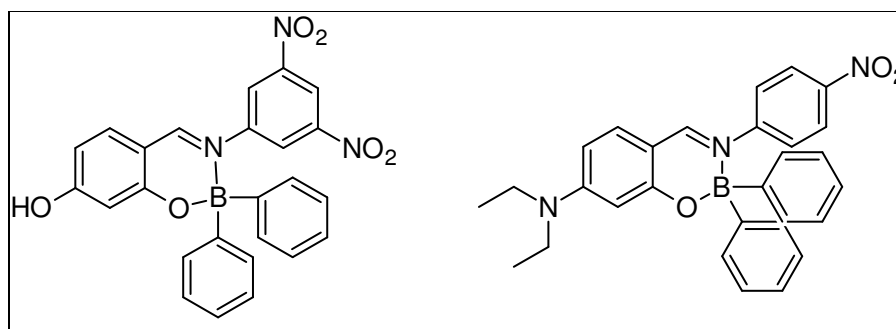


Fig. 2.5 Chemical structure of boron complexes

The role of metal in NLO response has been well illustrated by Ray and co-workers (2010). They found that on probing the coumarin derived dyes by femtosecond laser, none of the compounds showed any two-photon activity in the wavelength range 760-860 nm. However, in presence of Zn(II) (Fig. 2.6) and Mg(II) metal ions, the compounds exhibited large two-photon absorption as well as emission in the same wavelength region.

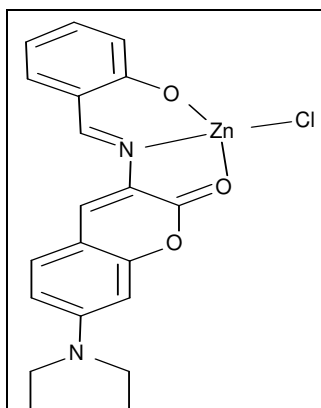


Fig. 2.6 Chemical structure of coumarin derived Zn(II) complexes

To improve the nonlinearity, ionic liquids are being tagged to the inorganic complexes. This is mainly due to the liquid crystalline property of ionic liquids (Bowlas et al. 1996, Gordon et al. 1998). Organic materials with nonlinear optical responses have been used for the fabrication of opto-electronic devices such as optical limiters, optical modulators and optofluidic lens (Yin et al. 2007, Xu et al. 2005). Calixto and co-workers (2009) have carried out NLO studies for two different ionic liquid compounds, 1-n-butyl-3-methylimidazolium tetrafluoroborate ([BMI]BF₄) and 1-n-butyl-3-methylimidazolium hexafluorophosphate ([BMI]PF₆) using Z-scan technique at 514 and 810 nm (Fig. 2.7). They observed large nonlinear refractive indices of thermal origin at both the wavelengths. The results revealed that depending on the anion, different ionic liquid structures are a suitable media for the investigation of nonlocal nonlinear optical phenomena.

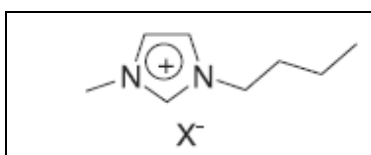


Fig. 2.7. Schematic illustration of [BMI]BF₄ and [BMI]PF₆ ionic liquid structures
(X = BF₄, PF₆)

In the past two years, there has been a remarkable thrust to understand the conjugated structure and nonlinear optical property of the inorganic complexes. Concerning this, there are evidences for the enhancement of nonlinear optical properties due to the presence of donor-acceptor groups in the metal Schiff base complex, resulting in delocalization of electrons. The Schiff base complexes of Co(II), Ni(II), Cu(II) and Zn(II) were prepared by the condensation of 2-aminothiazole and 3-formylchromone (Kalanithia et al. 2011) (Fig. 2.8). The Cu(II) complex exhibited a distorted square planar geometry whereas the other metal complexes exhibited distorted tetrahedral geometry. The SHG efficiency of Cu(II) complex was found to be one fourth that of urea.

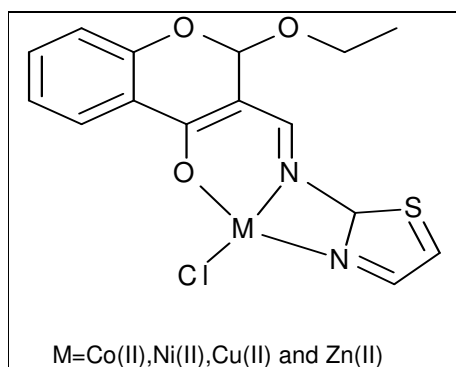


Fig. 2.8 Chemical structure of 2-aminothiazole and 3-formylchromone metal complexes

The present research is focused on understanding the structure-property relationship for the observed nonlinearity in metal complexes. For this, the optical properties and geometrical arrangement of the complexes are being systematically investigated. Tang and co-workers (2011) studied series of asymmetric donor-acceptor substituted salen-type Schiff bases and their structures and electronic properties. The complex with NO₂ substituent showed a large second-order hyperpolarizability. The enhancement in hyperpolarizability was investigated by studying the HOMO and LUMO energy gaps. Tang found that the smaller the HOMO-LUMO energy gap, the larger the

hyperpolarizability. Ying (2012) synthesized a tetra co-ordinated non-centrosymmetric $[\text{Zn}(\text{HL})_2(\text{H}_2\text{O})_2]$ complexes showing SHG response that is ~ 1.5 times higher than that of KDP making them potential candidates for photoactive materials. Anitha and co-workers (2012) have found that the SHG efficiency of azo Schiff base ligand 4-((E)-(4-chlorophenyl)diazenyl)-2-hydroxybenzylideneamino)-1,5-dimethyl-2-phenyl-1H-pyrazol-3(2H)-one (Fig. 2.9) is 2.1 times more active than KDP due to their relative delocalization of π -electronic clouds.

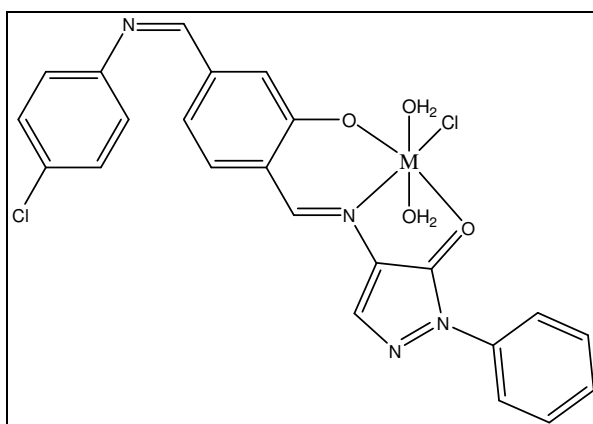


Fig. 2.9 Chemical structure of 4-((E)-(4-chlorophenyl)diazenyl)-2-hydroxybenzylideneamino)-1,5-dimethyl-2-phenyl-1H-pyrazol-3(2H)-one

The inorganic complexes showing third-order nonlinear behavior by 3PA have also been discovered. Cai et al. (2011) synthesized three mixed ligand Ni(II) complexes (Fig. 2.10) and studied their third-order nonlinear optical properties using femtosecond laser and degenerate four-wave mixing technique. The third-order nonlinear optical susceptibilities were $3.20 - 3.51 \times 10^{-13}$ esu and nonlinear refractive indexes were $5.89 - 6.45 \times 10^{-12}$ esu with a response time of 55-81 fs.

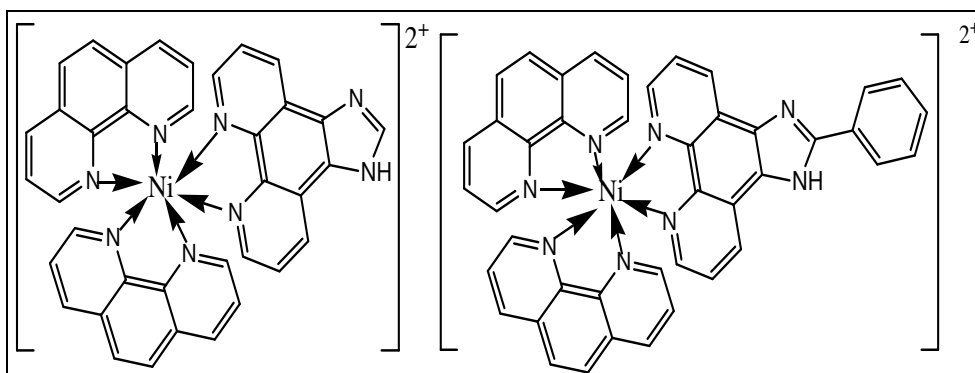


Fig. 2.10 Chemical structure of mixed ligand Ni(II) complexes

Few more reports on Schiff base derivatives exhibiting third-order nonlinear optical properties have come into picture. Sudeesh and Chandrashekar (2012) have studied the third-order nonlinear optical properties of Schiff's derivatives and the effect of Ag and Au nanoparticles on their nonlinear properties. The third-order optical nonlinearity of [PdLPPh₃] (L=N-(2-pyridyl)-N-(salicylidene) hydrazine) (Fig. 2.11) was investigated by our group (Rudresha et al. 2012) using Differential Optical Kerr Gate and Z-scan techniques. The nonlinear response time and third-order optical susceptibility were found to be ~90 fs and $3.9 \times 10^{-10} \text{ esu}^{-1}$ respectively.

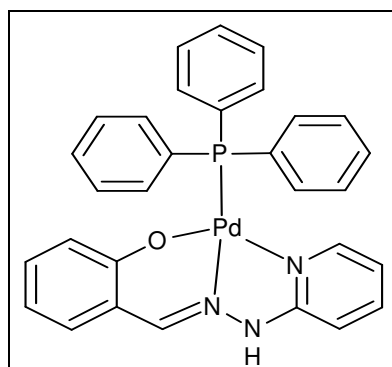


Fig. 2.11 Chemical structure of [PdLPPh₃] (L=N-(2-pyridyl)-N-(salicylidene) hydrazine)

Recently Di Bella (2012) has further reported an unprecedented mode of NLO switching in bis(salicylaldiminato) Zn(II) Schiff base complex. Here, addition of a Lewis base such as pyridine led to a switch-on of the quadratic hyperpolarizability. With an increasing demand to design novel metal complexes with useful NLO response, theoretical approach is being adopted by a large group of chemists to study the nonlinear optical properties of coordination complexes by using various theories like density functional theory (DFT) (Sun et al. 2011, Liu et al. 2012). Thus, in a span of just two decades, the progress of metal complexes in nonlinear optics has been incredible and still there is much scope of improvement in this field.

2.2 SCOPE AND OBJECTIVES OF THE WORK

It is well known that nonlinear optical materials have promising applications in the field of information storage, transmission and display. However, to design materials with the required NLO response is challenging. In the optics world, which was initially dominated by organic chromophores as being the best NLO materials, reports on the wonder a metal can do to the NLO property, is a noteworthy breakthrough. Coordinated complexes can be easily tunable to achieve the desired target. The ease of preparation of metal complexes is attributed to the flexibility it offers in terms of metal variation, ligand variation, coordination geometry, oxidation state, stabilization of organic fragments and electron donating/withdrawing capabilities of the metal or ligand. The ligands attached to the metal atom influence the donor-acceptor nature of the metal atom. Electron-withdrawing ligands coordinated to the metal increase the electronegativity of the metal; whereas electron-donating ligands decrease the electronegativity of the metal. A large difference in the electronegativity between metal and ligand introduces large polarities in the complex molecular system. Further, even greater intramolecular interactions are expected in metal complexes that possess conjugated ligands because of the effective overlapping of the π -electron orbitals of the ligand with the metal ion π -orbitals. By

coordinating a central metal atom with different ligands, it is possible to introduce a chiral centre making the complex noncentrosymmetric. Keeping in mind these architectural flexibility provided by the ligands, one can design a metal complex to tailor the NLO properties to a maximum level.

Among the coordinated complexes, metal complexes of Schiff base ligands are being extensively explored mainly because of their excellent chelating ability towards a large number of metal ions. This is mainly due to the lone pair of electrons on the sp^2 hybridized orbital of nitrogen atom of azomethine group. Depending on the substituent groups, Schiff base can behave as a monodentate, bidentate or even tridentate ligand. Further, substitution of the R and R' group of Schiff base ($RCH=NR'$) with extended conjugation of π -electrons, like aryl groups, leads to an enhancement of NLO activity.

The N_2O_2 Schiff base ligands can be used for the preparation of NLO compounds, owing to their synthetic versatility relative to the introduction of electron donor/acceptor moieties and creation of extensive π -delocalization to introduce large electron asymmetry (Freire and de Castro 1998). Since they can coordinate with several transition metal ions, further fine-tuning of the NLO responses is possible as the metal centers can impart important structural and electronic properties to the organic ligands (Coe 2004). Also, thiosemicarbazones $\{R^1R^2C=N^3-N^2H-C(=S)-NR^3R\}$ possess several donor atoms and generally bind to metals via N^2 , N^3 , S donor atoms forming four membered or five membered rings. Because of the strong chelating ability of these ligands towards metal ions like Fe, Cu and Ni, they are of great biological importance. The presence of extensive π -conjugation in the aromatic ring can also lead to strong hyperpolarizability. Ligands like 1,10-phenanthroline and triphenylphosphine display strong π -acceptor character. When they are coordinated to any metal ion which acts as electron donor, it will lead to acceptor-donor-acceptor type of electronic transitions between ligands and metals. Further, if these ligands are tagged to an ionic liquid, then due to the charge separation in the ionic liquid, an enhancement in the optical property of the metal complex is expected.

The main purpose of the present research work is to design new molecular systems with transition metal ions as the central metal ion and Schiff base derivatives as ligands to yield an affordable and useful NLO material. Consequently, the present work has been focused on the following objectives:

- To design and synthesize organic chromophores with extensive π -conjugation and/or donor-acceptor groups.
- To synthesize metal [Fe(II), Co(II), Ni(II), Cu(I), Cu(II), Zn(II)] complexes with ligand/its derivatives.
- To characterize the synthesized ligands and complexes by analytical and spectral methods.
- To study the nonlinear optical response of the newly synthesized complexes by using open aperture Z-scan and Optical Kerr gate (for selected complex) techniques.

CHAPTER 3

SYNTHESIS, CHARACTERIZATION AND NONLINEAR OPTICAL STUDIES OF Fe(II), Ni(II) AND Zn(II) SCHIFF-BASE COMPLEXES

Abstract

Schiff base complexes of N,N'-bis(2-hydroxynaphthalidene)phenylene-1,2-diamine ligand with metal M (M= Ni(II), Zn(II) and Fe(II)) have been synthesized and characterized by their UV-Vis, FTIR, NMR, elemental analysis and magnetic susceptibility measurements. Nonlinear optical measurements of the complexes carried out at 532 nm using nanosecond laser pulses show appreciable third-order optical nonlinearity. Among the samples, nickel complex displayed maximum optical limiting capability. Being optical limiters, these complexes have potential applications in optoelectronics and photonics.

3.1 INTRODUCTION

Of late, much interest has been aroused in the exploration of new materials with large third-order optical nonlinearities, not only from the perspective of understanding nonlinear optical (NLO) phenomena (Marder et al.1991, Bredas 1994) but also from their potential technological applications related to telecommunications, optical computing, optical storage and optical information processing (Zyss 1994, Dalton 1995, Marks and Ratner 1995). New nonlinear optical (NLO) materials are essential for the advancement of various optoelectronic and nano technologies, e.g. optical communications, high speed electro-optical information processing, light modulation, light switching and high density data storage. In the past nonlinear optical research primarily focused on purely inorganic semiconductors, organic molecules and conjugated polymers (Huang 1998, Burland et al.

1994). However, after the report by Green et al. (1987), in which good second-harmonic generation (SHG) efficiency was revealed for a ferrocenyl derivative, attention has been paid to metal complexes also as potential NLO materials (Long 1995, Whittall et al. 1998). Thus various classes of metal complexes and organometallic compounds (Renx 2008) have systematically been explored for new and optimized NLO materials. Early and more recent review articles on NLO of metal complexes indicate the breadth of active research in this field. Despite these efforts, the vast potential of organometallic and coordination complexes as NLO materials still remain largely untapped. Moreover, the design and preparation of new NLO active materials required for practical devices is still a challenging task (Miguel et al. 1999, Sagayaraj and Selvakumar 2009, Yu et al. 2006).

In organic compounds the increase of the optical response is not only due to the high level of π -conjugated charge transfer but also due to the increase of conjugation length which plays a determining role in the delocalisation of π -electrons under light excitation. As a result, the values of $\chi^{(3)}$ and β increase with the number of branches of the molecule (Fuks-Janczarek et al. 2002). Proceeding to organometallics, one hopes to combine the advantages of organic molecules which possess design flexibility and fast response with those of inorganic salts which possess properties of mechanical strength and thermal stability. The flexibility available for organometallics like metal variation, ligand variation, coordination geometry, oxidation state, electron donating/withdrawing capabilities of the metal or ligand and stabilization of unstable organic fragments can all, in principle, be modified to optimize targeted responses (Pignatello et al. 1994, Whittall 1998). In particular, transition metal Schiff base complexes have attracted considerable attention recently since metal ions can play a central role in many fields such as materials research, photonics and biology (Powell and Humphrey 2004). Schiff bases are widely used as analytical reagents because they allow simple and inexpensive determination of several organic and inorganic substances (Cimernman 1997). They also form stable complexes with metals that perform an important role in biological systems (Raptopoulou

et al. 1998). Schiff bases derived from salicylaldehyde are well known as polydentate ligands (Holm et al. 1966) coordinating as deprotonated or neutral forms. There are many reports available for metal complexes with bidentate or tridentate ligands.

In this chapter, the synthesis, characterization and NLO measurements of metal M (M = Fe(II), Ni(II) and Zn(II)) complexes of Schiff base derived from 1,2-diaminobenzene and 2-hydroxynaphthaldehyde have been reported. Their nonlinear optical property has also been studied using Z-scan technique with a discussion on the nonlinear mechanism adapted by the complexes.

3.2 EXPERIMENTAL

3.2.1 Materials

All the chemicals used were of analytical grade. Solvents were purified and dried according to standard procedure (Vogel 1989). NiCl₂·6H₂O was purchased from Merck, ZnCl₂ and FeCl₂·4H₂O were procured from Nice chemicals and were used without further purification.

3.2.2 Physical measurements

Electronic spectra of the complexes in 200-800 nm range were measured on a GBC UV-Vis double beam spectrophotometer in N,N-dimethylformamide solution. FT-IR spectra were recorded on a Thermo Nicolet Avatar FT-IR spectrometer as KBr powder in the frequency range 400-4000 cm⁻¹. The C, H, N and S contents were determined by Thermoflash EA1112 series elemental analyzer. ¹H NMR spectra were recorded in Bruker AV-400 instrument using TMS as internal standard. Thermal analysis, differential thermal analysis (DTA) and thermogravimetric analysis (TGA) measurements were recorded on SII-EXSTAR6000-TG/DTA6300 thermal analyzer with

heating rate of $10^{\circ}\text{Cmin}^{-1}$. Magneto-chemical measurement was recorded on a Sherwood Scientific instrument.

3.2.3 Z-scan Measurement

Open-aperture Z-scan measurements were performed to determine the nonlinear transmission of laser light through the samples. The Z-scan is a widely used technique developed by Sheik Bahae et al. (1990) to measure optical nonlinearity of materials, and the open aperture Z-scan gives information about the nonlinear absorption coefficient. Here a laser beam which is spatially Gaussian is focused using a lens and passed through the sample. The beam's propagation direction is taken as the Z-axis, and the focal point is taken as $Z = 0$. The beam will have maximum energy density at the focus, which will symmetrically reduce towards either side for the positive and negative values of Z. The experiment was done by placing the sample in the beam at different positions with respect to the focus (different values of Z), and measuring the corresponding light transmission. The graph plotted between the sample position Z and the normalized transmittance of the sample T (norm.) (transmission normalized to the linear transmission of the sample) is known as the Z-scan curve. For a Gaussian beam, each Z position corresponds to an input laser energy density of $F(z) = 4\sqrt{\ln 2}E_{in} / \pi^{3/2}\omega(z)^2$, and intensity of $I(z) = F(z)/\tau$, where E_{in} is the input laser pulse energy, $\omega(z)$ is the beam radius, and τ is the laser pulse width. The curve drawn between $F(z)$ (or $I(z)$) and T (norm.) is known as the nonlinear transmission curve. The nonlinear absorption coefficient of the sample can be numerically calculated either from the Z-scan curve or the nonlinear transmission curve.

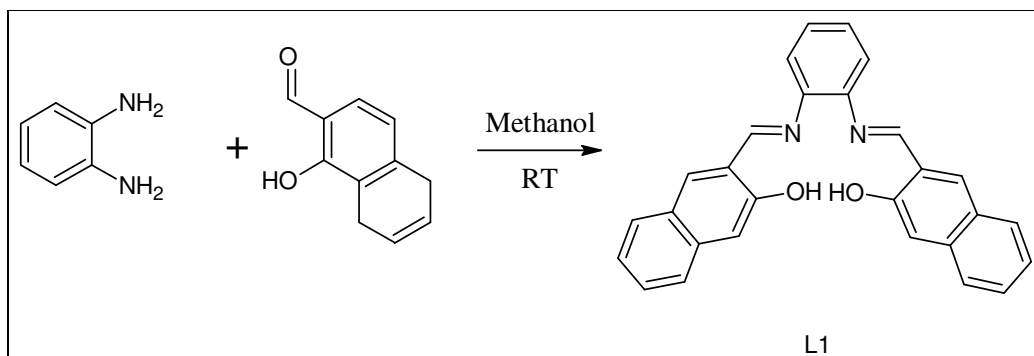
The third-order optical nonlinearity of complexes in DMSO, at the concentration of 2.5mmol/L, was measured by Z-scan technique. At this concentration the solutions show a linear transmission of 75%, 60% and 70% respectively for Fe(II), Ni(II) and Zn(II) complexes at the excitation wavelength of 532 nm.

3.3 SYNTHESIS OF METAL COMPLEXES

3.3.1 Synthesis of ligand (L1)

Methanolic solution of 1, 2-diaminobenzene (0.138g, 1.2mmol) was added to a methanolic solution of 2-hydroxynaphthaldehyde (0.108g, 0.63 mmol). The mixture was stirred for 3 hours in room temperature to give orange yellow precipitate. The precipitate was washed thoroughly with ethanol and recrystallized using chloroform. The synthetic route for the ligand is given in Scheme 3.1.

Yield: (86%). M.P: 231°C Anal. Calc. for $C_{28}H_{20}N_2O_2$ (416.47): C, 80.75; H, 4.84; N, 6.73. Found: C, 80.51; H, 4.77; N, 6.65%. IR (KBr, cm^{-1}): 3658 (m), 1617(m), 1323(m), 1083(m), 750(m), 826(m). 1H NMR (400 MHz, DMSO): 9.68 (d, 2H)(OH), 8.51 (d, 2H)(-C-N-), 7.96-7.04 (m, 16H)(aromatic), UV-Vis: λ_{max} (nm) intraligand interactions: 320, 400.



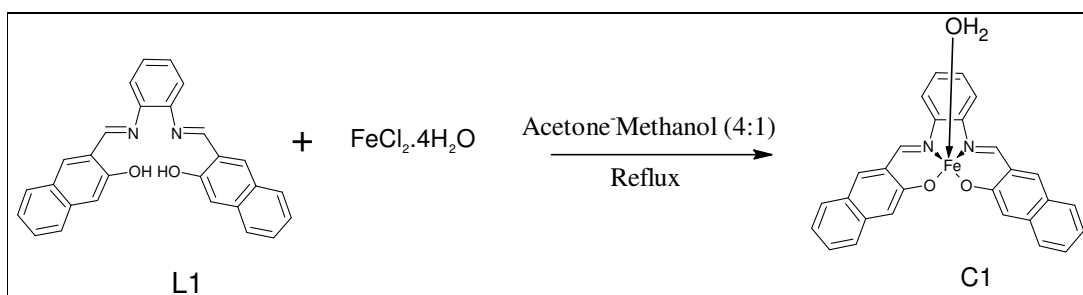
Scheme 3.1 Synthetic scheme for **L1**

3.3.2 Synthesis of iron complex (C1)

$FeCl_2 \cdot 4H_2O$ (0.237g, 1.2mmol) in methanol was added to the ligand (**L1**) (0.497g, 1.2mmol) in minimum quantity of (4:1) acetone-methanol solvent mixture. The reaction

mixture was refluxed at 80°C for 2 hours. The resulting dark blackish precipitate was filtered and washed with methanol followed by hexane and dried in *vacuo*. The synthetic method for metal complex **C1** is given in Scheme 3.2.

Yield: (70%). M.P: > 330 °C. Anal. Calc. for C₂₈H₂₂FeN₂O₄ (488.31): C, 68.87; H, 4.13; N, 5.74. Found: C, 68.62; H, 4.05; N, 5.65%. IR (KBr, cm⁻¹): 3450(m), 1595(s), 750(m), 830(w), 554(m), 421(m). UV-Vis: λ_{max}(nm) intraligand interactions: 332, 415, d→d forbidden transition: 466.



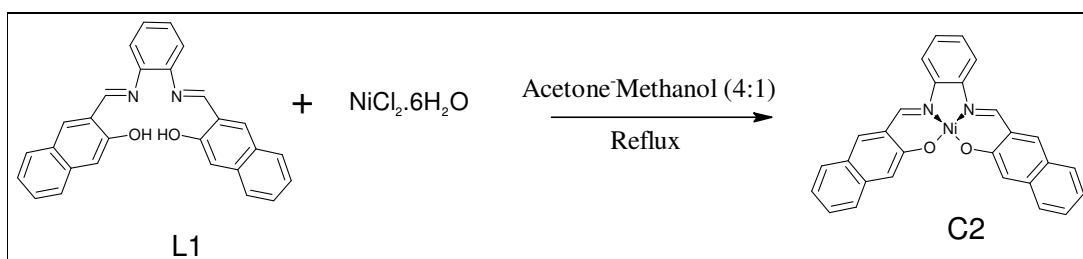
Scheme 3.2 Synthetic scheme for **C1**

3.3.3 Synthesis of nickel complex (C2)

NiCl₂·6H₂O (0.288g, 1.2mmol) in methanol was added to the ligand (**L1**) (0.497g, 1.2mmol) in minimum quantity of (4:1) acetone-methanol solvent mixture. The reaction mixture was refluxed at 80°C for 2 hours. The resulting bright red coloured precipitate was filtered, washed with methanol followed by hexane and dried in *vacuo*. The synthetic method for metal complex **C2** is given in Scheme 3.3.

Yield: (76%). M.P: > 330 °C. Anal. Calc. for C₂₈H₂₀N₂NiO₂ (473.14): C, 71.08; H, 3.83; N, 5.92. Found: C, 70.97; H, 3.80; N, 5.86%. IR (KBr,cm-1): 1607(s), 1317(m), 750(m),

830(w), 565(m), 423(m). ^1H NMR (400MHz, DMSO): 8.55(d, 2H)(-C-N-), 7.97-7.04 (m,16H)(aromatic), UV-Vis: λ_{max} (nm) intraligand interactions: 330, 387, d→d forbidden transition: 484.

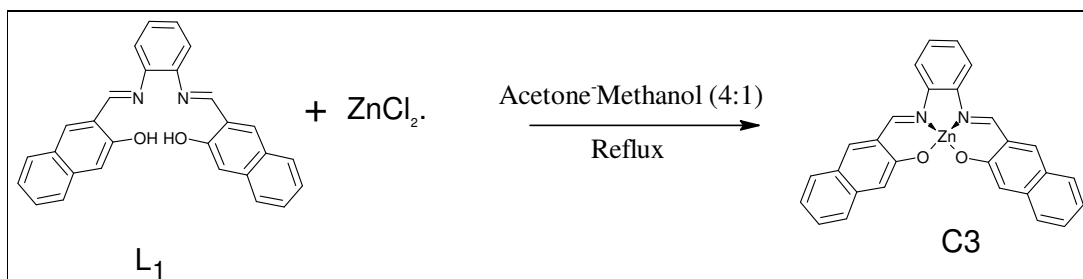


Scheme 3.3 Synthetic scheme for **C2**

3.3.4 Synthesis of zinc complex (C3)

ZnCl_2 (0.194g, 1.2mmol) taken in methanol was added to the ligand (**L1**) (0.497g, 1.2mmol) taken in minimum quantity of (4:1) acetone-methanol solvent mixture. The reaction mixture was refluxed at 80°C for 2 hours. The resulting orange coloured precipitate was filtered, washed with methanol followed by hexane and dried in *vacuo*. The synthetic method for metal complex **C3** is given in Scheme 3.4.

Yield: (80%). M.P: $> 330^\circ\text{C}$. Anal. Calc. for $\text{C}_{28}\text{H}_{20}\text{N}_2\text{O}_2\text{Zn}$ (479.86): C, 70.08; H, 3.78; N, 5.84. Found: C, 69.92; H, 3.71; N, 5.80%. IR (KBr, cm^{-1}): 1591(s), 1353(s) 755(m), 832(m), 551(m), 463(m). ^1H NMR (400 MHz,DMSO): 8.54 (d,2H)(-C-N-), 7.97-6.97 (m,16H)(aromatic). UV-Vis: λ_{max} (nm) intraligand interactions: 343.



Scheme 3.4 Synthetic scheme for **C3**

3.4 RESULTS AND DISCUSSION

The analytical data showed that the observed values were in good agreement with the theoretical values (Table 3.1).

Table 3.1 Analytical data of Schiff base complexes

Complex /Ligand	Decomp temp (°C)	% Found (Theoretical)			UV-Vis Data, λ_{\max} (nm)	
		C	H	N	Intra ligand Transition	d-d Transition
L1	231	80.51 (80.75)	4.77 (4.84)	6.65 (6.73)	320,400	-
C1	>330	68.62 (68.87)	4.05 (4.13)	5.65 (5.74)	332,415	466
C2	>330	70.97 (71.08)	3.80 (3.83)	5.86 (5.92)	330,387	484
C3	>330	69.92 (70.08)	3.71 (3.78)	5.80 (5.84)	343	-

3.4.1 FT-IR Spectra

The FT-IR spectra of complexes **C1-C3** show that the coordination geometry around Fe(II), Ni(II) and Zn(II) ions are same for all the complexes. The characteristic stretching frequencies of ligand and complexes are shown in Table 3.2. FT-IR absorption band due to $\nu(\text{C}=\text{N})$ of the free ligand appears in the region $1610\text{-}1620\text{ cm}^{-1}$. For all complexes, $\nu(\text{C}=\text{N})$ undergoes a negative shift by $5\text{-}20\text{ cm}^{-1}$ indicating the coordination of azomethine nitrogen to the metal (Prabhakaran et al. 2005, Kovacic 1967). The band in the region $1315\text{-}1330\text{ cm}^{-1}$ which is assigned to phenolic $\nu(\text{C}-\text{O})$ in the free ligand, is shifted to higher wave number in the complexes suggesting the coordination of phenolic oxygen to metal ion (Prabhakaran et al. 2005, Philip 2004, Soliman and Mohamed 2004). The bands around 550 cm^{-1} and 470 cm^{-1} in the complexes are assigned to $\nu(\text{M}-\text{O})$ and $\nu(\text{M}-\text{N})$ respectively (Karvembu et al. 2008). In Fe(II) complex, the observed band in the region 3450 cm^{-1} is assigned to $\nu(\text{O}-\text{H})$ of coordinated water. FT-IR spectra of ligand, iron, nickel and zinc complexes are shown in Fig. 3.1 to Fig. 3.4 respectively.

Table 3.2 Infrared spectral data (cm^{-1}) for ligands and its Schiff base complexes

Ligand/Complex	$\nu(\text{C}=\text{N})$	$\nu(\text{C}-\text{O})$	$\nu_{(\text{M}-\text{O})}$	$\nu_{(\text{M}-\text{N})}$
L1	1612	1367	-	-
C1	1595	1338	554	421
C2	1607	1317	565	423
C3	1591	1322	551	463

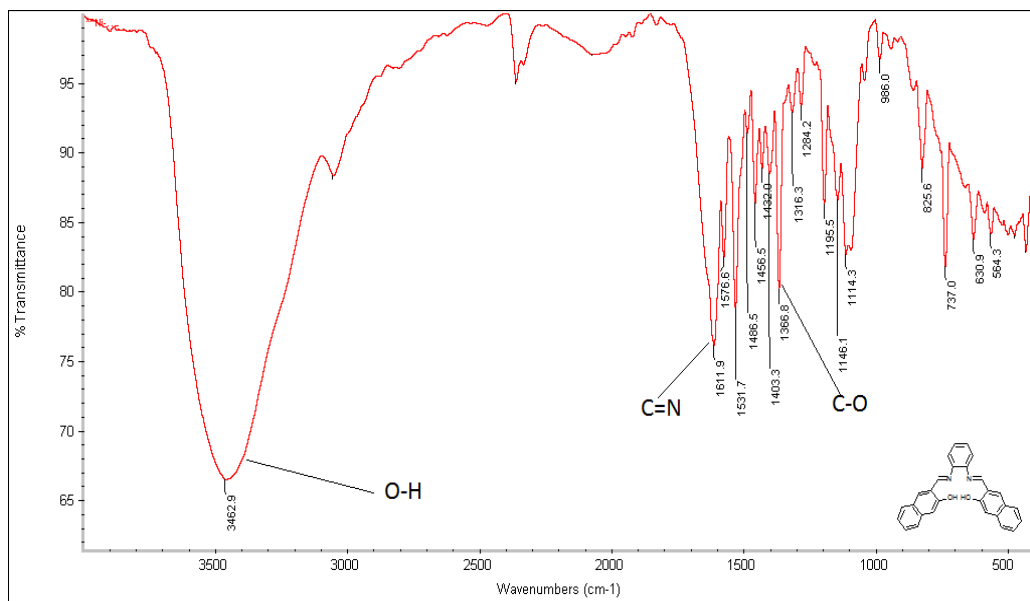


Fig. 3.1 IR spectrum of L1

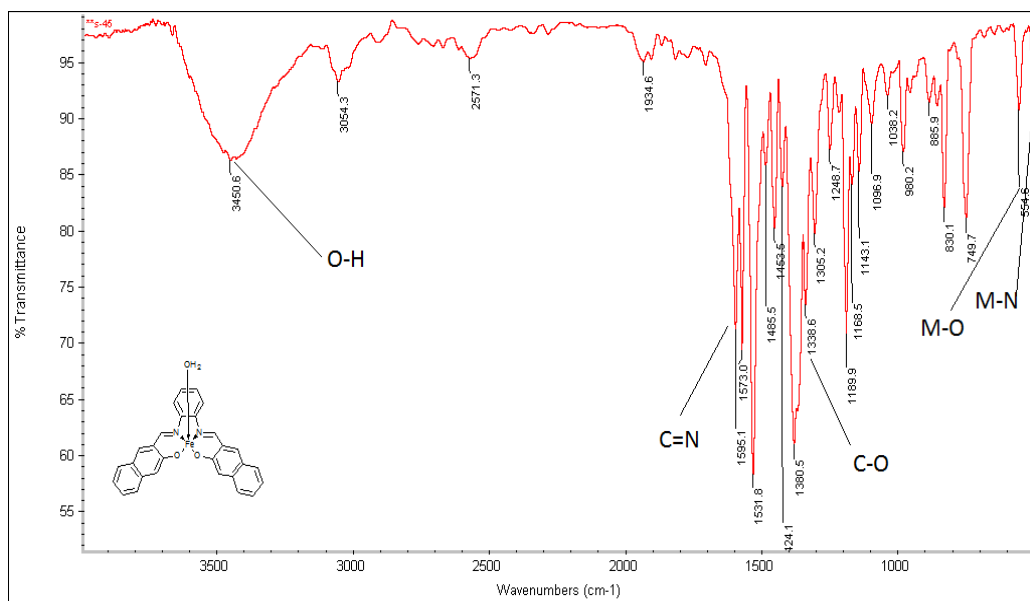


Fig. 3.2 IR spectrum of C1

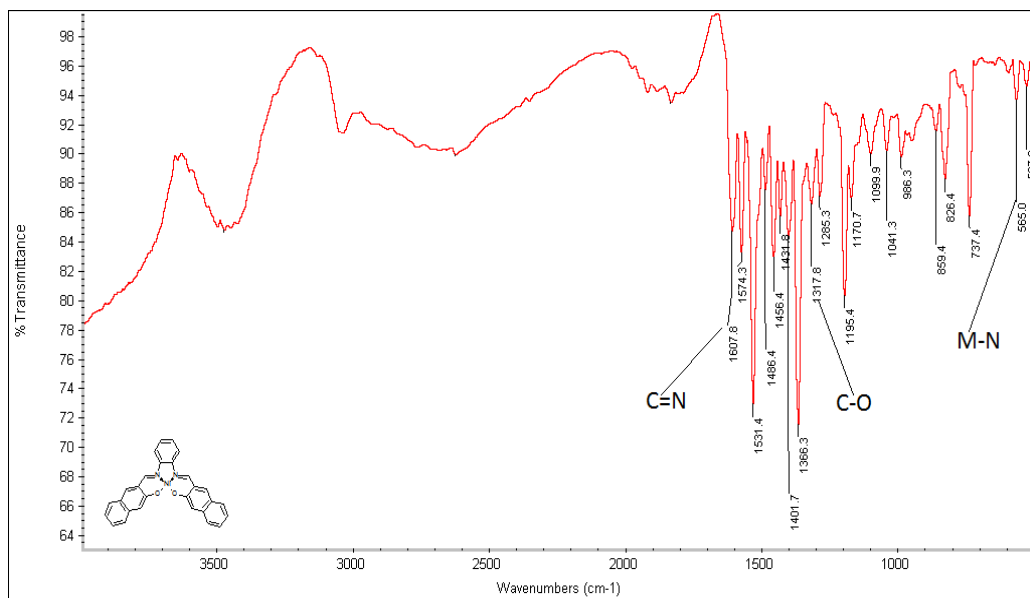


Fig. 3.3 IR spectrum of C2

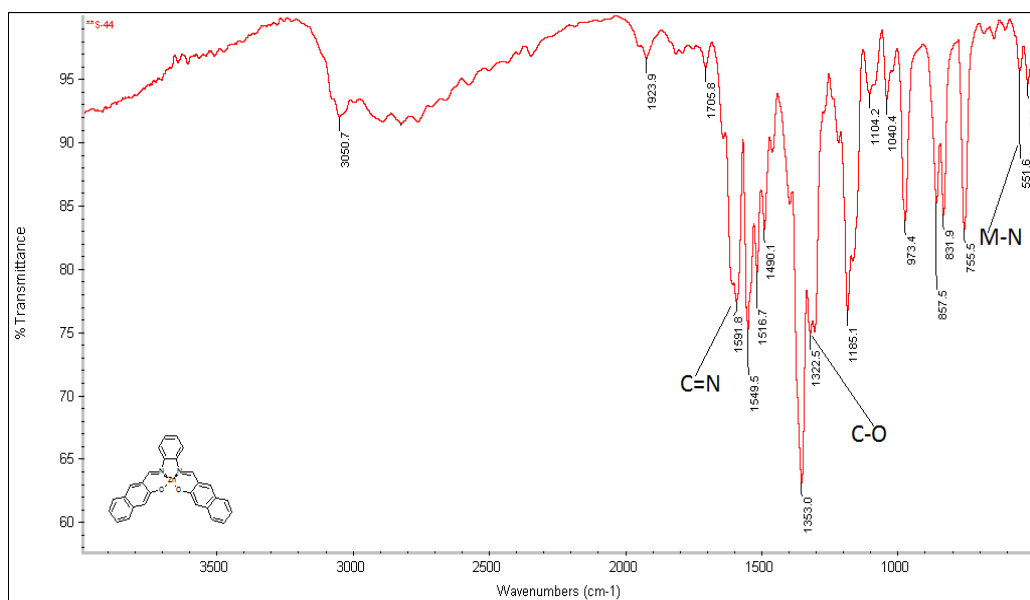


Fig. 3.4 IR spectrum of C3

3.4.2 ¹H-NMR spectra

The ¹H NMR spectra of ligand, Ni(II) and Zn(II) complexes exhibit a multiplet around 6.9–7.9 ppm which has been assigned to the protons of phenyl groups present in Schiff base ligand. A peak observed at 10.31 ppm in the complex has been assigned to azomethine proton (–C=N–) (Angela Sorkau et al. 2005, Vettaikaranpudur et al. 2005, Balasubramanian et al. 2007). In ligand, resonance due to phenolic hydrogen observed at 13.61 ppm is absent in complexes indicating the deprotonation of Schiff base (Table 3.3). ¹H-NMR shifts of ligand and Ni(II) complex are shown in Fig 3.5 and Fig 3.6 respectively.

Table 3.3 ¹H-NMR spectral details of ligands and complexes

Complex/Ligand	Position (δ)
L1	13.61 (d, 2H)(OH), 10.11 (d, 2H)(-C-N-), 7.96-7.04 (m, 16H)(aromatic),
C1	Paramagnetic.
C2	10.32 (d, 2H)(-C-N-), 7.94-7.04 (m, 16H)(aromatic)
C3	10.31 (d, 2H)(-C-N-), 7.97-6.97 (m, 16H) (aromatic)

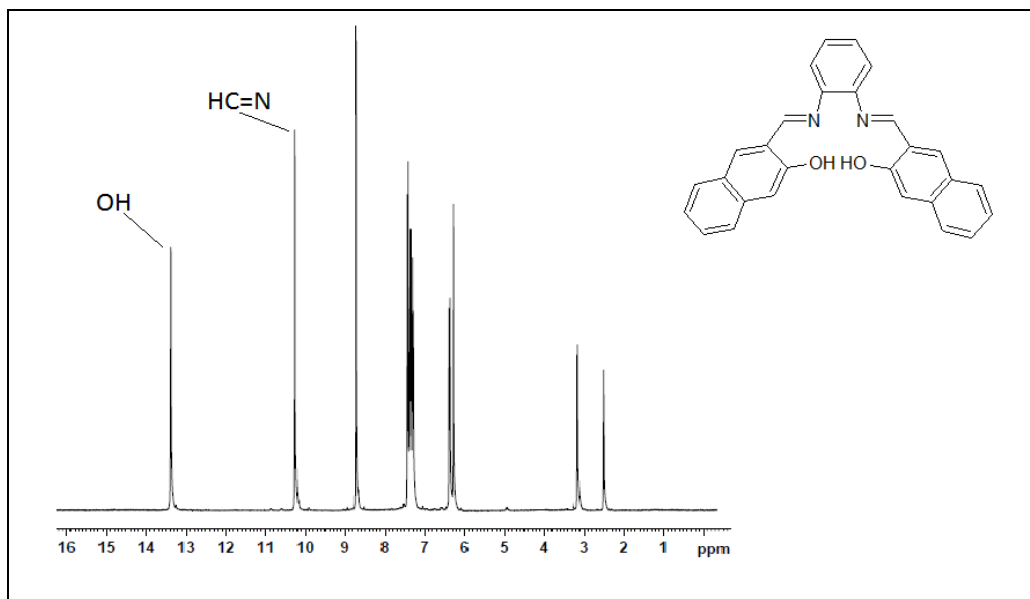


Fig. 3.5 ¹H-NMR spectrum of **L1**

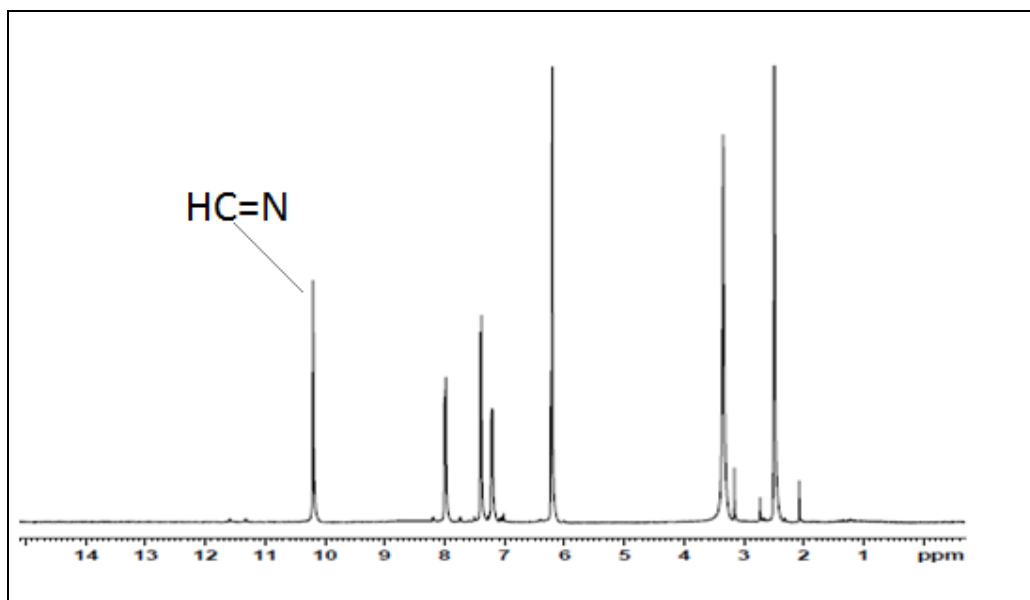


Fig. 3.6 ¹H-NMR spectrum of **C2**

3.4.3 Thermogravimetric analysis

The TGA and DTA curve for Fe(II) complex shows a peak around 200°C which is due to coordinated water molecule. An endothermic peak in DTG further supports this. Thermo gravimetric analysis (Fig. 3.7) results show that Fe(II) complex contains one coordinated water molecule. The TG curves clearly indicate that the complex loses no weight at all below 180 °C and then loses 3.2% weight (calculated from % TG curve) in the temperature range of about 180 °C - 230 °C. This matches well with the theoretical weight loss (~3.68%) of one water molecule. Moreover, according to Nikolaev et al. (1969) water eliminated above 150 °C can be considered as coordinated water. This confirms the presence of one coordinated water molecule in the Fe(II) complex. The complex is thermally stable up to 300 °C and undergoes complete decomposition by about 550 °C.

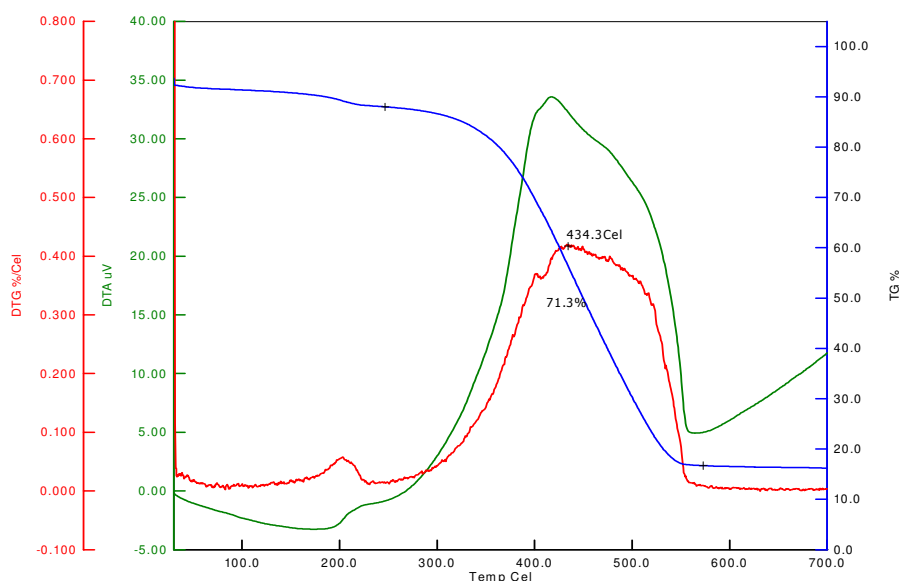


Fig. 3.7 Thermal analysis of C1

3.4.4 UV-Visible spectra

The UV–Visible spectral data of the ligand and complexes recorded in dry DMSO are depicted in Fig. 3.8. The values of the electronic spectra of ligand and complexes (C1-C3) are given in Table 3.1. Bands in the region 250-350 nm correspond to intra ligand transition whereas the region 420-490 nm corresponds to forbidden $d-d$ transitions.

The electronic spectra of Ni(II) complex with an electronic configuration of d^8 shows new absorption bands in the visible region at 484 nm which is attributed to the electronic transition $^1A_{1g} \rightarrow ^1A_{2g}$. This assignment infers that Ni(II) complexes are square planar (Lever 1968). The electronic configuration of Zn(II) complex is d^{10} in which the metal ions are diamagnetic thereby confirming the absence of any $d-d$ electronic transitions.

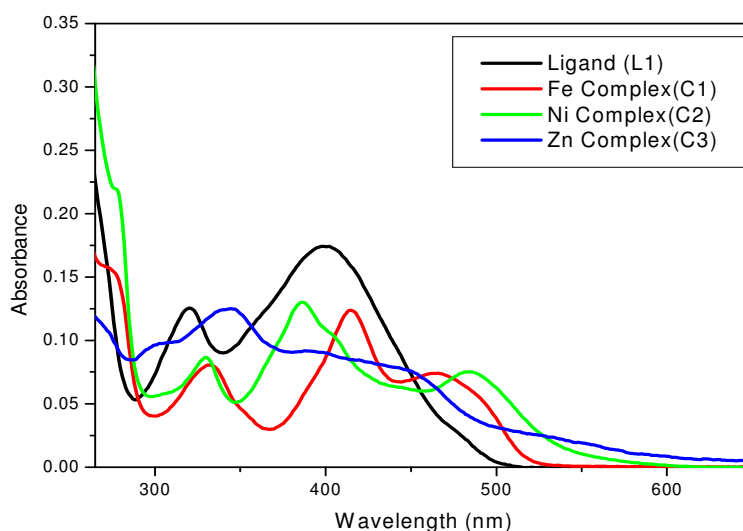


Fig 3.8 Linear absorption spectra of Ligand L1 and complexes C1-C3

3.5 NONLINEAR OPTICAL MEASUREMENTS

In our experiment, samples taken in 1 mm cuvettes were irradiated by laser pulses of 7 nanoseconds width at the wavelength of 532 nm, available from an Nd:YAG laser (Quanta Ray, Spectra Physics) provided with the second harmonic option. The laser beam is spatially Gaussian, as found from a knife-edge measurement (Fig. 3.9). The beam diameter (FWHM) is found to be 7.84 mm. The Rayleigh range in our experiment was 1.9 mm. The Z-scan and nonlinear transmission curves are shown in Fig. 3.10 to Fig. 3.12. As seen, the transmission is reduced at higher intensities, showing that the samples behave as optical limiters. Maximum nonlinearity was found in nickel complex (C2) and minimum in iron complex (C1). It is well known that optical limiters have potential applications in protecting human eyes and other light sensitive devices like cameras from accidental exposure to intense light.

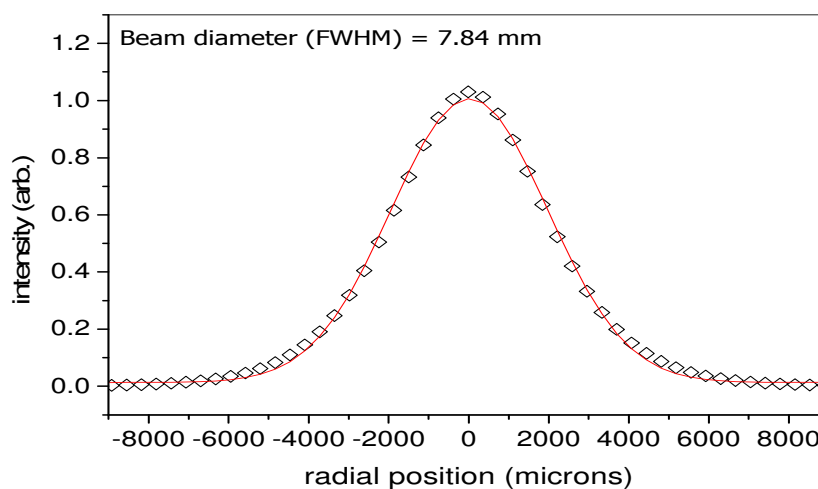


Fig. 3.9 Spatial profile of the Nd:YAG laser beam used for the Z-scan experiment, measured using the knife-edge technique. The solid line is a Gaussian fit to the measured data.

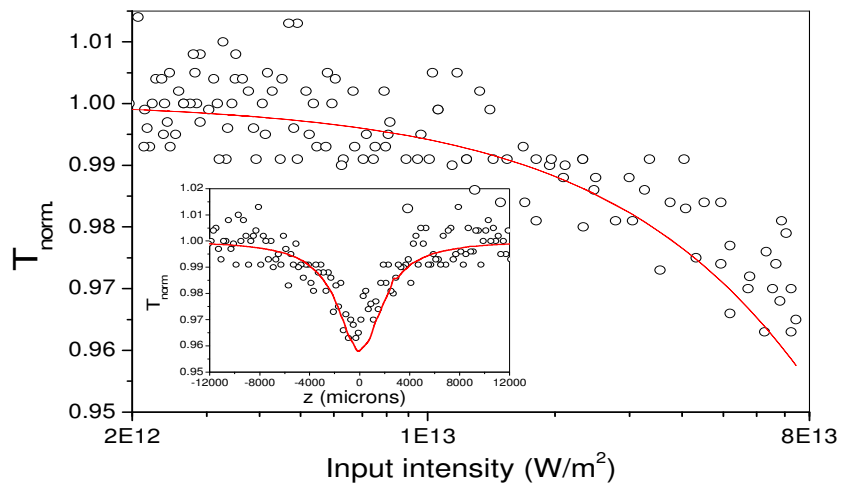


Fig. 3.10 Nonlinear transmission curve of C1. Inset shows the open aperture Z-scan curve. Linear transmission of the sample (corresponding to T (norm.) = 1) is 75%. Circles are data points while solid curves are numerical fits using equation 3.1.

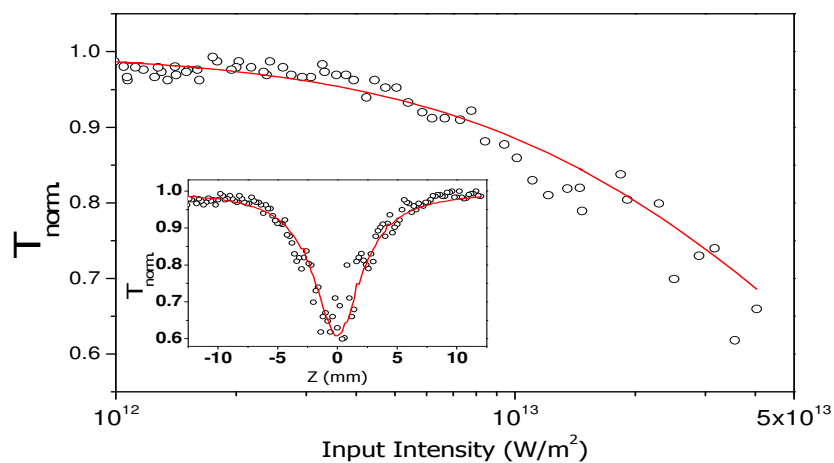


Fig. 3.11 Nonlinear transmission curve of **C2**. Inset shows the open aperture Z-scan curve. Linear transmission of the sample (corresponding to $T(\text{norm.}) = 1$) is 60%. Circles are data points while solid curves are numerical fits using equation 3.1.

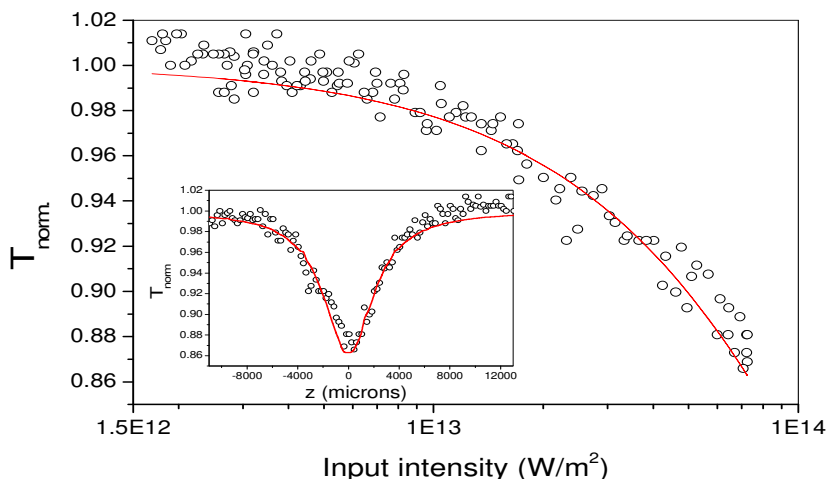


Fig. 3.12 Nonlinear transmission curve of **C3**. Inset shows the open aperture Z-scan curve. Linear transmission of the sample (corresponding to $T(\text{norm.}) = 1$) is 70%. Circles are data points while solid curves are numerical fits using equation 3.1.

The nonlinear absorption of nanosecond pulses is generally explained by a five-level model (Yim et al. 1998, Giuliano 1967). It consists of S_0 as the ground state, S_1 and S_2 as the first and second excited singlet states and T_1 and T_2 as the first and second excited triplet states, respectively. Each electronic state has many vibrational levels. Exposure of the molecule to 532nm, 7ns laser pulses may lead to excitation from ground state S_0 to one of the vibrational levels of the first excited singlet state S_1 [$S_1 \leftarrow S_0(v=0)$] by absorbing two photons simultaneously. This process is known as two-photon absorption (2PA) and is characterized by an absorption cross section σ_0 . From state S_1 , the molecule may further get excited to the higher excited state S_2 [$S_2 \leftarrow S_1$]. The singlet

transition [$S_2 \leftarrow S_1$] does not deplete the population in S_1 appreciably as atoms excited to S_2 decay to S_1 ($v=0$) within picoseconds. However, they can be transferred from S_1 ($v=0$) to a lower triplet state T_1 ($v=0$) through intersystem crossing from where transitions to a higher triplet state T_2 can occur (Poornesh et al. 2010, Yim et al. 1998). The molecules in the excited state S_1 can be further excited to the higher energy state S_2 and similarly from state T_1 to T_2 with absorption cross section of σ_S and σ_T , respectively. Such a process is called excited state absorption (ESA). In particular, if singlet excited state S_1 or triplet state T_1 or both have larger absorption cross section than the ground state S_0 , then the absorption mechanism is termed reverse saturable absorption (RSA). Since we have used nanosecond laser pulses in all our experiments, the triplet-triplet transitions are expected to make significant contribution to the observed nonlinear absorption. Moreover, a positive nonlinear absorption coefficient implies that RSA is the dominant mechanism for absorption (Zhang et al. 2007).

It was found that numerically, a two-photon absorption (2PA) type process gives the best fit to the obtained open aperture Z-scan data. In the present context, strong two-step excited state absorption also will happen concurrently with genuine 2PA and hence the effect is an effective 2PA process. The data obtained are fitted to the nonlinear transmission equation 3.1 for a two-photon absorption process, given by (Sutherland 1996).

$$T = \left((1-R)^2 \exp(-\alpha L) / \sqrt{\pi q_0} \right) \int_{-\infty}^{+\infty} \ln \left[\sqrt{1 + q_0 \exp(-t^2)} \right] dt \quad \dots\dots\dots (3.1)$$

where T is the sample transmission given by $T(\text{norm.}) \times$ linear transmission of the sample and L and R are the length and surface reflectivity of the sample respectively. α is the linear absorption coefficient. q_0 is given by $\beta(1-R)I_0L_{\text{eff}}$, where β is the effective 2PA coefficient, and I_0 is the on-axis peak intensity. L_{eff} is given by $\int_0^L \exp(-\alpha z) dz = (1 - \exp(-\alpha L)) / \alpha$. The calculated values of the effective 2PA coefficient for synthesized complexes are given in Table 3.4. For comparison, under similar excitation conditions, NLO

materials like Cu nanocomposite glasses had given effective 2PA coefficient values of 10^{-10} to 10^{-12} m/W (Karthikeyan et al. 2008), bismuth nanorods gave 5.3×10^{-11} m/W (Sivaramakrishnan 2007) and CdS quantum dots gave 1.9×10^{-9} m/W (Kurian 2007) respectively. This shows that the present samples have a comparable optical nonlinearity, so that they can find potential applications in optical limiting devices. It may be worthwhile here to consider whether over and above the effective 2PA mechanism, any thermal effect is contributing to the observed optical limiting behavior. In general, when excited with laser pulses of nanoseconds duration, the possibility of sample heating cannot be excluded. However, this will contribute to the optical limiting action only if substantial nonlinear scattering takes place in the system. We measured nonlinear scattering using a photodiode attached at an angle to the beam path in front of the sample, but it did not give any appreciable signal. Another aspect of the experiment is that since we used detectors having large apertures, even if the sample shows any nonlinear refraction it will not contribute to the observed optical limiting behavior. Therefore it is clear that the nonlinearity arises mostly from two-step excited state absorption in the system, which is the cause behind the effective 2PA mechanism.

Table 3.4 2PA coefficient β of Schiff base complexes

Complex	2PA coefficient β (mW^{-1})
Iron Complex (C1)	2×10^{-12}
Nickel Complex (C2)	5×10^{-11}
Zinc Complex (C3)	8×10^{-12}

CHAPTER 4

SYNTHESIS, CHARACTERIZATION AND THIRD-ORDER NONLINEAR OPTICAL STUDIES OF Co(II), Ni(II) AND Zn(II) - 3,4- DIAMINOBENZOPHENONE SCHIFF BASE COMPLEXES

Abstract

The synthesis, structural characterization and nonlinear optical properties of metal M [M = Co(II), Ni(II) and Zn(II)] complexes with 3,4-diaminobenzophenone and 2-hydroxynaphthaldehyde ligands are reported in this chapter. Nonlinear optical (NLO) measurements were achieved by Z-scan method using nanosecond laser pulses at 532 nm to probe the role of M[ONNO] chromophores and the π -conjugation of the aromatic ring in the nonlinearity. All the complexes exhibit optical limiting behavior due to effective two-photon absorption (2PA). The 2PA coefficient was found to be highest for nickel complex. A rationalization of the structure and the nonlinear behavior of the title compounds have been provided. Based on their nonlinear properties, the complexes have a fair chance to be employed as optical limiting materials.

4.1 INTRODUCTION

Schiff base complexes have remained an important and popular area of research due to their simple synthesis and versatility. Among the Schiff base ligands, the tetradentate Schiff base ligands are known to form stable complexes with different metal cations (Akine and Nabeshima 2009). Several metal chelates of the ONNO donor class of Schiff bases have received considerable attention due to their potential use as catalysts (Gupta et al. 2009, Zhang et al. 2010), inhibitors (Soltani et al. 2010) and antifungal

(Negm et al. 2010), antibacterial (Liu et al. 2009), antitumour (Jin et al. 2005) and herbicidal (Samadhiya and Halve 2001) activities.

Further, interest in the synthesis, design and characterization of the transition metal complexes of unsymmetrical Schiff base ligands has increased pace in the recent years. Unsymmetrical Schiff base ligands have clearly offered many advantages over their symmetrical counterparts in the elucidation of the composition and geometry of the metal ion binding sites in the metallo-proteins and the enzymes and the selectivity of the natural systems with synthetic materials (Asadi and Khaha 2010, Daneshvar et al. 2003). Recently, this class of compound has also attracted much attention in the field of optoelectronic technologies for their large non linear responses (Gradinaru et al. 2007).

In this chapter, the synthesis, characterization and NLO measurements of metal M (M = Co(II), Ni(II) and Zn(II)) complexes of Schiff base derived from 3,4-diaminobenzophenone and 2-hydroxynaphthaldehyde have been reported.

4.2 EXPERIMENTAL

4.2.1 Materials

All the chemicals used were of analytical grade. Solvents were purified and dried according to standard procedure (Vogel 1989). Ni(OCOCH₃)₂·4H₂O, Co(OCOCH₃)₂·4H₂O, Zn(OCOCH₃)₂·4H₂O, 3,4-diaminobenzophenone and 2-hydroxynaphthaldehyde were purchased from Sigma Aldrich and were used without further purification.

4.2.2. Physical measurements

The C, H, N and S contents were determined by Thermoflash EA1112 series elemental analyzer. FT-IR spectra were recorded on a Thermo Nicolet Avatar FT-IR spectrometer as KBr powder in the frequency range 400-4000 cm⁻¹. ¹H-NMR spectra

were recorded in Bruker AV-400 instrument using TMS as internal standard. Electronic spectra of the complexes in the 200-800 nm range were measured on a GBC UV-Vis double beam spectrophotometer in N,N-dimethylformamide solution.

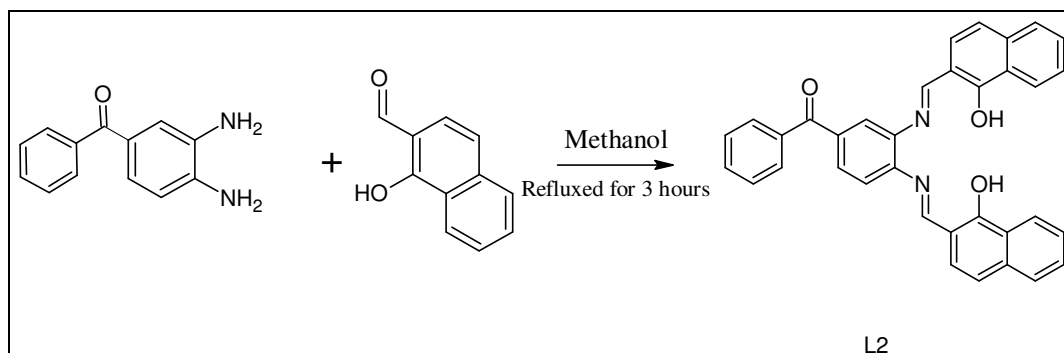
The third-order optical nonlinearity of complexes in DMF solution, at the concentration of 2.5mmol/L, was measured by Z-scan technique. At this concentration the solutions show a linear transmission of 60%, 64% and 68% respectively for Co(II), Ni(II) and Zn(II) complexes at the excitation wavelength of 532 nm.

4.3 SYNTHESIS OF METAL COMPLEXES

4.3.1 Synthesis of ligand (L2)

Methanolic solution of 3,4-diaminobenzophenone (0.233g, 1.1mmol) was added to methanolic solution of 2-hydroxynaphthaldehyde (0.396g, 2.3mmol). The mixture was refluxed for 3 hours to give yellow precipitate. The precipitate was washed thoroughly with ethanol and recrystallized using chloroform. The synthetic route for ligand **L2** is given in Scheme 4.1.

Yield: (75%). M.P: 267°C Anal. Calc. for $C_{35}H_{24}N_2O_3$ (520.57), C: 80.75; H: 4.65; N: 5.38 Found: C: 80.91; H: 4.69; N: 5.65%. IR (KBr, cm^{-1}): 3343(O-H), 1721(C=O), 1598(C=N), 1265(C-O). 1H NMR (400 MHz, DMSO): 15.07 (s, 1H), 14.80(s, 1H) (O-H), 9.76 (d, 2H)(-C-N-), 8.57-7.04 (m, 24H)(aromatic), UV-Vis: λ_{max} (nm) intraligand interactions: 286, 356.

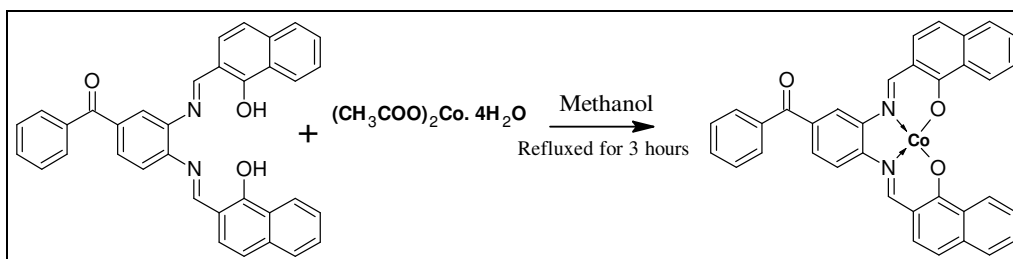


Scheme 4.1 Synthetic scheme for **L2**

4.3.2 Synthesis of cobalt complex (C4)

$\text{Co}(\text{CH}_3\text{COO})_2 \cdot 4\text{H}_2\text{O}$ (0.273g, 1.1mmol) in methanol was added to the ligand (**L2**) (0.624g, 1.2mmol) in minimum quantity of chloroform (20ml)-methanol (15ml) solvent mixture. The reaction mixture was refluxed at 80°C for 3 hours. The resulting blackish precipitate was filtered, washed with methanol followed by ethanol and dried in *vacuo*. The synthetic method for metal complex **C4** is given in Scheme 4.2.

Yield: (71%). M.P: $> 330^\circ\text{C}$. Anal. Calc. for $\text{C}_{35}\text{H}_{22}\text{CoN}_2\text{O}_3$ (577.49): C, 72.79; H, 3.84; N, 4.85. Found: C, 72.62; H, 3.95; N, 4.89%. IR (KBr, cm^{-1}): 1650(C=O), 1604(C=N), 1268(C-O), 570(N-M), 426(O-M). ^1H NMR (400 MHz, DMSO): 9.14 (d, 2H)(-C-N-), 8.52-7.11 (m, 24H)(aromatic), UV-Vis: λ_{max} (nm) intraligand interactions: 254,391, d→d forbidden transition: 495

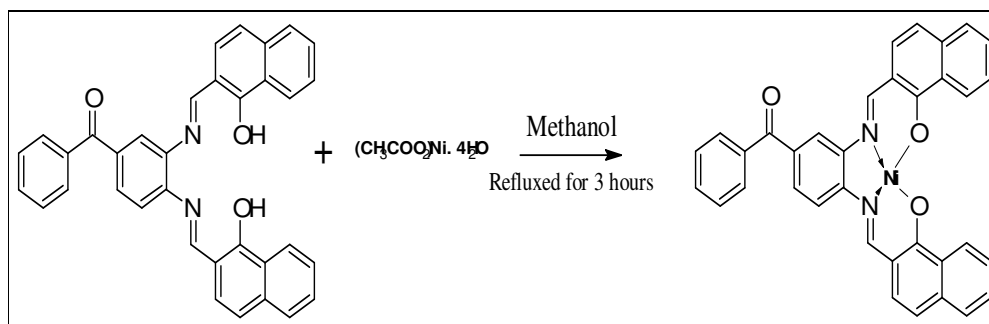


Scheme 4.2 Synthetic scheme for **C4**

4.3.3 Synthesis of nickel complex (**C5**)

$\text{Ni}(\text{OCOCH}_3)_2 \cdot 4\text{H}_2\text{O}$ (0.273g, 1.1mmol) in methanol was added to the ligand (**L2**) (0.624g, 1.2mmol) taken in minimum quantity of chloroform (20ml)-methanol (15ml) solvent mixture. The reaction mixture was refluxed at 80°C for 3 hours. The resulting blackish precipitate was filtered, washed with methanol followed by ethanol and dried in *vacuo*. The synthetic method for metal complex **C5** is given in Scheme 4.3.

Yield: (80%).M.P: $> 330^\circ\text{C}$. Anal. Calc. for $\text{C}_{35}\text{H}_{22}\text{N}_2\text{NiO}_3$ (577.25): C, 72.82; H, 3.84; N, 4.85. Found: C, 72.89; H, 3.80; N, 4.92%. IR (KBr, cm^{-1}): 1651(C=O), 1607(C=N), 1260(C-O), 569 (N-M), 425(O-M). ^1H NMR (400 MHz, DMSO): 9.50 (d, 2H)(-C-N-), 8.78-7.16 (m, 24H)(aromatic), UV-Vis: λ_{max} (nm) intraligand interactions: 295,376, d \rightarrow d forbidden transition: 487.

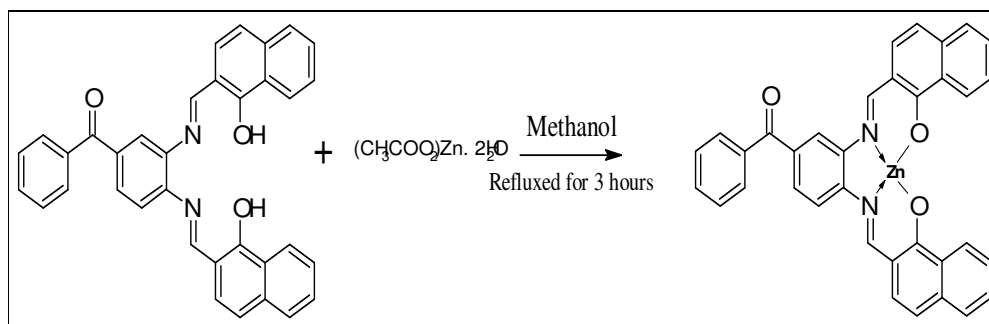


Scheme 4.3 Synthetic scheme for **C5**

4.3.4 Synthesis of zinc complex (C6)

Zn(OCOCH₃)₂·4H₂O (0.241g, 1.1mmol) taken in methanol was added to the ligand (**L2**) (0.624g, 1.2mmol) taken in minimum quantity of chloroform (20ml)-methanol (15ml) solvent mixture. The reaction mixture was refluxed at 80°C for 3 hours. The resulting blackish precipitate was filtered, washed with methanol followed by ethanol and dried in *vacuo*. The synthetic method for metal complex **C6** is given in Scheme 4.4.

Yield: (72%). M.P: > 330 °C. Anal. Calc. for C₃₅H₂₂N₂O₃Zn (583.96): C, 71.99; H, 3.80; N, 4.80. Found: C, 71.92; H, 3.91; N, 4.88%. IR (KBr, cm⁻¹): 1647(C=O), 1605(C=N), 1256(C-O), 545 (N-M), 446(O-M). ¹H NMR (400 MHz, DMSO): 9.88 (d, 2H)(-C-N-), 8.48-7.00 (m, 24H)(aromatic), UV-Vis: λ_{max} (nm) intraligand interactions: 258, 385



Scheme 4.4 Synthetic scheme for **C6**

4.4 RESULTS AND DISCUSSION

The analytical data showed that the observed values were in good agreement with the theoretical values (Table 4.1).

Table 4.1 Analytical data of Schiff base complexes

Complex /Ligand	Decomp. Temp.	% Found (Theoretical)			UV-vis Data, λ_{\max} (nm)	
		C	H	N	Intra ligand Transition	d-d Transition
	(°C)					
L2	267	80.91 (80.75)	4.69 (4.65)	5.65 (5.38)	286, 336	-
C4	>330	72.62 (72.79)	3.95 (3.84)	4.89 (4.85)	254, 391	495
C5	>330	72.89 (72.82)	3.80 (3.84)	4.92 (4.85)	295, 376	487
C6	>330	71.92 (71.99)	3.91 (3.80)	4.88 (4.80)	258, 385	-

4.4.1 FT-IR Spectra

The IR spectra of ligand, cobalt, nickel and zinc complexes are shown in Fig. 4.1 to Fig. 4.4 respectively. As seen from Fig. 4.2 to Fig. 4.4, the IR spectra of complexes have similar stretching bands suggesting a similar kind of ligand geometry around the central metal ion. The band in the region 1250–1270 cm^{-1} is assigned to phenolic $\nu(\text{C-O})$. The absorption band the region 1590-1610 cm^{-1} is due to the stretching of $-\text{C}=\text{N}$ group of the free ligand. This band of $\nu(\text{C}=\text{N})$ undergoes a negative shift by 5–25 cm^{-1} in the IR spectra of complexes. This is because of the coordination of azomethine nitrogen to the metal (Prabhakaran et al. 2005, Kovacic 1967). The strong broad band in the IR spectra of the ligands in the range 3340–3463 cm^{-1} is assigned to O–H stretching vibrations, which is affected by the intramolecular hydrogen bond to the azomethine group ($\text{O-H}\cdots\text{N}=\text{C}$). These bands disappeared on complexation with the metal ions. The bands in the region 540-570 cm^{-1} and 425-460 cm^{-1} in the complexes are assigned to $\nu(\text{M-O})$ and $\nu(\text{M-N})$ respectively (Asadi et al. 2011). Thus the primary IR spectral analysis confirms the complexation of the ligands to the metal ions via O and N atoms. The characteristic stretching frequencies of ligand and complexes are shown in Table 4.2.

Table 4.2 Infrared spectral data (cm^{-1}) for ligands and its Schiff base complexes

Ligand/Complex	$\nu(\text{O-H})$	$\nu(\text{C=O})$	$\nu(\text{C=N})$	$\nu(\text{C-O})$	$\nu(\text{M-O})$	$\nu(\text{M-N})$
L2	3343	1721	1598	1265	-	-
C4	-	1650	1604	1268	570	426
C5	-	1651	1607	1260	569	425
C6	-	1647	1605	1256	545	446

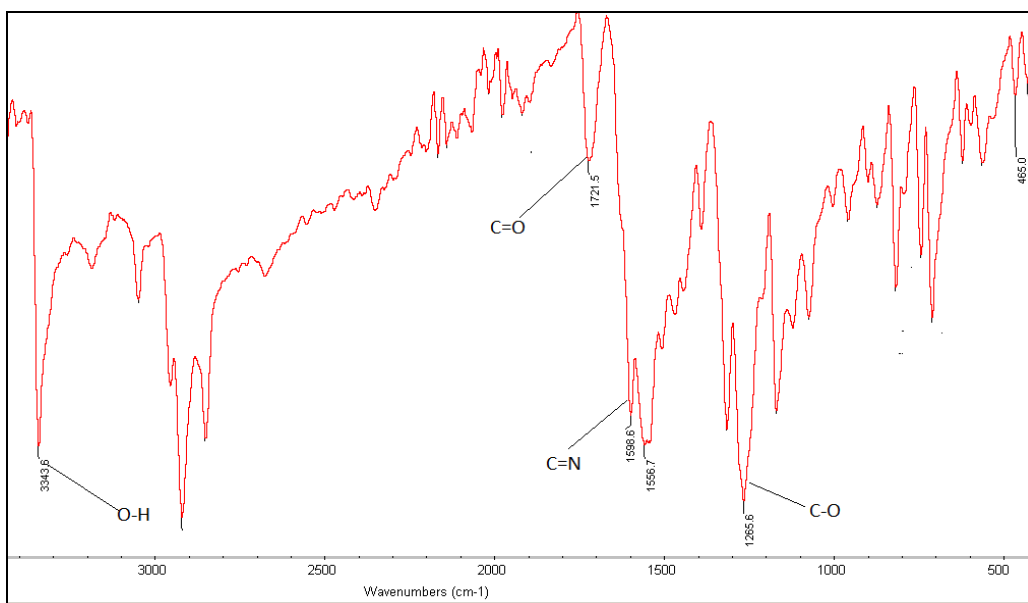


Fig. 4.1 IR spectrum of L2

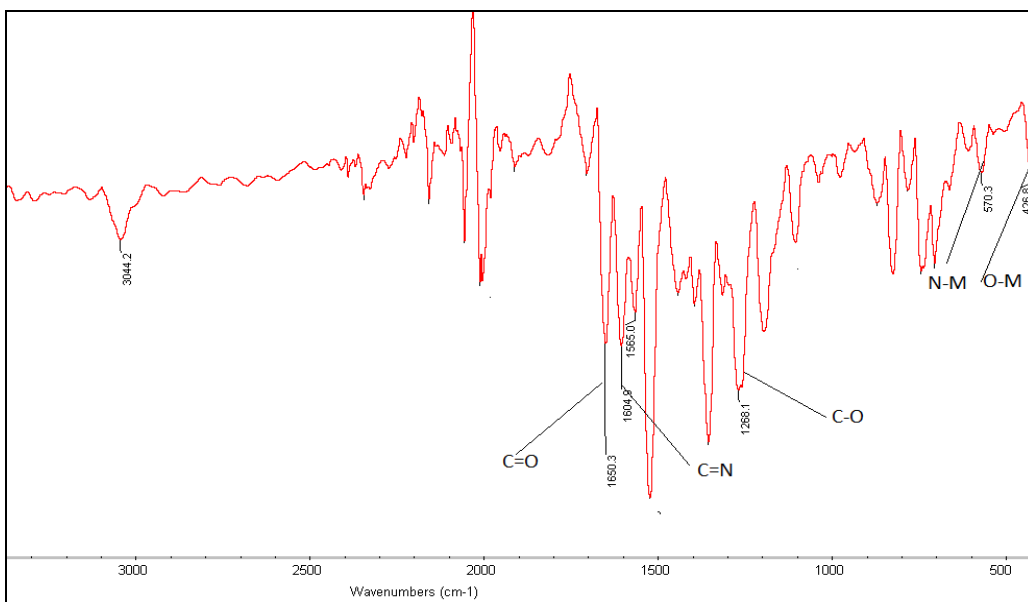


Fig. 4.2 IR spectrum of C4

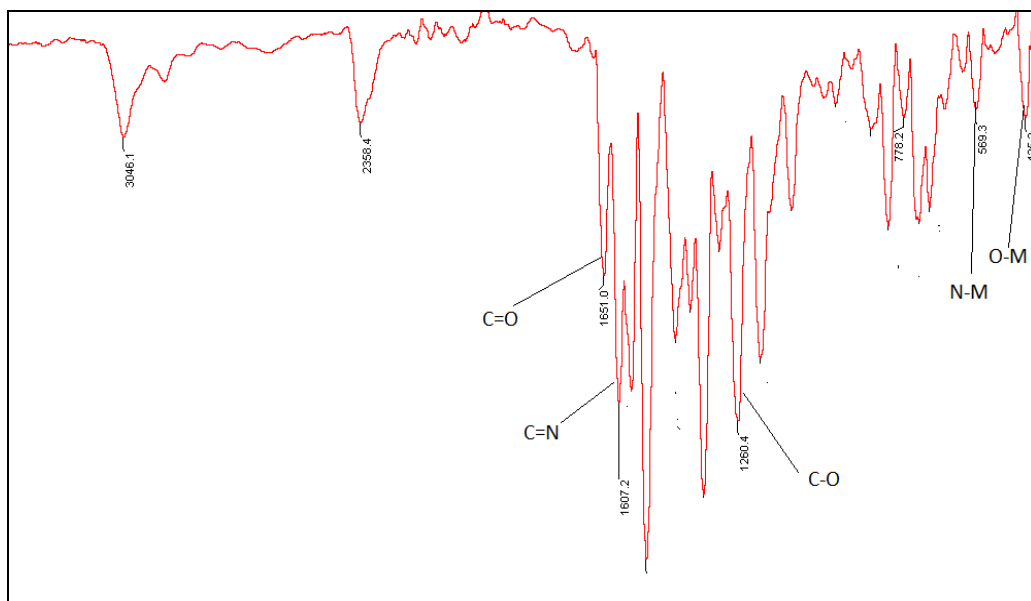


Fig. 4.3 IR spectrum of C5

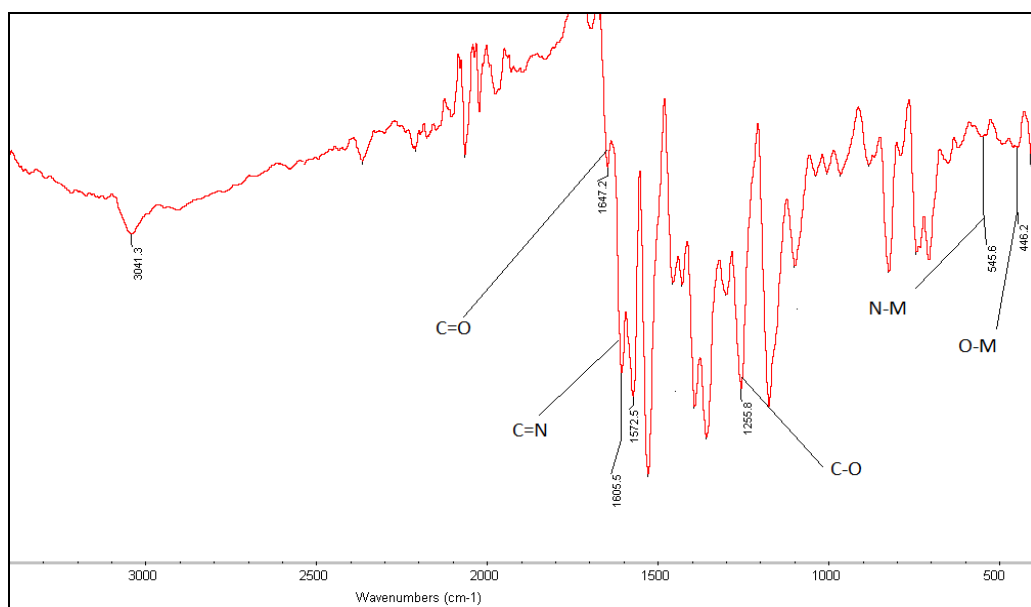


Fig. 4.4 IR spectrum of C6

4.4.2 $^1\text{H-NMR}$ spectra

$^1\text{H-NMR}$ shifts of the ligand and the three complexes are given in Fig. 4.5 to Fig. 4.8. The spectral data of the complexes exhibit a multiplet around 7.0 – 8.6 ppm which corresponds to the aromatic protons of the Schiff base ligand. A peak observed at 9.7 ppm in the complex has been assigned to azomethine proton ($-\text{C}=\text{N}-$) (Sorkau et al. 2005, Gnanasoundari and Natarajan 2005, Balasubramanian et al. 2007). Further, two peaks resonating at 14.8 and 15.0 ppm in ligand were absent in the metal complex spectra. These two peaks are assigned to the hydroxyl group in the ligand, and the absence of a resonance due to these phenolic hydrogens in the metal complexes indicates the deprotonation of the Schiff base, to form the metal complex. It is worth mentioning here, that the presence of two hydroxyl peaks confers an unsymmetrical environment to the ligand.

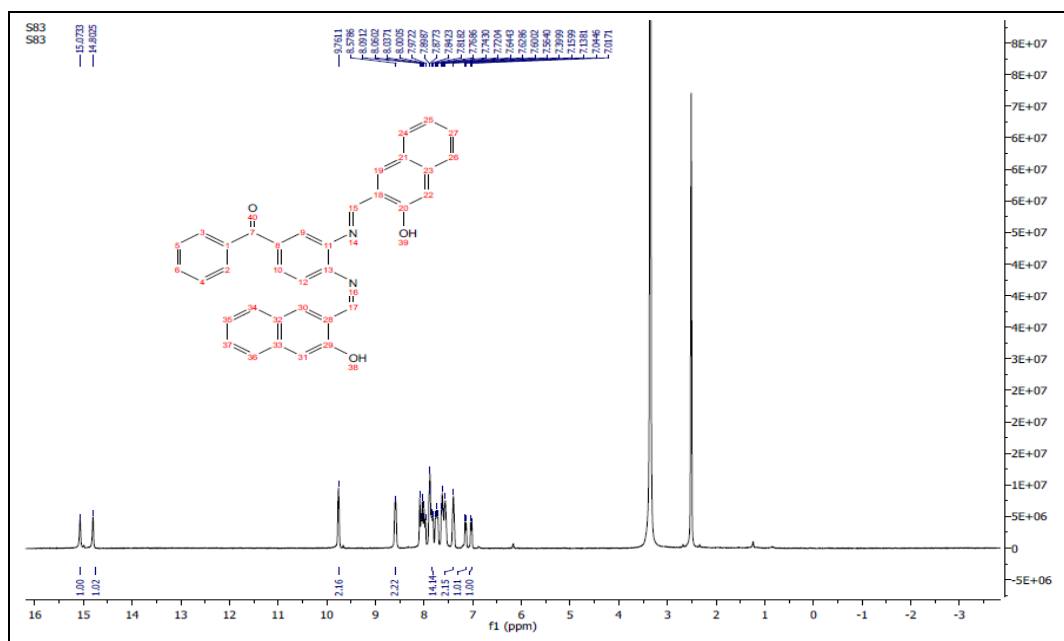


Fig. 4.5 $^1\text{H-NMR}$ spectrum of L2

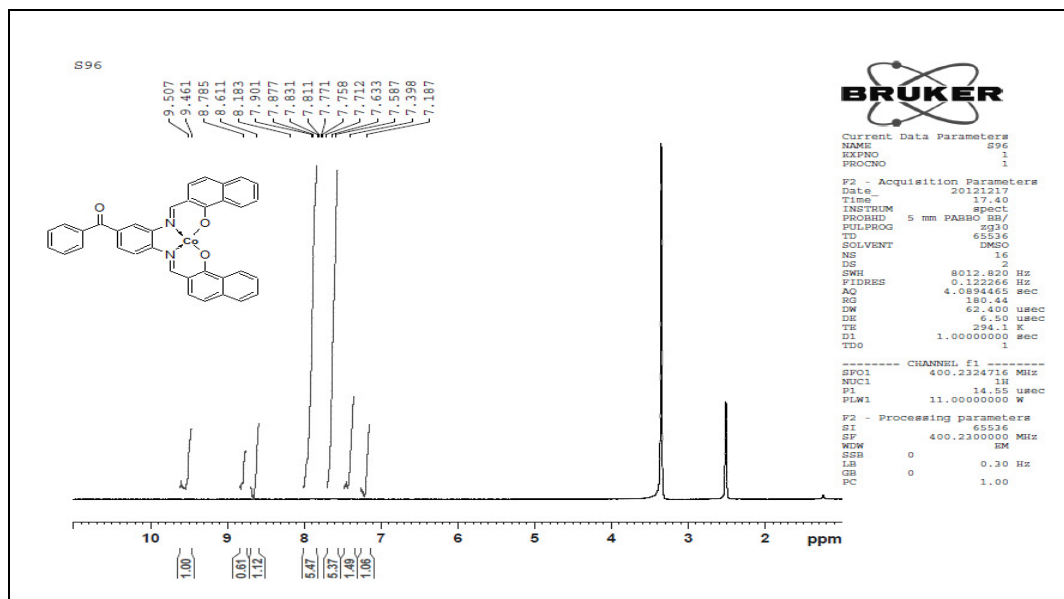


Fig. 4.6 ^1H -NMR spectrum of C4

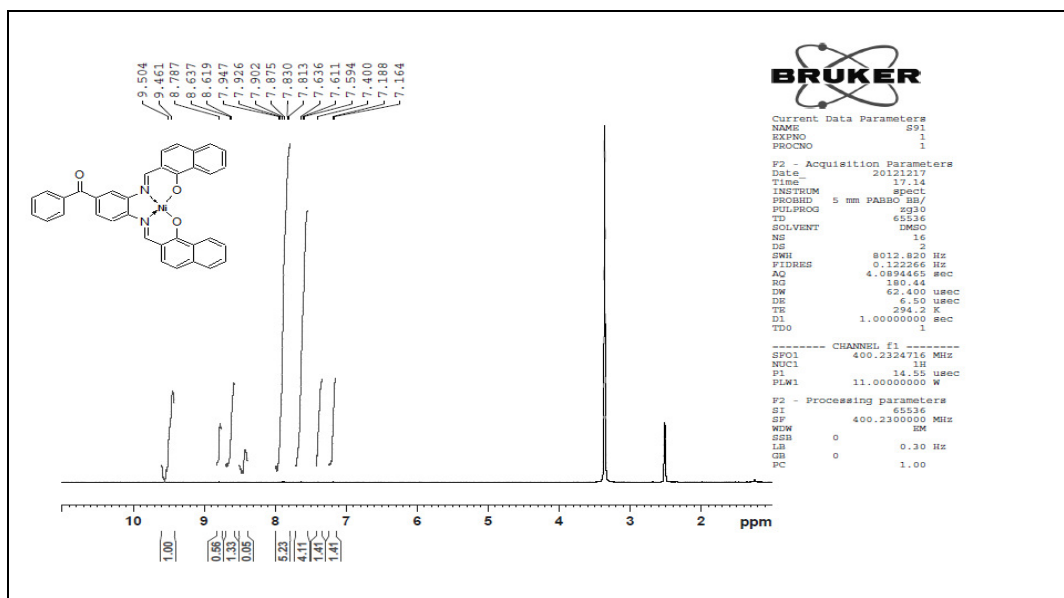


Fig. 4.7 ^1H -NMR spectrum of C5

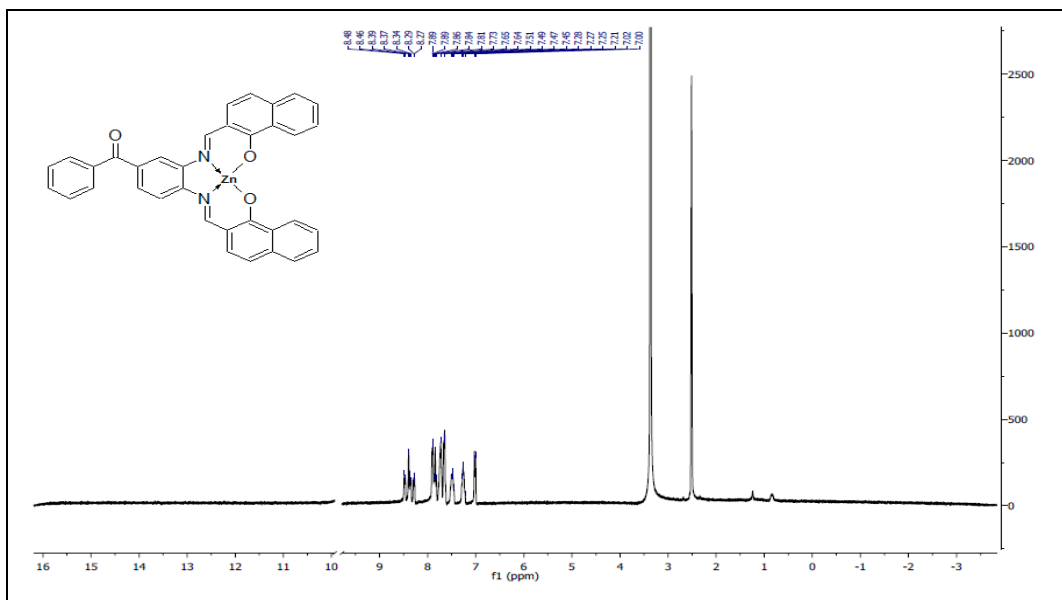


Fig. 4.8 $^1\text{H-NMR}$ spectrum of **C6**

4.4.3 UV-Visible spectra

The linear absorption spectral data of the ligand and complexes were recorded in dry DMSO and are given in Fig. 4.9. The values of the electronic spectra of ligand and complexes (**C4-C6**) are given in Table 4.1. Linear absorption in a transition metal complex is generally due to metal-to-ligand charge transfer (MLCT), ligand-to-metal charge transfer (LMCT) and intra-ligand charge transitions (ILCT). The presence of one broad band between 450 nm to 600 nm in the spectral data of the complexes, corresponds to the non resolved $d-d$ transitions from the four low-lying d-orbitals (d_{xz} , d_{yz} , d_z^2 and $d_{x^2-y^2}$) to the empty (in case of Ni(II)) or half-filled (in case of Co(II)) d_{xy} orbital. This broad band is not observed for Zn(II) complex due to the absence of $d-d$ electronic transitions in the diamagnetic Zn^{2+} ion (d^{10} configuration). This eliminates the possibility of octahedral

geometry. On the basis of this, for all the three complexes square planar structure has been proposed (Lever 1984).

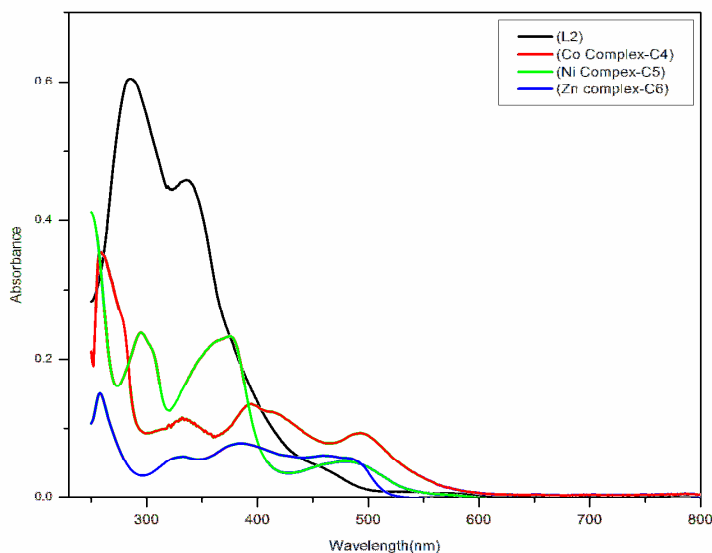


Fig. 4.9 Linear absorption spectra of ligand **L2** and complexes **C4-C6**

The electronic spectra of Co(II) and Ni(II) complexes with an electronic configuration of d^7 and d^8 respectively, show new absorption bands in the visible region at 487 nm and 497 nm respectively, which are attributed to the electronic transition $^1A_{1g} \rightarrow ^1A_{2g}$. This further confirms that the Ni(II) and Co(II) complexes are square planar (Lever 1968).

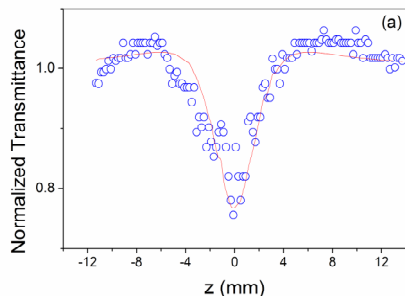
4.5 NONLINEAR OPTICAL MEASUREMENTS

The nonlinear absorption of the complexes was determined by open-aperture Z-scan technique using high intensity laser light. The Z-scan is a widely used technique

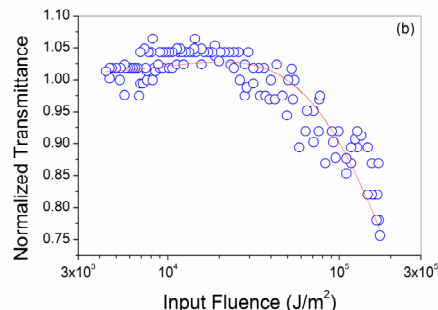
developed by Sheik Bahae et al. (1990) to evaluate the NLO properties of a material. It is based on the transformation of phase distortion during beam propagation. The advantage of this technique is that it requires simple experimental set-up and provides direct measurement of both nonlinear refractive index and absorption coefficient, along with their sign (Gomez et.al 2003). This helps in the estimation of third order susceptibility coefficient. Here a Gaussian beam is focused on the sample which is moved along the Z-axis. The nonlinear absorption coefficient is calculated from the Z-scan curve or the nonlinear transmission curve.

In the present experiment, a Nd:YAG Laser (Quanta Ray, Spectra Physics), which produces 7 ns laser pulse at 532 nm was used as the light source. The laser beam is spatially Gaussian, as found from a knife-edge measurement. Liquid samples in DMF were taken in a cuvette of thickness 1 mm cuvettes and mounted on a motorized linear translation stage. The beam diameter (FWHM) was found to be 7.84 mm and the corresponding Rayleigh range was 1.9 mm.

The Z-scan and nonlinear transmission curves are shown in Fig. 4.10 to 4.12. As seen, the transmission is reduced at higher intensities, showing that the samples behave as optical limiters. Maximum nonlinearity was found in nickel complex (**C5**) and minimum in cobalt complex (**C4**).

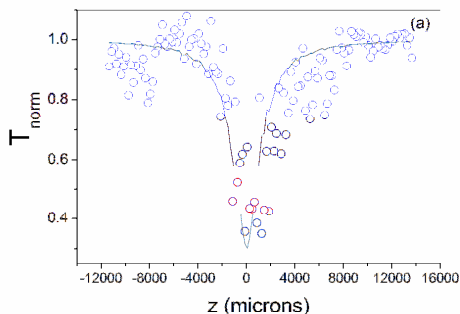


(a)

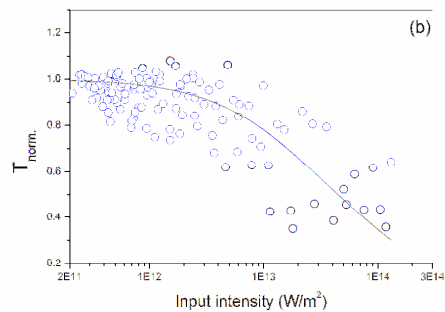


(b)

Fig. 4.10 (a) Open aperture Z-scan curve. Linear transmission of the sample (corresponding to T (norm.) = 1) is 60%. Circles are data points while solid curves are numerical fits using equation 4.1. (b) Nonlinear transmission curve of **C4**



(a)



(b)

Fig. 4.11 (a) Open aperture Z-scan curve. Linear transmission of the sample (corresponding to T (norm.) = 1) is 64%. Circles are data points while solid curves are numerical fits using equation 4.1. (b) Nonlinear transmission curve of **C5**.

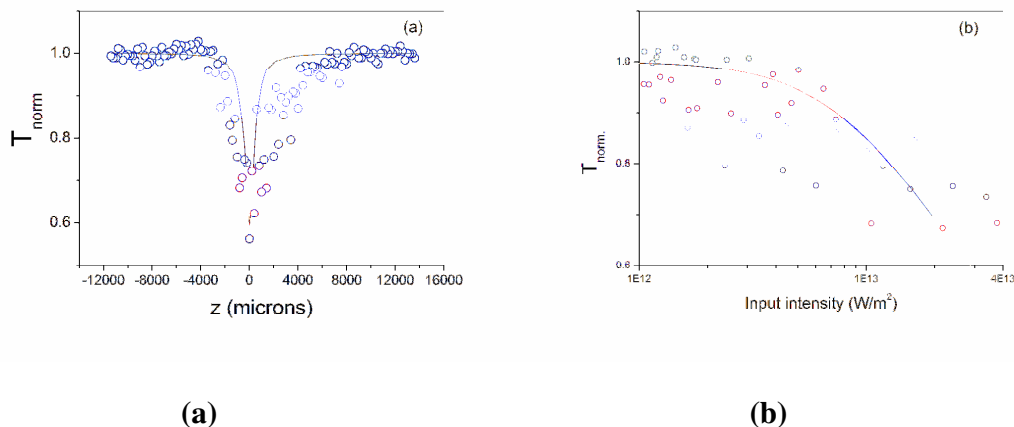


Fig. 4.12 (a) Open aperture Z-scan curve. Linear transmission of the sample (corresponding to T (norm.) = 1) is 68%. Circles are data points while solid curves are numerical fits using equation 4.1 (b) Nonlinear transmission curve of **C6**.

Large optical nonlinearity in materials is commonly associated with resonant transitions, which may be single or multi-photon in nature. Generally, nonlinear optical materials have different nonlinear absorption mechanisms viz., two photon absorption (2PA), three photon absorption (3PA), excited state absorption (ESA) or reverse saturable absorption (RSA). These phenomena can be explained based on a five level energy diagram (Yim.S.H et.al 1998, Giuliano.C 1967) as shown in Fig. 4.13. As per this model, a material has three singlet states (one ground state and two excited states) as well as two triplet states (excited states). Each of these electronic states is further divided into several vibrational levels. When a molecule is subjected to 532 nm laser pulse of 7 ns duration, simultaneous two photon absorption occurs from singlet ground state (S_0) to one of the vibrational levels of first singlet excited state (S_1). This corresponds to two photon absorption (2PA). From state S_1 , the molecule may further get excited to higher excited singlet state (S_2) or they may even transfer from S_1 state to a lower level triplet state (T_1) through intersystem crossing (ICS). However, the molecules from S_1 state can get excited to higher energy states S_2 (or similarly from T_1 to T_2 state). Such a process is

called excited state absorption (ESA) phenomena. Reverse saturable absorption (RSA) occurs if S_1 and/or T_1 states have larger absorption cross-section than the ground state S_0 . In the present experiment carried at 532 nm, it was found that numerically, a two-photon absorption (2PA) type process gives the best fit to the obtained open aperture Z-scan data. The data obtained are fitted to the nonlinear transmission equation 4.1 for a two-photon absorption process, given by Sutherland (1996).

$$T = \left((1-R)^2 \exp(-\alpha L) / \sqrt{\pi} q_0 \right) \int_{-\infty}^{+\infty} \ln \left[\sqrt{1 + q_0 \exp(-t^2)} \right] dt \quad \dots\dots\dots (4.1)$$

where T is the sample transmission given by T (norm.) x linear transmission of the sample, and L and R are the length and surface reflectivity of the sample respectively. α is the linear absorption coefficient, q_0 is given by $\beta(1-R)I_0L_{eff}$, where β is the effective 2PA coefficient, and I_0 is the on-axis peak intensity. L_{eff} is given by $1 - \exp(-\alpha/\alpha)$. It must be mentioned here that since the molecule is subjected to nanosecond laser pulses, thermal effects in the system may also contribute to the optical limiting behavior. However, this becomes substantial only if non-linear scattering is observed in the system. But since in the present experiment, detectors with large apertures were used, any non-linear refraction becomes insignificant. For further confirmation, we measured non-linear scattering using a photodiode attached at an angle to the beam path in front of the sample but did not receive any appreciable signal thereby clarifying that 2PA is the dominant mechanism prevailing in the system.

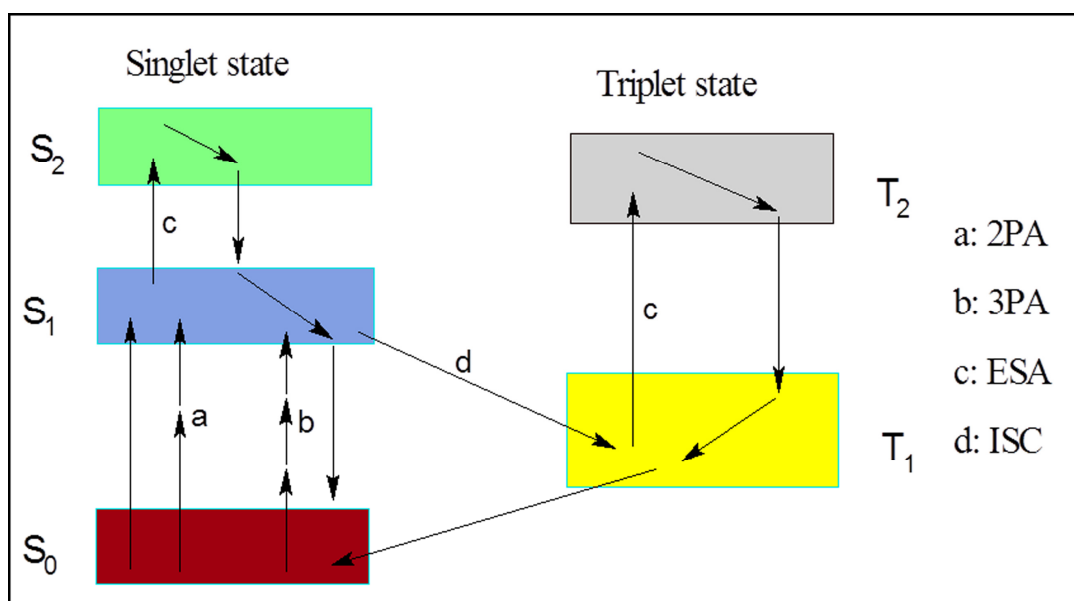


Fig. 4.13 Five level energy diagram showing nonlinear absorption mechanisms

The nonlinearity in inorganic metal complexes is due to the presence of metal ions which can assemble simple organic ligands in a variety of multipolar arrangements which can induce charge transfer transitions between metal and ligands. Hence the molecules were designed to have a donor- π bridge-acceptor (D- π -A) system. As seen in Chapter 3, nonlinear optical properties of metal Schiff base complexes of 1,2-diaminobenzene and 2-hydroxynaphthaldehyde have been studied by us. The β value for Ni(II) complex have improved by an order (refer Table 3.4 of Chapter 3) by just replacing 1,2-diaminobenzene with 3,4-diaminobenzophenone. This is mainly because the introduction of the latter not only extends the π -conjugation but also increases the electron asymmetry around the metal center, thereby enhancing the NLO response. Thus, a comparative study shows that extensive conjugation helps in attaining a better optical nonlinearity, thereby extending their optical limiting applications.

The calculated values of the effective 2PA coefficient for the metal complexes are given in Table 4.3. As seen from Table 4.3, among the three metal complexes, Ni(II)

complexes show higher β value, thereby indicating that NLO responses not only depend on the electron distribution in the ligand, but also on the metal center. Better insights on the metal center influence can be obtained by the survey of the linear optical properties of the metal complexes. A study of the UV-Vis spectra of the metal complexes in the range of 250-400 nm (Fig. 4.5) shows that bands of the Ni(II) complexes are more intense than that of Co(II) and Zn(II) complexes. NLO responses also follow the same trend. Ni(II) complexes exhibit the highest non-linear absorption coefficient whereas the lowest value is observed for Zn(II) complexes. This suggests that the metal center plays an important role in fine tuning the nonlinear responses of a complex (Tedim et al. 2006).

Table 4.3 2PA coefficient β of Schiff base complexes

Complex	2PA coefficient β (mW^{-1})
Cobalt Complex (C4)	2.3×10^{-12}
Nickel Complex (C5)	1.1×10^{-10}
Zinc Complex (C6)	1.4×10^{-12}

CHAPTER 5

SYNTHESIS, CHARACTERIZATION AND NONLINEAR OPTICAL STUDIES OF THIOSEMICARBAZIDE COMPLEXES OF Ni(II), Cu(II) AND Zn(II)

Abstract

In this chapter, thiosemicarbazide complexes of Ni(II), Cu(II) and Zn(II) metal ions were synthesized and well characterized by several analytical techniques. The stereochemistry of the ligand around the metal ion has been discussed. The linear and nonlinear optical behavior of the complexes were studied by UV-Vis spectroscopy and Z-scan measurement respectively. The complexes exhibited good three photon absorption behaviour.

5.1 INTRODUCTION

In recent years there has been growing interest in organic materials for nonlinear optical applications because of their high potential in optical behavior (Prasad and Williams 1991, Chemla and Zyss 1987). The organic molecular materials have emerged as a new class of promising nonlinear optical materials because of their superior qualities over inorganic systems. These materials exhibit strong nonlinear polarization in the presence of high-intensity electromagnetic fields. The properties and performance of nonlinear optical and photonic materials depend critically upon their composition, purity and microstructure.

Among the various organic materials, the chemistry of thiosemicarbazone complexes of transition metal ions has been receiving significant current attention, mainly because of the variable binding modes displayed by these ligands in their complexes. Thiosemicarbazones $\{R^1R^2C=N^3-N^2H-C(=S)-NR^3R\}$ and thiosemicarbazides $\{R^1R^2C=N^3-N^2H-C(=O)-NR^3R\}$ possess several donor atoms and generally bind to metals via N^2 , O (or S) or N^3 , S donor atoms forming four or five membered rings, respectively.

Thiosemicarbazones (TSC), as well as their metal complexes, have been the subject of great interest for many researchers since a number of years. Apart from their diverse chemical and structural characteristics, the interest in these compounds also stems from their wide spectrum biological activity, which is already well established. Their biological importance is evident by a wide range of antibacterial, antimalarial, antiviral, antineoplastic and antileprotic activities (Bauer 1972, Williams 1972). Such pharmacological activities are due to the strong chelating ability of these ligands with biologically important metal ions such as Fe, Cu, Ni and their reductive capacities (Padhye and Kaufman 1985, Cymerman et al 1955, Cambell 1975, Chattopadhyay et al 1990). Other than bioinorganic applications, thiosemicarbazone, which has a π -electron delocalized system containing mixed sulphur and nitrogen donors, is expected to display two-photon exciting dual fluorescence (Xue et al 2003).

5.2 EXPERIMENTAL

5.2.1 Materials

All the chemicals used were of analytical grade. Solvents were purified and dried according to standard procedure (Vogel 1989). $NiCl_2 \cdot 6H_2O$, $ZnCl_2 \cdot 6H_2O$ and $CuCl_2$ were purchased from Merck. Thiosemicarbazide was procured from Nice chemicals and was used without any further purification.

5.2.2 Physical measurements

The C, H, N and S contents were determined by ThermoFlash EA1112 series elemental analyzer. FT-IR spectra were recorded on a Thermo Nicolet Avatar FT-IR spectrometer as KBr powder in the frequency range 400-4000 cm^{-1} . $^1\text{H-NMR}$ spectra were recorded in Bruker AV-400 instrument using TMS as internal standard. Electronic spectra of the complexes in the 200-800 nm range were measured on a GBC UV-Vis double beam spectrophotometer in N, N-dimethylformamide solution.

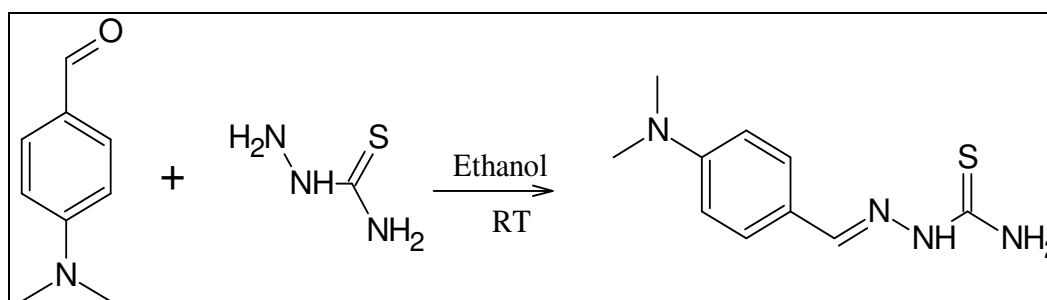
The third-order optical nonlinearity of complexes in DMF solution, at the concentration of 2.5mmol/L, was measured by Z-scan technique. At this concentration, the solutions show a linear transmission of 65%, 62% and 65% respectively, for Ni(II), Cu(II) and Zn(II) complexes at the excitation wavelength of 532 nm.

5.3 SYNTHESIS OF METAL COMPLEXES

5.3.1 Synthesis of ligand (L3)

The synthetic procedure for the synthesis of the ligand 4-[(dimethylamino)benzylidene]hydrazinecarbothioamide (**L3**) followed in the present work is similar to that carried out by Chattopadhyay et al. (1988). 4-dimethylaminobenzaldehyde (0.164g, 1.1mmol) was taken in minimum amount of ethanol solution and dissolved by stirring in room temperature. Later to this a solution of thiosemicarbazide (0.0914g, 1.0mmol) and sodium acetate (0.127g, 1.5mmol) in water and ethanol mixture was added. The above mixture was stirred for 2 hours at room temperature to yield yellow precipitate. The obtained precipitate was washed thoroughly with ethanol and recrystallized using dichloromethane. The synthetic route for the ligand **L3** is given in Scheme 5.1.

Yield: (72%). M.P: 210°C Anal. Calc. for C₁₀H₁₄N₄S (222.3): C, 54.03; H, 6.35; N, 25.20. S, 14.42. Found: C, 54.21; H, 6.17; N, 25.45, S: 14.14%. IR (KBr, cm⁻¹): 3122(N-H), 1589(C=N), 941(C=S). ¹H NMR (400 MHz, DMSO): 11.19(s, 1H) (N-H-), 8.01-7.93 (d,2Ar-H), 7.59-7.57 (d,2Ar-H), 7.77(s,1H) (N=CH-) 6.69 (d,2H) (-NH₂) , 2.96 (m,6H) (CH₃). MS:m/z = 223(M⁺). UV-Vis: λ_{max}(nm) intraligand interactions: 281, 339.

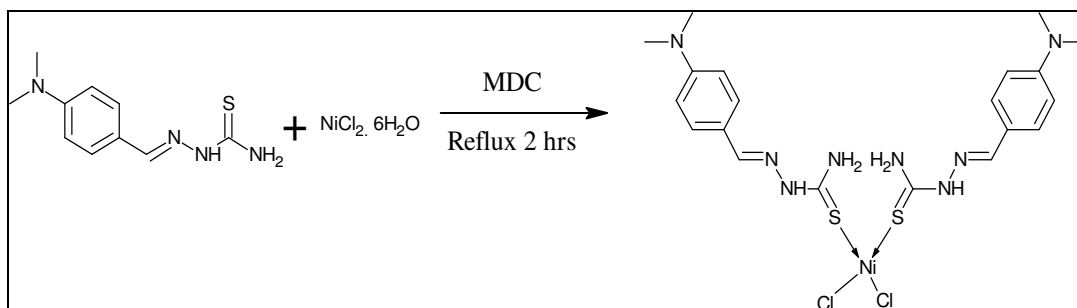


Scheme 5.1 Synthetic scheme for **L3**

5.3.2 Synthesis of nickel complex (C7)

NiCl₂·6H₂O (0.261g, 1.1mmol) in methanol was added to the synthesized ligand (**L3**) (0.486g, 2.2mmol) taken in dichloromethane solvent. The reaction mixture was then refluxed for 2 hours. The resulting greenish yellow coloured precipitate was thoroughly washed with ethanol and dried in vacuum. The synthetic method for metal complex **C7** is given in Scheme 5.2.

Yield: (76%). M.P: 294 °C. Anal. Calc. for C₂₀H₂₈Cl₂N₈NiS₂(574.21): C, 41.83; H, 4.91; N, 19.51; S, 11.71. Found: C, 41.97; H, 4.80; N, 19.86; S, 11.56%. IR (KBr, cm⁻¹): 3374(N-H), 3252(NH₂), 1606(C=N), 955(C=S). ¹H NMR (400 MHz, DMSO): 11.13(s, 1H) (N-H-), 8.11-7.94 (d,2Ar-H), 7.78-7.53 (d,2Ar-H), 7.88(s,1H) (N=CH-) 6.64 (d,2H) (-NH₂) , 2.91 (m,6H) (CH₃).UV-Vis: λ_{max}(nm) intraligand interactions: 309, 339. d→d Transitions : 413

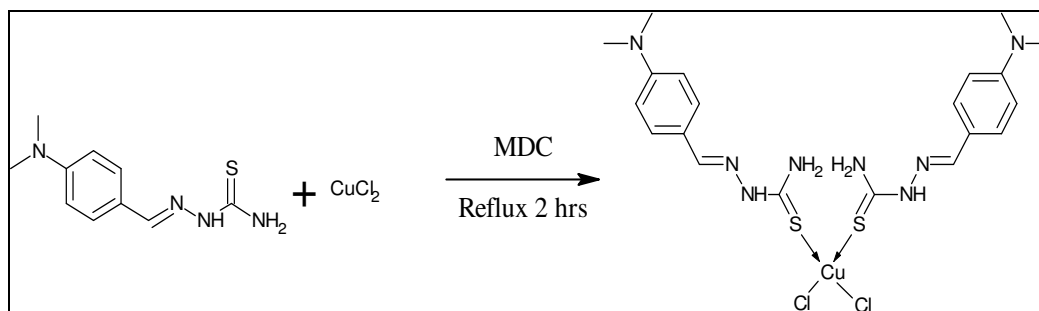


Scheme 5.2 Synthetic scheme for **C7**

5.3.3 Synthesis of copper complex (C8)

CuCl_2 (0.187g, 1.1mmol) taken in methanol was added to the synthesized ligand (**L3**) (0.486g, 2.2mmol) taken in dichloromethane solvent. The reaction mixture was then refluxed for 2 hours. The resulting yellow coloured precipitate was thoroughly washed with ethanol and dried in vacuum. The synthetic method for metal complex **C8** is given in Scheme 5.3.

Yield: (68%). M.P: 282 °C. Anal. Calc. for $\text{C}_{20}\text{H}_{28}\text{Cl}_2\text{CuN}_8\text{S}_2$ (579.07): C, 41.48; H, 4.87; N, 19.35; S, 11.07. Found: C, 41.42; H, 4.95; N, 19.65; S, 11.01%. IR (KBr, cm^{-1}): 3420 (N-H), 1595(C=N), 951(C=S). ^1H NMR (400 MHz, DMSO): 11.52(s, 1H) (N-H-), 8.37-8.17 (d,2Ar-H), 7.84-7.65 (d,2Ar-H), 7.96(s,1H) (N=CH-) 6.77 (d,2H) (-NH₂) , 2.99 (m,6H) (CH₃). UV-Vis: λ_{max} (nm) intraligand interactions: 306, 335. d→d Transitions : 403

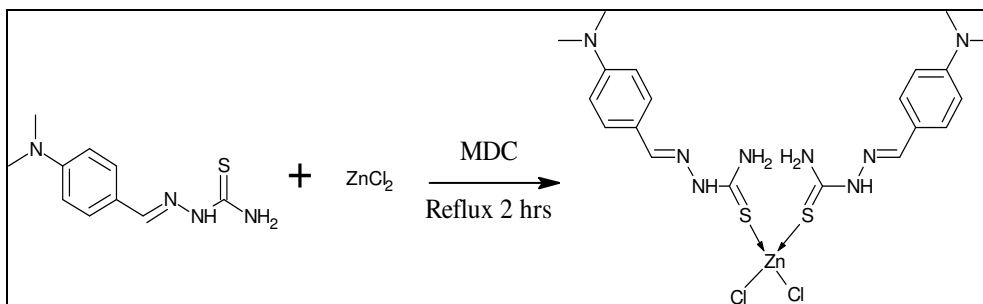


Scheme 5.3 Synthetic scheme for **C8**

5.3.4 Synthesis of zinc complex (**C9**)

ZnCl₂ (0.149g, 1.1mmol) taken in methanol was added to the synthesized ligand (**L3**) (0.486 g, 2.2mmol) taken in minimum quantity of (4:1) acetone-methanol solvent mixture. The reaction mixture was then refluxed for 2 hours. The resulting orange coloured precipitate was filtered, washed with methanol followed by hexane and dried in vacuum. The synthetic method for metal complex **C9** is given in Scheme 5.4.

Yield: (68%). M.P: > 290 °C. Anal. Calc. for C₂₀H₂₈Cl₂N₈S₂Zn(580.93): C, 41.35; H, 4.86; N, 19.29. S, 11.04. Found: C, 41.92; H, 4.71; N, 19.40; S, 11.32 %. IR (KBr, cm⁻¹): 3320(N-H), 1581(C=N), 941(C=S). ¹H-NMR (400 MHz, DMSO): 11.19(s, 1H) (N-H-), 8.01-7.93 (d,2Ar-H), 7.74-7.58 (d,2Ar-H), 7.78(s,1H) (N=CH-), 6.70 (d,2H) (-NH₂), 2.95 (m,6H) (CH₃). UV-Vis: λ_{max}(nm) intraligand interactions: 303, 337.



Scheme 5.4 Synthetic scheme for **C9**

5.4 RESULTS AND DISCUSSION

The analytical data showed that the observed values are in good agreement with the theoretical values (Table 5.1).

Table 5.1 Analytical data of Schiff base complexes

Complex /Ligand	Decomp. Temp. (°C)	% Found (Theoretical)			UV-vis Data, λ_{\max} (nm)	
		C	H	N	Intra ligand Transition	d-d Transition
L3	210	54.21 (54.03)	6.17 (6.35)	25.45 (25.20)	281, 339	-
C7	294	41.97 (41.83)	4.80 (4.91)	19.86 (19.51)	309, 339	413
C8	282	41.42 (41.48)	4.95 (4.87)	19.65 (19.35)	306, 335	403
C9	290	41.92 (41.35)	4.71 (4.86)	19.40 (19.29)	303, 337	-

5.4.1 FT-IR Spectra

The IR spectra of the complexes exhibit a weak band around 3450cm^{-1} , which is assigned to secondary $\nu(\text{N-H})$ stretching vibration in all the three complexes and ligands and also a sharp band around $3160\text{-}3130\text{cm}^{-1}$ which is assigned to N-H of amide group. Band around 1610cm^{-1} is assigned to -C=N group. The band due to C=S is observed in the range of 950 cm^{-1} (Tian et al 2002). The characteristic peaks are given in Table 5.2. The typical IR spectra of ligand and complexes are given in Fig. 5.1 – Fig. 5.4.

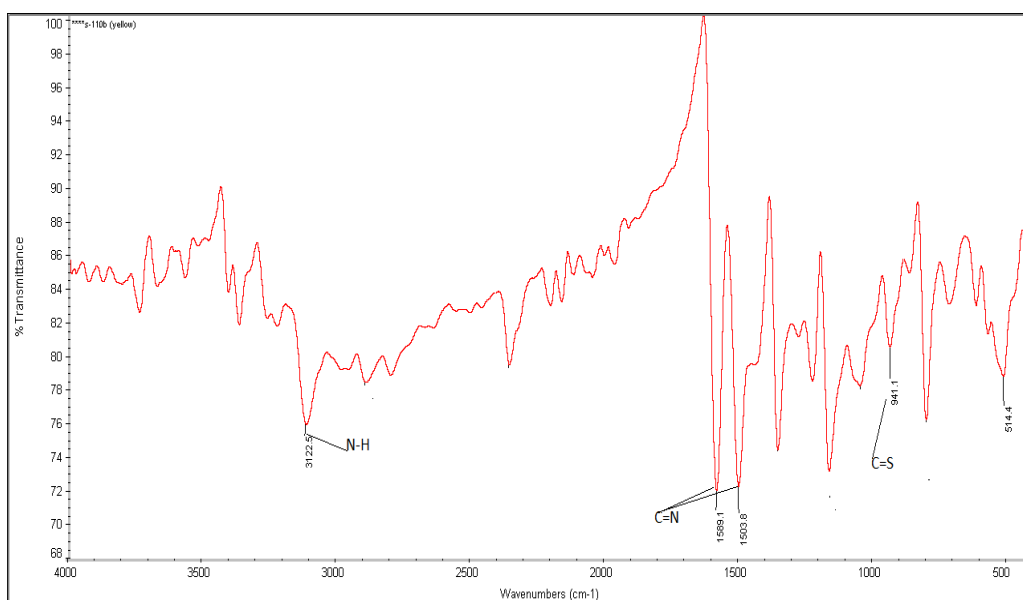


Fig. 5.1 IR spectrum of L3

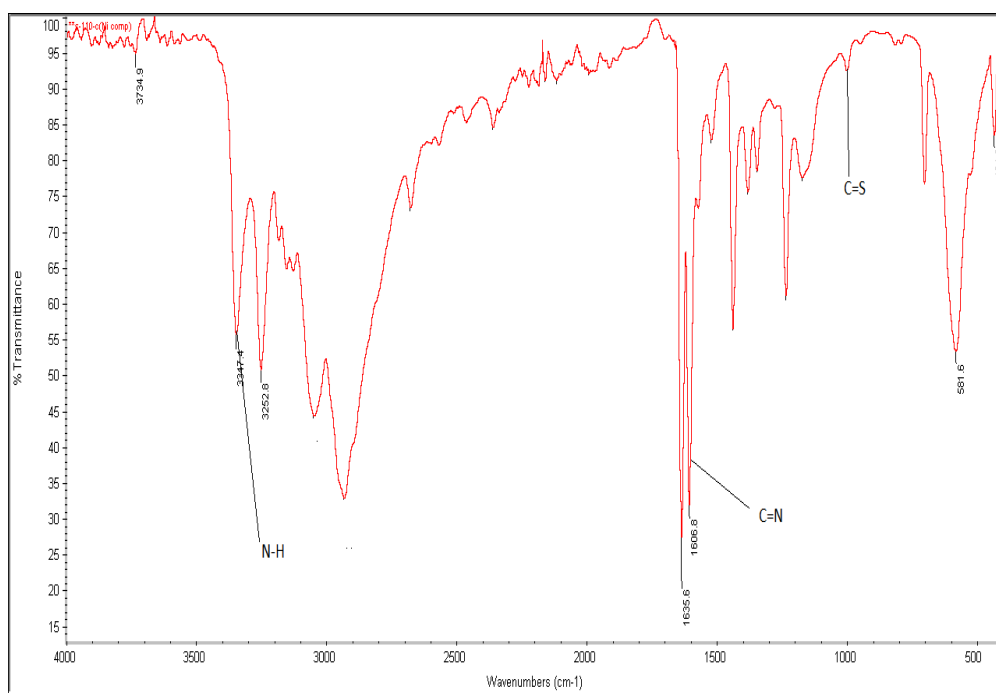


Fig. 5.2 IR spectrum of **C7**

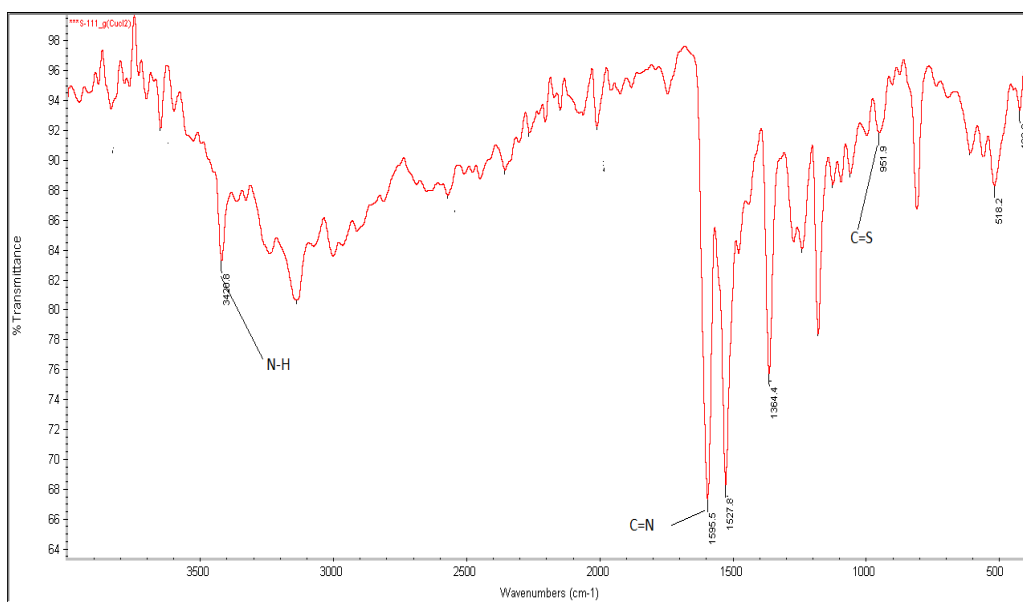


Fig. 5.3 IR spectrum of **C8**

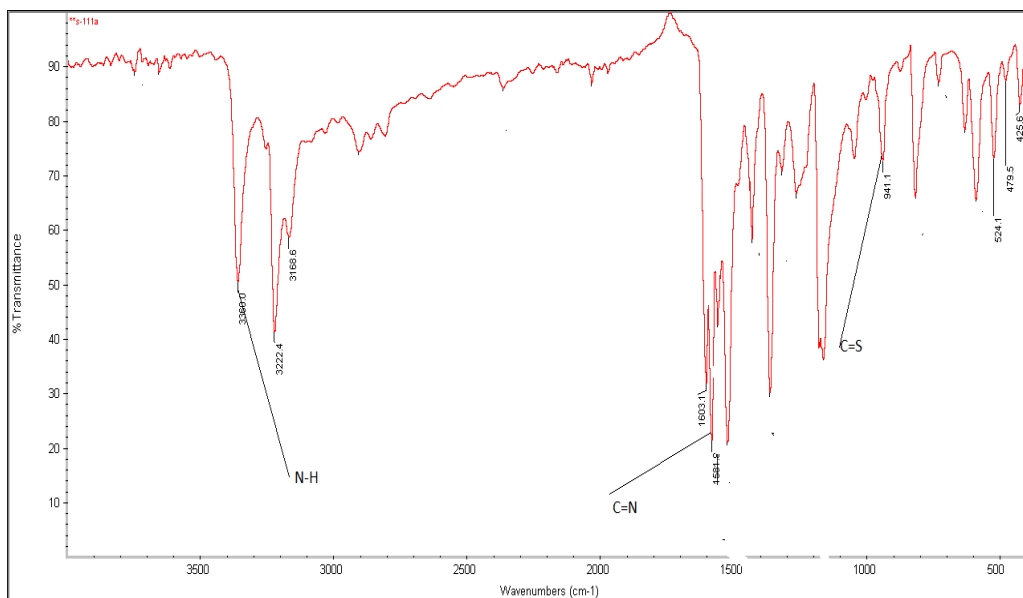


Fig. 5.4 IR spectrum of **C9**

Table 5.2 Infrared spectral data (cm^{-1}) for ligands and its complexes (**C7-C9**)

Ligand/Complex	ν (N-H)	ν (NH_2)	ν (C=N)	ν (C=S)
L3	3422	3123	1589	941
C7	3374	3130	1606	955
C8	3420	3137	1595	951
C9	3360	3168	1581	941

5.4.2 $^1\text{H-NMR}$ Spectra

$^1\text{H-NMR}$ spectra of ligand **L3** and metal complexes (**C7 to C9**) are shown in Fig. 5.5 to Fig. 5.8. The spectra showed prominent peaks around 11.13 -11.52 ppm which has been assigned for N-H proton. In ligand **L3** a peak around 7.77 ppm which is assigned to azomethine proton (HC=N-) is slightly shifted in the complexes. In ligand **L3** a peak

around 6.69 ppm is assigned to two protons of NH₂ which also shifted in the all the complexes. A Peak around 2.96 ppm is assigned to two methyl groups. As the complexation takes place through the sulphur moiety there are no much variations in the NMR spectra of ligand and metal complexes.

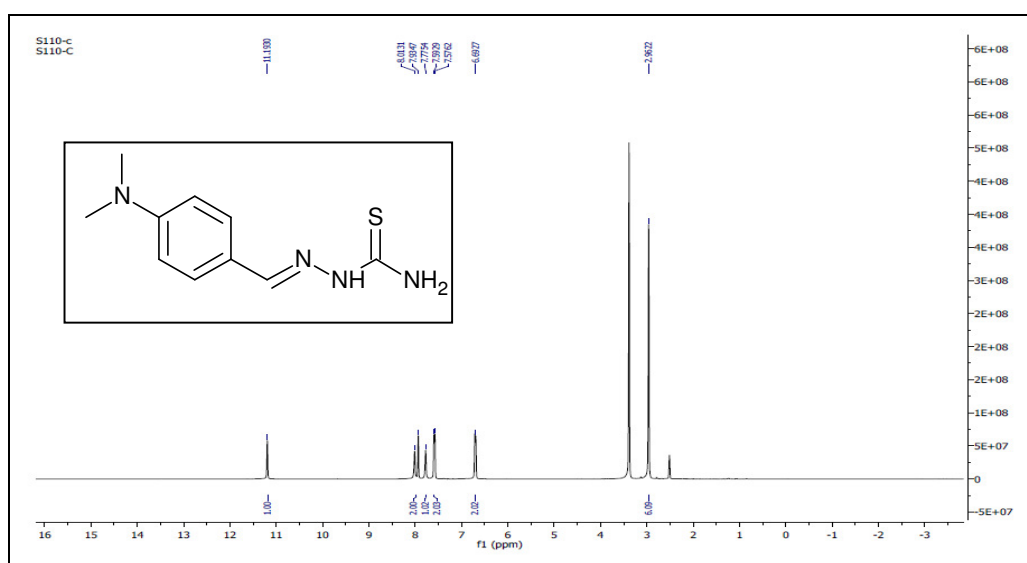


Fig. 5.5 ¹H-NMR spectrum of L3

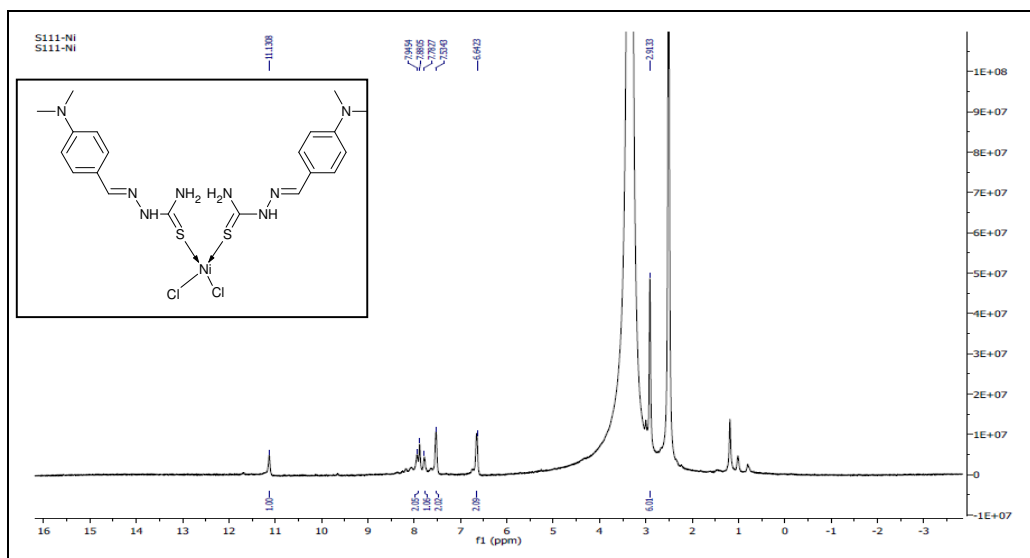


Fig. 5.6 $^1\text{H-NMR}$ spectrum of **C7**

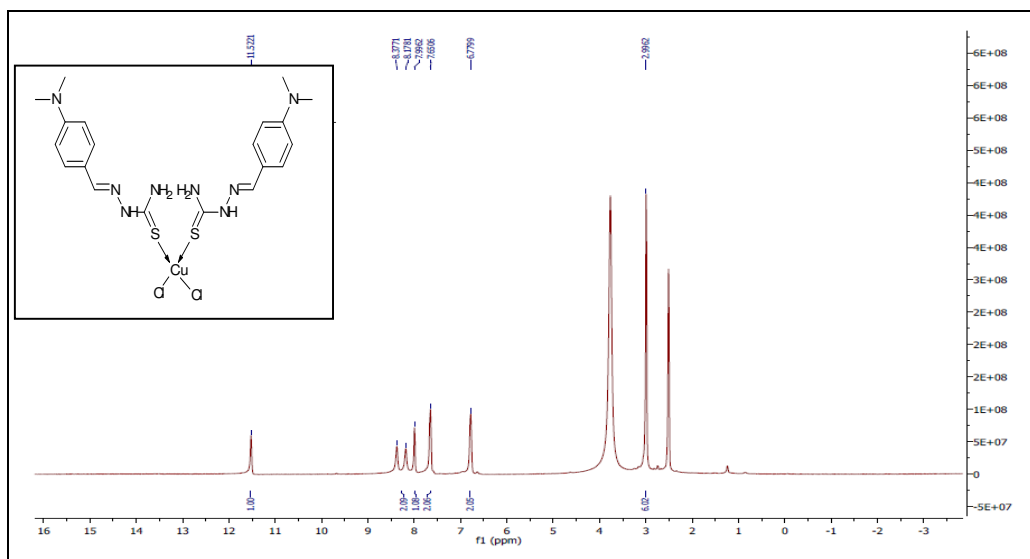


Fig. 5.7 $^1\text{H-NMR}$ spectrum of **C8**

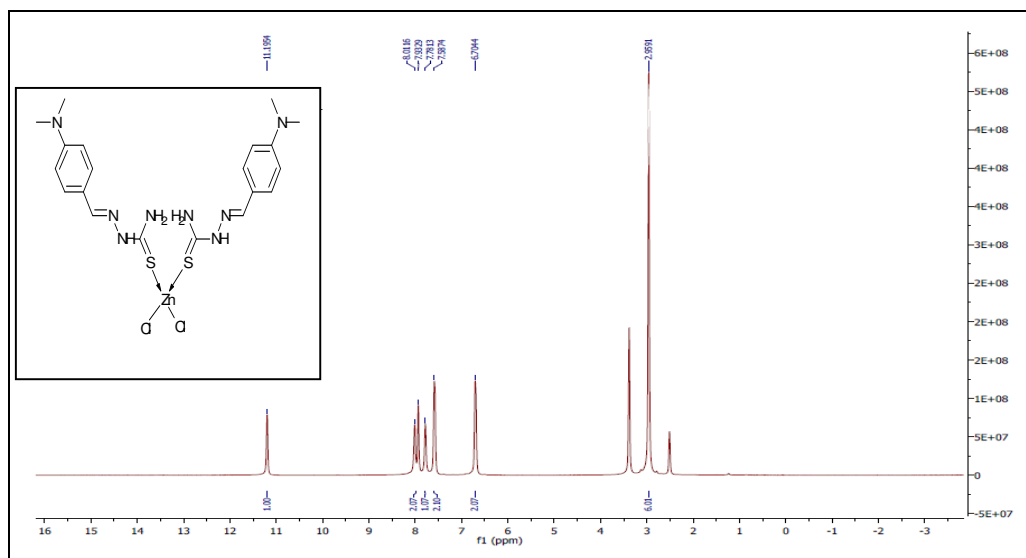


Fig. 5.8 ¹H-NMR spectrum of **C9**

5.4.3 UV-Visible spectra

The electronic absorption spectra (Fig. 5.9) of the complexes were recorded in dimethylformamide (DMF). The spectra of the complexes are dominated by one main absorption band in the region 281 nm in ligand and whereas in ligand the λ_{max} is shifted by 5 to 20 nm, i.e. the λ_{max} varies from 300 to 310 nm (Table 5.1). It is observed that the λ_{max} of the metal complexes is shifted to the visible region indicating the complex formation and this transition may be attributed to $\pi \rightarrow \pi^*$ electronic transition (Sutton 1968). Also a peak around 335 nm is observed which can be attributed to $n \rightarrow \pi^*$ transitions of nonbonding electron pairs of N and S atoms (Tian et al 2002).

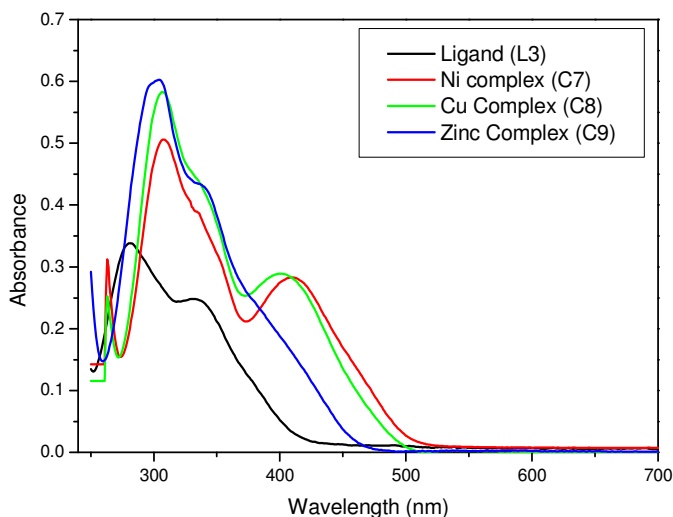


Fig. 5.9 Linear absorption spectra of ligand **L3** and complexes **C7-C9**

5.5 NONLINEAR OPTICAL MEASUREMENTS

The open aperture Z-scan curves of complexes (**C7** to **C9**) are given in Fig. 5.10 to Fig. 5.12 respectively. To determine the nature of the nonlinearity, we tried fitting the data numerically to two-photon and three-photon absorption equations, given by equation (5.1) and (5.2) respectively. The best fit was obtained for the transmission equation corresponding to a three-photon nonlinear absorption (3PA), given by equation (5.2) (Sutherland 2003).

$$T = \left((1-R)^2 \exp(-\alpha L) / \sqrt{\pi} q_0 \right) \int_{-\infty}^{+\infty} \ln \left[\sqrt{1 + q_0 \exp(-t^2)} \right] dt \quad \dots\dots\dots (5.1)$$

$$T = [(1-R)^2 \exp(-\alpha_o l) / p_o \sqrt{\pi}] \times \int_{-\infty}^{+\infty} \ln \left[\sqrt{1 + p_o^2 \exp(-2t^2)} + p_o \exp(-t^2) \right] dt \quad \dots\dots\dots (5.2)$$

where T is the light transmission through the sample, and R is the surface reflectivity. p_o is given by $2\gamma(1-R)^2I_o^2L$, where γ is the three photon absorption co-efficient and I_o is the on-axis peak intensity. α_o is the linear absorption coefficient.

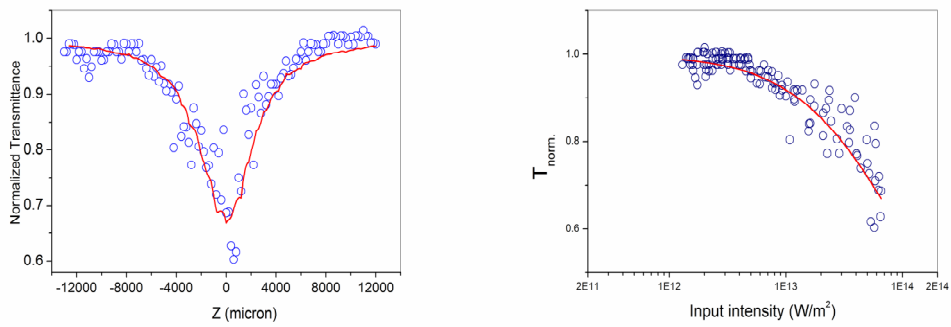


Fig. 5.10 (a) Open aperture Z-scan curve.. Circles are data points while solid curve is a numerical fit for three-photon absorption. (b) Nonlinear transmission in **C7**.

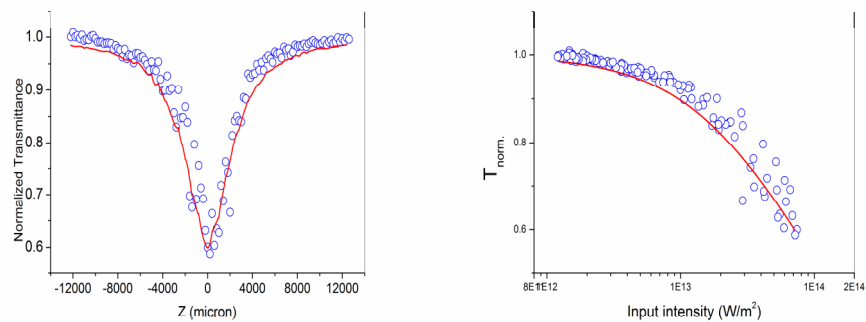


Fig. 5.11 (a) Open aperture Z-scan curve. Circles are data points while solid curve is a numerical fit for three-photon absorption. (b) Nonlinear transmission in **C8**

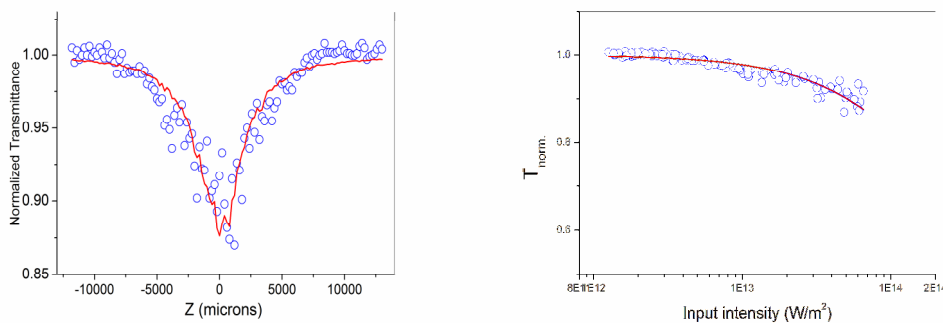


Fig. 5.12 (a) Open aperture Z-scan curve. Circles are data points while solid curve is a numerical fit for three-photon absorption. (b) Nonlinear transmission curve of **C9**

3PA is a process in which an electron transits to the conduction band from the valence band by simultaneously absorbing three photons. This involves two virtual (Fig. 5.13) transitions in which photon energies of at least one-third the band-gap are absorbed. In other words, the 3PA resonance peak occurs at wavelengths three times longer than the single photon absorption peak. During the 3PA process, excitation is proportional to the cube of the incident intensity. This feature may help to obtain higher contrast and resolution in imaging, since 3PA provides a stronger spatial confinement. With the usage of ultrafast pulsed lasers, it is possible to extend the applications of 3PA materials like three-photon pumped lasing and 3PA based optical limiting and stabilization (Zheng et al. 2005). On incorporation of transition metals to organic chromophores, the rate of intersystem crossing (ISC) can be enhanced. This generates long-lived triplet excited states. Such materials have the potential to display nonlinear absorption enhanced from an excited state absorption (ESA). As seen from Fig. 5.10 to Fig. 5.12, a decrease in

transmittance is observed as photon intensity increases. This characteristic presents this class of metal complexes as potential optical limiting materials (Reinhardt et al. 1998, McKay et al. 2001).

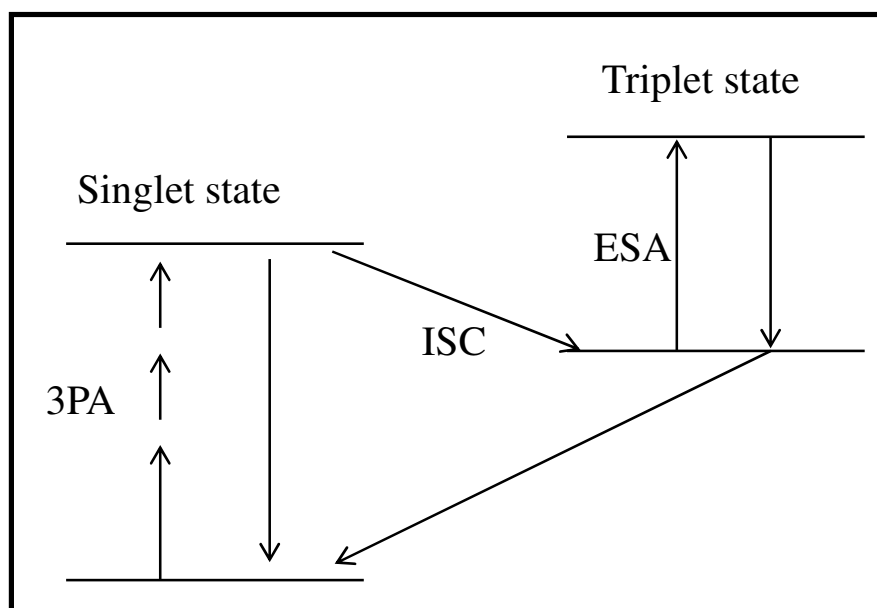


Fig. 5.13 Energy level diagram showing three photon absorption

Considerable interest in the development of three photon absorbing (3PA) materials has grown in the past decade and significant advances in the design of these materials have been recently made, but still there is scope for improvement. In the design of nonlinear optical materials, the metal plays a very important role contributing to increased NLO activity. The metal behaves as a template to configure ligands in a predictable octupolar arrangement. The metal can also induce metal to ligand charge transfer (MLCT) and a strong intraligand charge transfer (ILCT) due to its Lewis acid character. While building the architecture of multiphoton absorbing materials, the essential elements are the presence of electron accepting and electron releasing moieties

in the ligand environment. Keeping this in view, the configuration of the organic chromophore used in this project is an electron donating species with polarizable π -conjugation linked through the metal ion to the electron accepting halogen ligands.

In the present work, the calculated 3PA coefficients are $2.0 \times 10^{-24} \text{ m}^3/\text{W}^2$ for **C9**, $5.9 \times 10^{-24} \text{ m}^3/\text{W}^2$ for **C7** and $8.49 \times 10^{-24} \text{ m}^3/\text{W}^2$ for **C8**. It may be noted that what we observe is not a genuine 3PA as seen in transparent media where the intermediate levels are virtual; rather we are dealing with a resonant nonlinearity which is enhanced due to linear absorption at the excitation wavelength. Such kind of nonlinearities has been earlier reported in fullerenes, semiconductors, metal nanoclusters, phthalocyanines and some fluorine derivatives (Cassano et al. 2001, Harilal et al. 1999, Tutt and Boggess 1933, Philip et al. 2000, Santosh kumar et al. 2007, Cohanoschi et al. 2006, Nair et al. 2008). As a comparison, the hyperpolarizability value for $[\text{Ag}(\text{L})_2](\text{NO}_3) \cdot (\text{MeOH}) \cdot (\text{EtOH})$ and $[\text{HgI}_2(\text{L})]$ {L = 1,2-bis[(ferrocen-1-ylmethylene)amino]ethane} complexes was found to be 2.68×10^{-30} esu and 1.44×10^{-30} esu respectively (Hou et al. 2003). A novel zinc (II) 1,3,5 -triazine-based complex $[\text{Zn}(\text{TIPT})\text{Cl}_2] \cdot 2\text{CH}_3\text{OH}$ (TIPT = 2,4,6-tri(2-isopropylidene-1-ly)hydrazono-1,3,5-triazine) was prepared and structurally characterized and the hyperpolarizability γ value was found to be 8.26×10^{-30} esu (Yaoting et al. 2004). From Table 5.3 it can be observed that the synthesized complexes exhibited a very good 3PA coefficients γ , thereby making them potential alternatives for applications in optoelectronics.

Table 5.3 Three photon coefficient γ of thiosemicarbazide complexes

Complex	3PA coefficient γ (m^3/W^2)
Nickel complex (C7)	5.9×10^{-24}
Copper complex (C8)	8.4×10^{-24}
Zinc complex (C9)	2×10^{-24}

CHAPTER 6

THIRD-ORDER NONLINEAR OPTICAL STUDY OF COPPER COMPLEXES USING Z-SCAN TECHNIQUE

Abstract

Three Cu(I) halide complexes [Cu(L)(PPh₃)X] (L=1,10-phenanthroline, X= Cl (C10), Br (C11) and I (C12), PPh₃ = triphenylphosphine) have been synthesised and characterised by spectroscopic techniques. Further, structure of the complex C10 was confirmed by single crystal X-ray diffraction analysis. The nonlinear optical properties of the complexes were investigated at 532 nm using single beam Z-scan technique with nanosecond laser pulses. The complexes showed optical limiting behavior due to effective three-photon absorption (3PA). These studies demonstrate that the ligand→copper coordinative bonds facilitate the polarization of the electronic π -system which optimizes the third-order NLO response in the reported complexes. The contribution of the excited states to the total nonlinear absorption process has also been discussed. The results reveal the potential of this newly designed compound for multi-photon absorption-based photonic applications.

6.1 INTRODUCTION

The development of new materials that exhibit nonlinear optical response and have the potential for commercial device applications continues to be of primary interest in industrial and university laboratories (Marder 1995). Transition-metal and organometallic complexes are interesting subclass of molecular NLO compounds which offer extensive scope for the creation of multifunctional optical materials (Nalwa 1991), such as redox switchable NLO responses (Coe et al. 1999). The incorporation of

transition metal ions introduces more sublevels into the energy hierarchy, thus permitting more allowed electronic transitions and giving larger NLO effects (Chao et al. 1999). Organometallic and coordination compounds have highly polarisable *d*-orbitals, which can overlap effectively with ligand orbitals, either in the ground or excited states, leading to highly polarizable compounds with good third order NLO properties. The metal-ligand interaction can be tuned by varying the metal atom, the oxidation state of the metal or the surrounding ligands. It should thus be possible to exploit the good electronic flexibility of organometallic and coordination compounds to develop new third-order NLO materials (Lori et al. 1995).

Among the transition metal complexes, copper (I) complexes containing diimine and/or phosphine ligands have been extensively studied for their photophysical properties, photoinduced electron-transfer reactions, excited-state substrate-binding reactions (McMillin and McNett 1998, Yam and Lo 1999, Mao et al. 2003, Hu et al. 2005, Liu et al. 2006). Few Cu(I) compounds have also been reported for their nonlinear optical activities (Renouard et al. 1999, Kang et al. 2004, Kiran et al. 2005).

Despite a number of previous reports on the NLO properties of various metal complexes in solutions, the interest in ultrafast NLO properties of high-quality thin film and crystalline forms of novel metal complexes has sustained over past years since they are crucial for any photonic devices. Recent reports have indicated the importance of studies on the mechanisms of third-order nonlinear response and nonlinear absorption of metal complexes by using laser pulses with different pulse widths (Guo et al. 2007, He et al. 2008). Since both two-photon absorption (2PA) and three-photon absorption (3PA) are of interest and they are now easily achievable with the ultrafast lasers, there is a growing demand for such novel materials for multi-photon microscopy, data storage and optical power limiting (Bhawalkar et al. 1996, Zheng et al. 2005).

Based upon the consideration of the above requirements, in the present chapter we have synthesized three co-ordinated copper halogen complexes using 1,10-

phenanthroline and triphenylphosphine as ligands. Both these ligands (1,10-phenanthroline and triphenylphosphine) have strong π -accepting character. Cu(I) is a soft electron donor which can easily give out its electron density towards ligands through its switchable oxidation states. This will lead to acceptor-donor-acceptor type electron transitions between ligands and metal. Considering the above situation Cu(I) complexes were synthesized and tested for NLO applications.

6.2 EXPERIMENTAL

6.2.1 Materials

Reagent grade 1,10-phenanthroline, CuBr, CuI and CuCl were received from Merck, and triphenyl phosphine was purchased from Spectrochem Pvt. Ltd. Remaining chemicals and reagents were obtained from commercial sources and were used as supplied.

6.2.2 Physical measurements

Electronic spectra of the complexes in 200-800 nm range were measured on a GBC UV-Vis double beam spectrophotometer in N,N-dimethylformamide solution. FT-IR spectra were recorded on a Thermo Nicolet Avatar FT-IR spectrometer as KBr powder in the frequency range 400-4000 cm^{-1} . The C, H, N and S contents were determined by Thermoflash EA1112 series elemental analyzer. ^1H and ^{31}P NMR spectra were recorded on a Bruker AV-400 (at 400.08 MHz and 100.60 MHz). Individual spectra were referenced relative to residual solvent. Melting points were determined in open glass capillaries using a Stuart Scientific SMP1 apparatus and are uncorrected.

The single crystal X-ray diffraction experiment was carried out with a Oxford Diffraction X'calibur Mova diffractometer (graphite monochromated Mo $K\alpha$ radiation, $\lambda = 0.71073 \text{ \AA}$, ω -scan technique, $T = 295 \text{ K}$). CrysAlisPro CCD software was used for

collecting frames of data. The indexing of reflections, determination of lattice constants, integration of intensities of reflections, scaling and absorption correction and space group were carried out by CrysAlisPro RED of Oxford diffraction. The structure determination, refinements, graphics, and structure reporting are done by WinGX (Version 1.63.04a) (Farrugia 1999). The structures were solved by direct methods and refined by the full-matrix least-squares technique against F² using SHELXL97 (Sheldrick 2008) with the anisotropic thermal parameters for all non-hydrogen atoms. Hydrogen atoms were fixed to their position geometrically and refined using riding model.

A time-resolved DOKG (Sutherland 2003) experiment with a Ti:Sapphire laser delivering 90 fs pulses at a repetition rate of 92 MHz at 800 nm was used to investigate the third-order optical nonlinearity of the composite. The laser beam was divided into pump and probe beams with 20:1 intensity ratio by a beam splitter. The polarization of the probe beam was set to 45° with respect to that of the pump beam by a half-waveplate. Two beams were focused on the sample by a convex lens of focal length 7 cm. The time delay of the probe with respect to the pump was controlled by a PC-driven linear translator (PI, M-014.D01). At the zero time delay, the two beams overlap spatially and temporally, and the probe beam polarization rotates due to the birefringence induced in the sample by the pump beam. The pump beam, after passing through the sample, was blocked and the probe beam was passed through a quarter-waveplate. The circularly polarized probe beam was then split into two beams by a polarizing cube beam splitter and the two beams were detected by a photodetector pair connected to a lock-in amplifier. CS₂ was used to check the reliability of the set-up as well as to estimate the $\chi^{(3)}$ of the sample. Additionally, a single-beam Z-scan technique (Sheik-Bahae 1990) was used to investigate the nonlinear absorption property of the composite over a wide wavelength range. An optical parametric oscillator synchronously pumped with a Ti:Sapphire laser operating at 80 MHz, tunable in the wavelength range from 1000 to 1600 nm (150–320 fs, 80 MHz), was employed in the study. The laser beam was focused by a convex lens on the sample. Using the knife edge method, the beam waist at 800 and

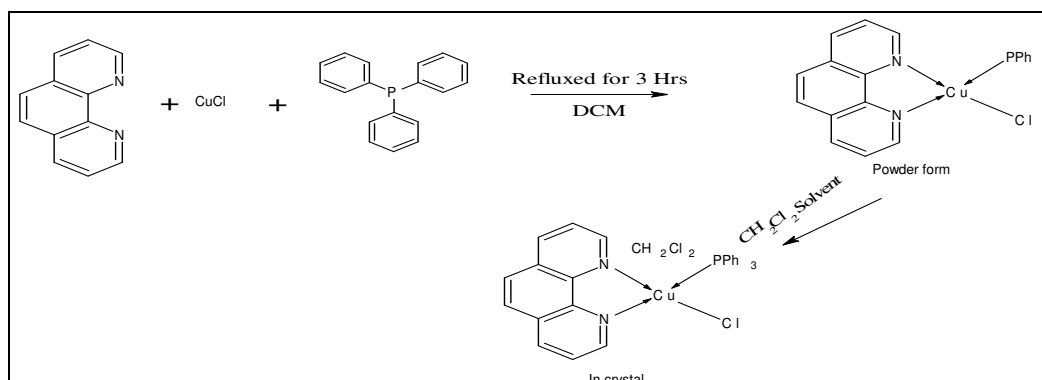
1250 nm was estimated as 16 and 18 μm , respectively.

6.3 SYNTHESIS OF METAL COMPLEXES

6.3.1 Synthesis of $\text{CuCl}(\text{Phen})\text{PPh}_3$ (C10)

1,10-phenanthroline monohydrate (0.24g, 1.24 mmol), triphenylphosphine (0.32g, 1.24 mmol) and cuprous chloride (0.12g, 1.24 mmol) were taken in dichloromethane solution (20 ml). This mixture was refluxed for 3 hours in nitrogen atmosphere and evaporated to 1/3rd of its content and precipitate was obtained by adding petroleum ether. After slow evaporation at room temperature, yellow crystals had formed in dichloromethane, which were suitable for X-ray diffraction. The synthetic scheme for metal complex **C10** is given in Scheme 6.1.

Yield: 86%. M.P: 250 °C Anal Calc. for crystal $\text{C}_{31}\text{H}_{25}\text{Cl}_3\text{CuN}_2\text{P}$ (626.08): C, 59.42; H, 4.02; N, 4.47. Found: C, 59.16; H, 3.89; N, 4.35 %. Anal Calc. for powder sample $\text{C}_{30}\text{H}_{23}\text{ClCuN}_2\text{P}$ (541.49): C, 66.54; H, 4.28; N, 5.17. Found: C, 66.05; H, 4.14; N, 5.05 %. $^1\text{HNMR}$, δ : 7.84 (m,2H), 8.08 (s,2H), 8.61 (d,2H), 8.99 (bs,2H), 7.38-7.15 (m,15H) $^{31}\text{PNMR}$, δ : 26.48. IR (KBr, cm^{-1}): 1434(m), 1094(s), 697(m), 740(s), 430(m). UV-Vis: λ_{max} , nm (DCM): 268, 386.

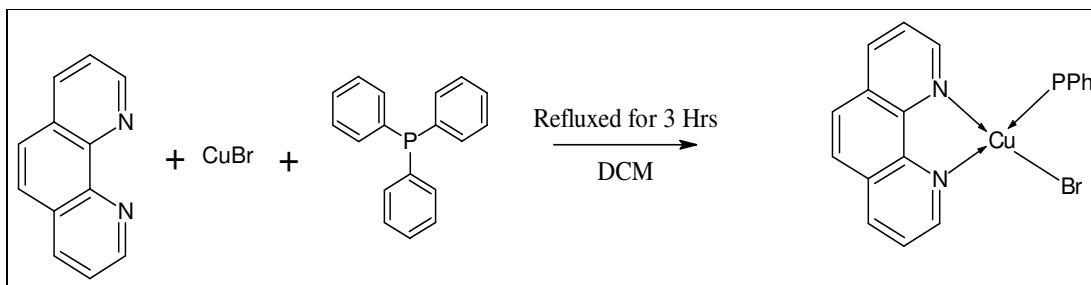


Scheme 6.1 Synthetic scheme for **C10**

6.3.2 Synthesis of CuBr(Phen)PPh₃ (C11)

1,10-phenanthroline monohydrate (0.24g, 1.24 mmol), triphenylphosphine (0.32g, 1.24 mmol) and cuprous bromide (0.17g, 1.24 mmol) were taken in dichloromethane solution (20 ml). This mixture was refluxed for 3 hours in nitrogen atmosphere and evaporated to 1/3rd of its content and precipitate was obtained by adding petroleum ether, filtered and washed repeatedly with petroleum ether and dried in *vacuo*. The synthetic scheme for metal complex **C11** is given in Scheme 6.2.

Yield: 85% M.P: 253°C. Anal Calc. for C₃₀H₂₃BrCuN₂P(585.94): C, 61.49; H, 3.96; N, 4.78. Found: C, 61.17; H, 3.60; N, 4.52%. ¹HNMR, δ: 7.94 (m,2H), 8.18 (s,2H), 8.74 (d,2H), 8.96 (bs,2H), 7.42-7.33 (m,15H). ³¹PNMR, δ: 26.47. IR (KBr, cm⁻¹): 1428(m), 1095(s), 696 (m), 738(s), 433(m). UV-Vis: λ_{max}, nm (DCM): 268, 367.



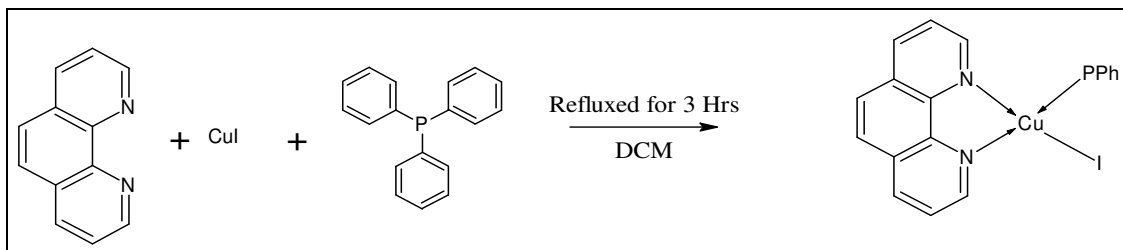
Scheme 6.2 Synthetic scheme for **C11**

6.3.3 Synthesis of CuI(Phen)PPh₃ (C12)

1,10-phenanthroline monohydrate (0.24g, 1.24 mmol), triphenylphosphine (0.32g, 1.24 mmol) and cuprous iodide (0.24g, 1.24 mmol) were taken in dichloromethane solution (20 ml). This mixture was refluxed for 3 hours in nitrogen atmosphere and evaporated to 1/3rd of its content and precipitate was obtained by adding petroleum ether,

filtered and washed repeatedly with petroleum ether and dried in *vacuo*. The synthetic scheme for metal complex **C12** is given in Scheme 6.3.

Yield: 82 %. M.P: 244°C Anal. Calc. for $C_{30}H_{23}ICuN_2P$ (632.94): C, 56.93; H, 3.66; N, 4.43. Found: C, 56.38; H, 3.35; N, 4.20%. 1H NMR, δ : 7.98 (m,2H), 8.19 (s,2H), 8.74 (d,2H), 9.01 (d,2H), 7.63-7.38 (m,15H). ^{31}P NMR, δ : 26.47. IR (KBr, cm^{-1}): 1432(m), 1097(s), 696(m), 748(s), 431(m). UV-Vis: λ_{max} , nm (DCM): 268, 367.



Scheme 6.3 Synthetic scheme for **C12**

6.4 RESULTS AND DISCUSSION

The analytical data showed that the observed values are in good agreement with the theoretical values (Table 6.1).

Table 6.1 Analytical and electronic spectral data of complexes **C10-C12**

Complex	Decom temp (°C)	% Found (Theoretical)			UV-vis Data, λ_{\max} (nm)	
		C	H	N	Intraligand transitions	
C10 crystal powder	250	59.16(59.42)	3.89(4.02)	4.35(4.47)	268	386
		66.05(66.54)	4.14(4.28)	5.05(5.17)		
C11	253	61.17(61.49)	3.60(3.96)	4.52(4.78)	268	367
C12	244	56.38(56.93)	3.35(3.66)	4.20(4.43)	268	367

6.4.1 FT-IR Spectra

The FT-IR spectra of the complexes exhibit a band around 430 cm^{-1} , which is assigned to $\nu(\text{Cu-N})$ stretching vibration in all the three complexes. Three bands due to triphenylphosphine were observed around 1438, 1095 and 695 cm^{-1} (Ramakrishna et al. 2010). The characteristic peaks are given in Table 6.2. The typical IR spectra of the complexes are given in Fig 6.1 to Fig. 6.3.

Table 6.2 Infrared spectral data (cm^{-1}) for complexes **C10-C12**

Compound	Bands due to PPh_3	$\nu(\text{Cu-N})$
C10	1434, 1094, 697	430
C11	1428, 1095, 696	433
C12	1432, 1097, 696	431

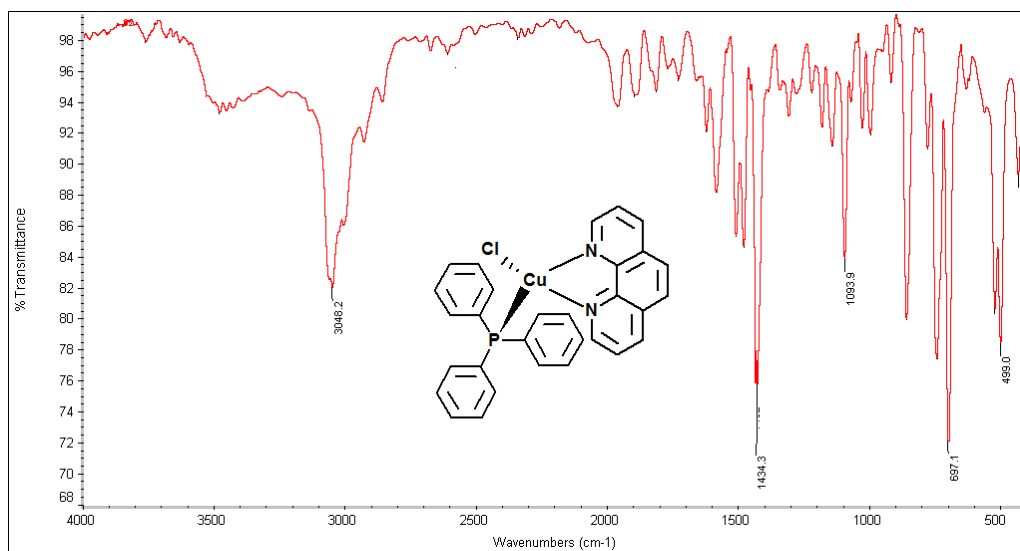


Fig. 6.1 IR spectrum of **C10**

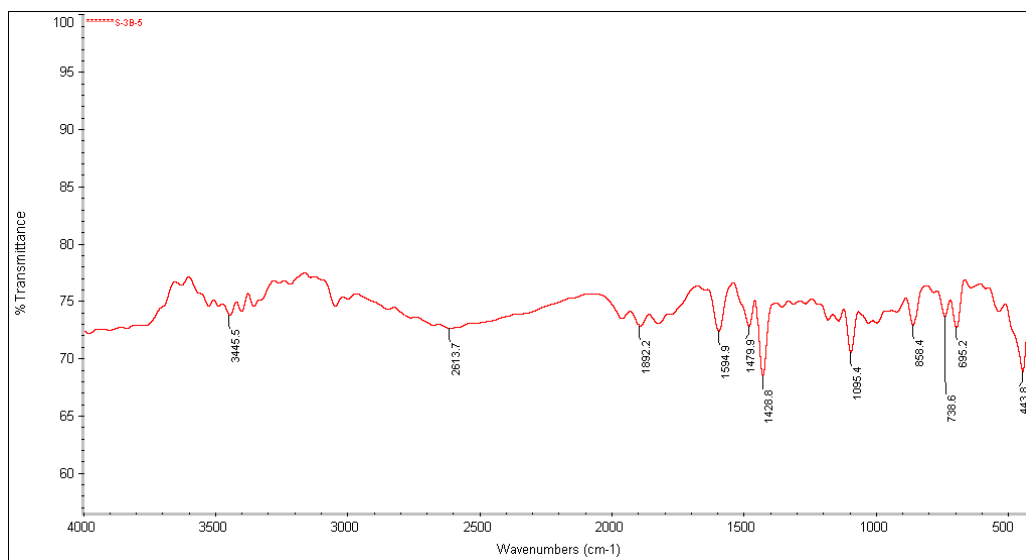


Fig. 6.2 IR spectrum of **C11**

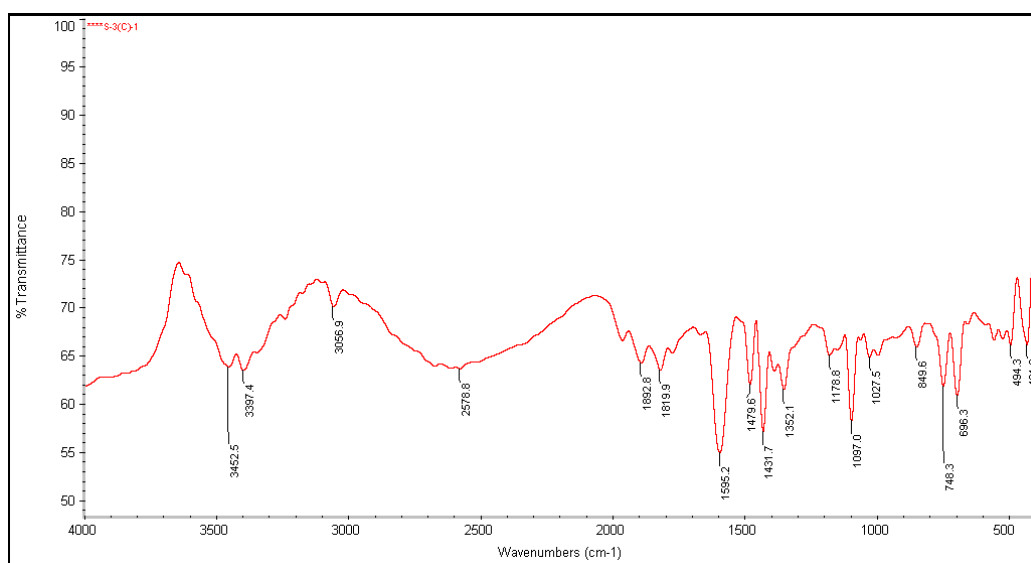


Fig. 6.3 IR spectrum of **C12**

6.4.2 NMR Spectra

To evaluate the incorporation of the ligand in the complex, both ^1H and ^{31}P -NMR of the complexes were recorded. The NMR spectra of all the complexes show presence of coordinated 1,10-phenanthroline and triphenylphosphine ligands in the region 7.1 to 9.2 δ value. The characteristic ^1H -NMR and ^{31}P -NMR shifts are shown in Table 6.3. The ^1H -NMR spectra of the complexes **C10-C12** are given in Fig 6.4 to Fig. 6.6.

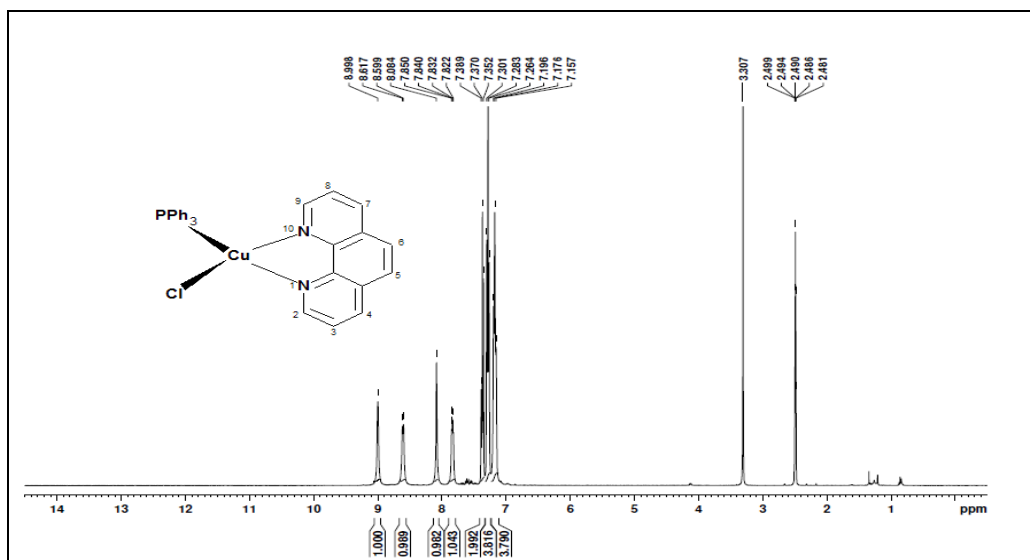


Fig. 6.4 ¹H-NMR spectrum of C10

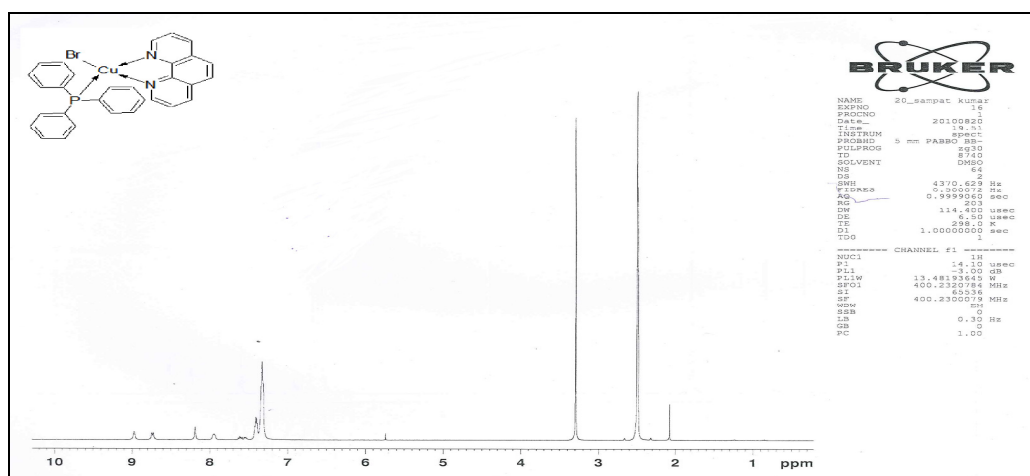


Fig. 6.5 ¹H-NMR spectrum of C11

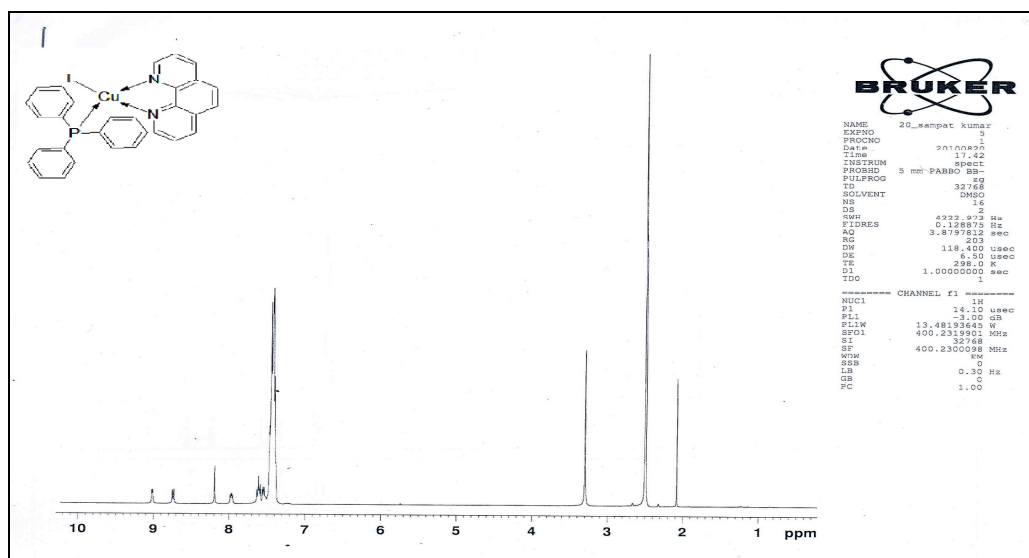


Fig. 6.6 ^1H -NMR spectrum of C12

Table 6.3 ^1H -NMR and ^{31}P -NMR spectral details of complexes

Complex	^1H NMR Position (δ)	^{31}P NMR (δ)
C10	δ : 7.84 (m, 2H), 8.08 (s, 2H), 8.61 (d, 2H,), 8.99 (bs, 2H,) δ : 7.38-7.15(m, 15H)	26.48
C11	δ : 7.94 (m, 2H), 8.18 (s, 2H), 8.74 (d, 2H,), 8.96 (bs, 2H,) δ : 7.42-7.33(m,15H)	26.47
C12	δ : 7.98 (m, 2H), 8.19 (s, 2H), 8.74 (d, 2H,), 9.01 (d, 2H,) δ : 7.63- 7.38(m,15H)	26.47

6.4.3 Single Crystal XRD

X-ray quality prismatic-shaped single crystal of complex **C10** was obtained by slow evaporation of the dichloromethane solution at room temperature. X-ray

crystallography data reveals that the main structure of these three complexes described as $[\text{Cu}(\text{X})(\text{phen})(\text{PPh}_3)]$ ($\text{X} = \text{Cl}, \text{Br}, \text{I}$) are similar to each other (Jin et al. 1999, Hua et al. 1998). In complex **C10**, 1,10-phenanthroline acts as a bidentate ligand coordinating via two N atoms to copper (Fig. 6.7). The coordination around the Cu atom is a distorted tetrahedron, with a Cu-P distance of 2.183 Å, Cu-N distance of 2.078 and 2.123 Å and Cu-Cl distance of 2.300 Å; with triclinic crystal system, space group P-1, cell lengths $a=9.350(5)$ $b=12.179(5)$ $c=13.721(5)$ and cell angles $\alpha=88.599(5)$ $\beta=73.405(5)$ $\gamma=77.593(5)$.

The molecular structure of the complex **C10** is shown Fig. 6.7a and Fig. 6.7b. Their selected geometric parameters and crystallographic data are provided in Table 6.4 and Table 6.5 respectively.

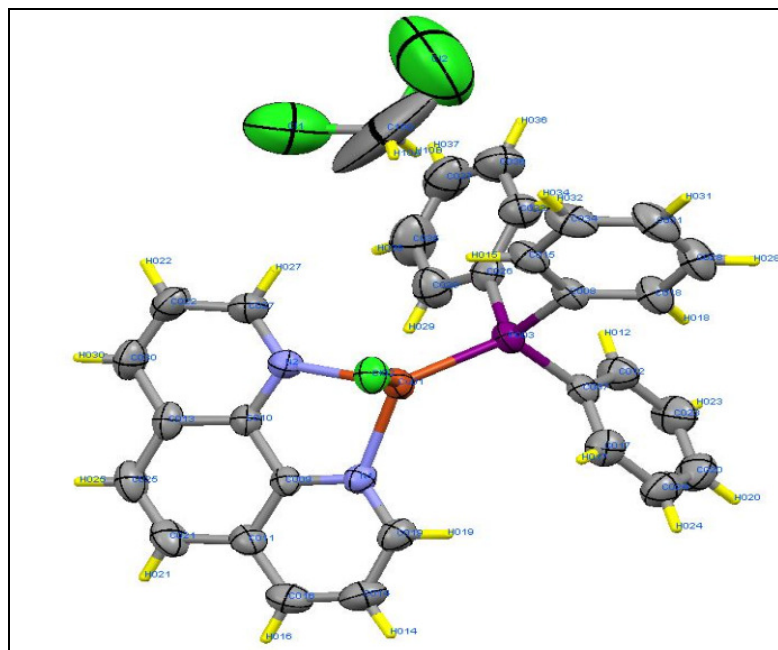


Fig. 6.7(a) Single crystal XRD structure of **C10** with solvent (CH_2Cl_2) of crystallization

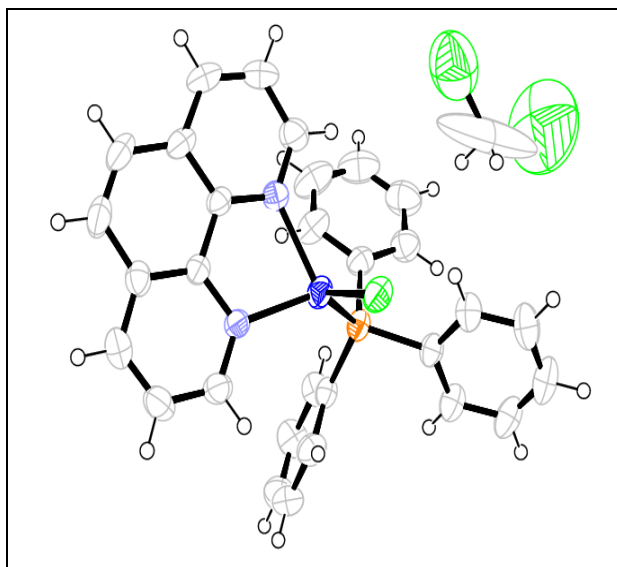


Fig. 6.7(b) View of complex **C10**. Displacement ellipsoids are shown at the 50% probability level. Hydrogen atoms are of arbitrary size.

Table 6.4 Selected geometric parameters (Å, °)

Cu-X	2.2999(11)	N1-Cu-X	103.18(8)
Cu-N1	2.0780(30)	N2-Cu-X	106.70(8)
Cu-N2	2.1228(28)	N1-Cu-P	124.90(8)
Cu-P	2.1829(11)	N2-Cu-P	117.72(7)
N2-Cu-N1	79.78(10)	P-Cu-X	117.75(3)

Table 6.5 Crystallographic data and structure refinement summary for **C10**

Crystal data	I
Crystal Size (mm)	0.30 × 0.28 × 0.25
Solvent	CH ₂ Cl ₂
Formula	C ₃₁ H ₂₅ Cl ₃ Cu ₁ N ₂ P ₁
Formula weight (g mol ⁻¹)	626.39
Temperature (K)	295(2)
Wavelength (Å)	0.71073
Crystal system	Triclinic
Space group	<i>P</i> - 1
<i>a</i> (Å)	9.350(5)
<i>b</i> (Å)	12.179(5)
<i>c</i> (Å)	13.721(5)
α (°)	88.599(5)
β (°)	73.405(5)
γ (°)	77.593(5)
Volume (Å ³)	1461.3(11)
Z	2
Density (g/cm ³)	1.424
μ (mm ⁻¹)	1.100
<i>F</i> (000)	640
$\theta_{\min, \max}$	3.10, 26.0
$h_{\min, \max}, k_{\min, \max}, l_{\min, \max}$	(-11, 11), (-15, 15), (-16, 16)
Treatment of Hydrogens	Isotropic
No of refln measured	29469
No of unique refln reflections	5735
No of parameters	343
R _{all} , R _{obs}	0.0710, 0.0468
wR _{2_all} , wR _{2_obs}	0.1371, 0.1308
$\Delta\rho_{\min, \max}$ (eÅ ⁻³)	-0.736, 0.642
G.o.F	1.075

Powder XRD Analysis

In order to confirm the difference of the original powder and the single crystal of sample **C10**, the powder XRD patterns were taken for the original powder (Fig. 6.8(a)). It was compared with the powder XRD pattern from the single crystal analysis (Fig 6.8(b)). It is observed that both the patterns show the difference in the diffraction pattern (in the range 10 to 20). This is possibly due to the presence of CH_2Cl_2 in the crystal structure. This is further supported by CHNS values of the powdered sample and crystal structure of the complex.

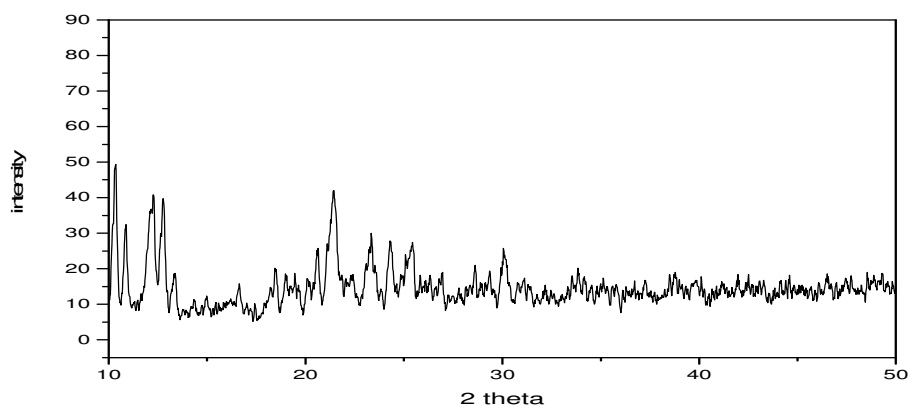


Fig. 6.8(a) Powder XRD of **C10** in powder form

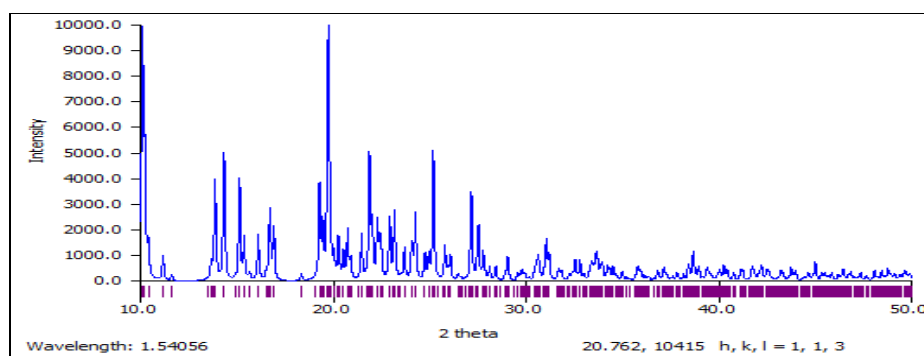


Fig. 6.8(b) Powder XRD of single crystal of **C10**

6.4.4 UV-Visible spectra

The electronic spectra (Fig. 6.9) of the complexes were recorded in dichloromethane. Spectrum of complexes are dominated by one main absorption band in the region 268 nm and a shoulder near 360-390 nm (Table 6.1) which are ascribed to the intra-ligand (π to π^*) transitions of triphenylphosphine. Also absence of bands ($d-d$) above 400 nm shows d^{10} electronic configuration of copper in the complexes. Since Cu(I) is reducing as well as oxidizing, MLCT and LMCT transitions will occur at relatively low energies (Horst et al. 2002).

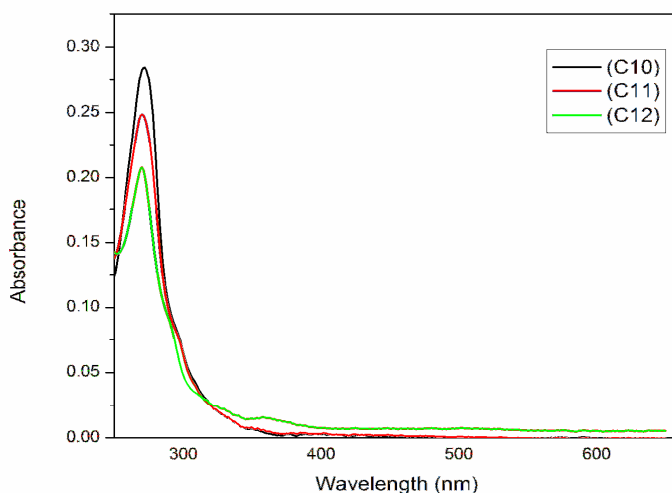


Fig. 6.9 Linear absorption spectra of complexes C10-C12

6.5 NONLINEAR OPTICAL MEASUREMENT

6.5.1 NLO measurement in solution state

6.5.1.1 Sample preparation

The third-order optical nonlinearity of complexes **C10**, **C11** and **C12** in DMF solution, at the concentration of 2.5mmol/L, was measured by Z-scan technique. At this concentration the solutions show a linear transmission of 65%, 62% and 65% respectively for complexes **C10**, **C11** and **C12**, at the excitation wavelength of 532 nm.

6.5.1.2 Z-scan measurement

The open aperture Z-scan curves of complexes (**C10** to **C12**) are given in Fig. 6.10 to Fig. 6.12 respectively. To determine the nature of the nonlinearity, we tried fitting the data numerically to two-photon and three-photon absorption equations. The best fit was obtained for the transmission equation corresponding to a three-photon nonlinear absorption (3PA), given by equation (Sutherland 2003)

$$T = [(1-R)^2 \exp(-\alpha_o l) / p_o \sqrt{\pi}] \times \int_{-\infty}^{\infty} \ln \left[\sqrt{1 + p_o^2 \exp(-2t^2)} + p_o \exp(-t^2) \right] dt \quad \dots\dots\dots (6.1)$$

where T is the light transmission through the sample and R is the surface reflectivity. p_o is given by $2\gamma(1-R)^2 I_o^2 L$, where γ is the three-photon absorption co-efficient and I_o is the on-axis peak intensity. α_o is the linear absorption coefficient. The calculated 3PA coefficients are $1.2 \times 10^{-23} \text{ m}^3/\text{W}^2$ for (**C12**), $3.2 \times 10^{-24} \text{ m}^3/\text{W}^2$ for (**C10**), and $6.0 \times 10^{-25} \text{ m}^3/\text{W}^2$ for (**C11**). It may be noted that what we observe is not genuine 3PA as seen in transparent media where the intermediate levels are virtual, rather we are dealing with a resonant nonlinearity which is enhanced due to linear absorption at the excitation wavelength. The calculated 3PA coefficients γ are given in Table 6.6.

Table 6.6 Three photon coefficient γ of copper complexes

Complex	3PA coefficient γ (m^3/W^2)
C10	3.2×10^{-24}
C11	6.0×10^{-25}
C12	1.2×10^{-23}

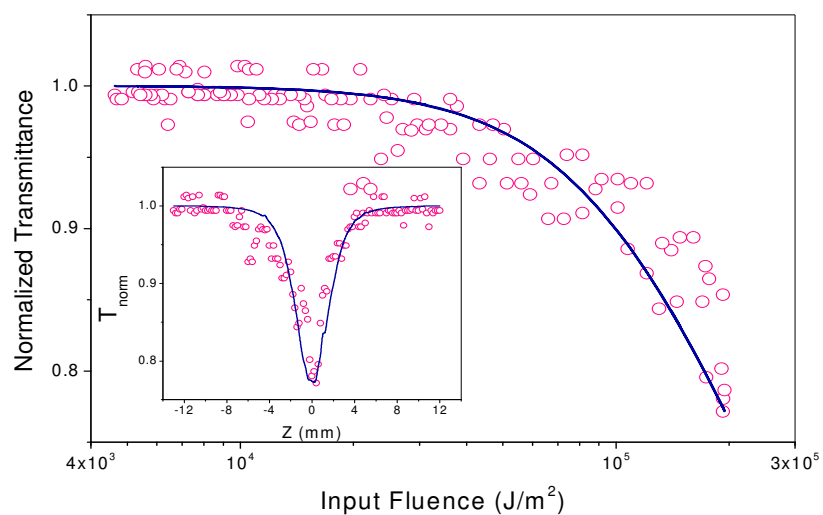


Fig. 6.10 Nonlinear transmission curve of **C10**. Inset shows the open aperture Z-scan curve. Linear transmission of the sample (corresponding to T (norm.) = 1) is 65%. Circles are data points while solid curves are numerical fits using equation 6.1.

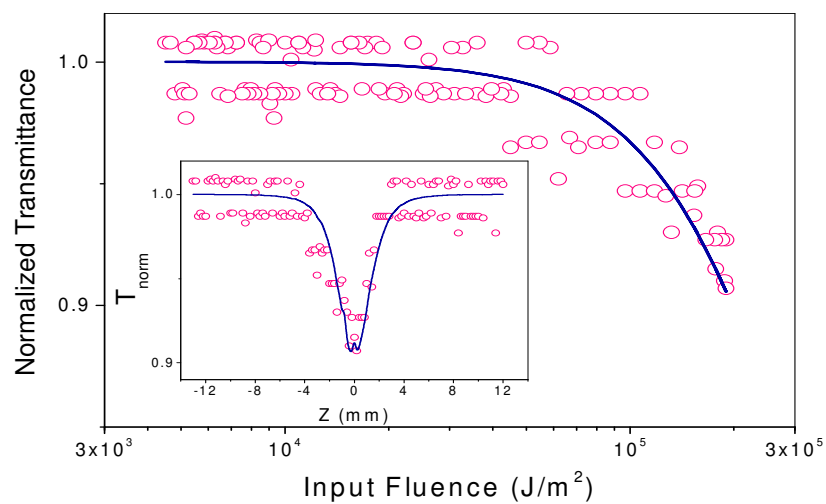


Fig. 6.11 Nonlinear transmission curve of **C11**. Inset shows the open aperture Z-scan curve. Linear transmission of the sample (corresponding to T (norm.) = 1) is 62%. Circles are data points while solid curves are numerical fits using equation 6.1.

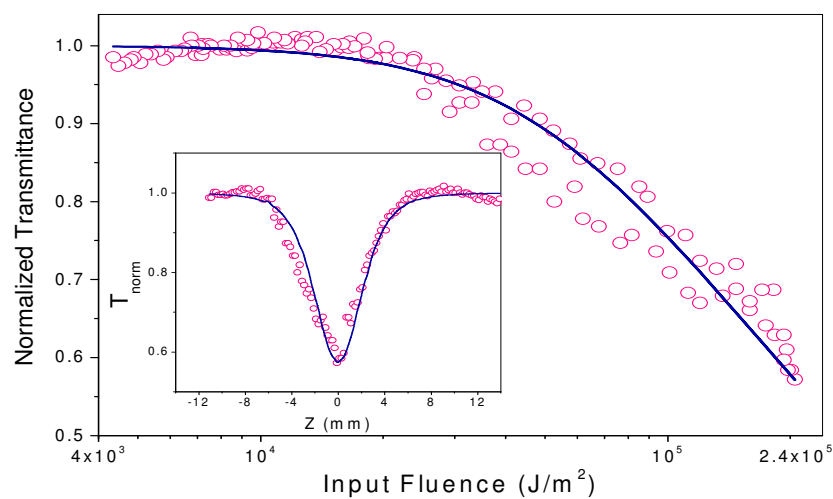


Fig. 6.12 Nonlinear transmission curve of **C12**. Inset shows the open aperture Z-scan curve. Linear transmission of the sample (corresponding to $T(\text{norm.}) = 1$) is 65%. Circles are data points while solid curves are numerical fits using equation 6.1.

6.5.2 NLO measurement using composite film

6.5.2.1 Composite film preparation

In order to prepare its composite with PMMA, 250 mg of PMMA (MW 140 000) and 2mg of compound were dissolved in 2.5 ml of dichlorobenzene (DCB). The concentration of the **C10** in the solution was 0.001 mol^{-1} . The solution was mixed thoroughly by stirring and via ultrasonication to ensure homogeneous mixing. The solution was subsequently spin coated at 1200 rpm on a glass substrate and the coated film was dried in a vacuum oven at 100°C for about 20 h. The film thickness (L) was measured to be $1.28 \mu\text{m}$, using an Alpha-step surface profiler (Tencor P-10). The films that were fabricated using DCB were clear, while those fabricated using dimethylformamide (DMF) as the solvent were hazy, whitish films due to the slow evaporation of DMF, despite the high solubility of the compound in the solvent.

6.5.2.2 NLO Measurement

It is already recognized that two major nonlinear absorption processes can be employed for optical limiting: one is the reverse saturable absorption (RSA) and the other is multi photon absorption (MPA) or MPA-initiated excited-state absorption (ESA). Investigation of nonlinear absorption at different wavelengths is required to examine such nonlinear absorption effects. The results of the nonlinear absorption measurements on the composite film at 800 nm are shown in Fig. 6.13. The nonlinear transmittance equation for an open aperture Z-scan, considering multiphoton absorption, is given by (Sutherland 2003).

$$TOA(nPA) = \frac{1}{[1 + (n - 1)\alpha_n L_{\text{eff}}(I_0/(1 + Z/Z_0)^2)]^{n-1}]^{1/(n-1)}} \dots\dots\dots (6.2)$$

where $n = 2$ and 3 represent 2P and 3PA, respectively, L_{eff} is the effective sample length define by $L_{\text{eff}}^{nPA} = (1 - e^{-(n-1)\alpha_0 L}) / (n - 1)\alpha_0$ (for $n = 2, 3$, etc), I_0 is the on-axis intensity and Z_0 is the Rayleigh range. The data corresponding to the input intensity of 8.7 GWcm^{-2} at 800 nm fit reasonably well if we assume 3PA. However, it should be noted that various organic materials exhibit 2P-assisted excited-state absorption when the intensity is sufficiently high; in the present case, considering the linear absorption near 400 nm . The 2P-assisted ESA process is considered as an intrinsically three-photon process, which is different from the coherent 3PA one (Das et al. 2001), i.e., 2P-assisted ESA is a three-photon process, although three photons are not absorbed simultaneously because of the finite lifetimes of the excited states. A qualitative formulation of 2P-assisted ESA is given by Das et al. (2001) and such a problem on a nanosecond (ns) timescale is treated as an effective 3PA case. The ESA varies linearly with both the width of the pulse and its strength, and for sufficiently large intensities the ESA can dominate MPA. Therefore, although the data seem to fit with equation (6.2) assuming a 3PA process, it is actually a two step process, where a large fraction of atoms are first generated in excited states by way of 2PA at low intensity which then, due to high intensity, linearly absorb the photons of the same wavelength. Additionally, there is an intraligand transition ($\pi-\pi^*$) at 268 nm (Fig. 6.9) in the **C10** compound, which sets the possibility of coherent 3PA at high intensity levels near 800 nm . This implies that the excited-state absorption process competes with the coherent 3PA process in this compound and, therefore, the measurement at 800 nm at higher intensity indicates a combined effect of the two processes.

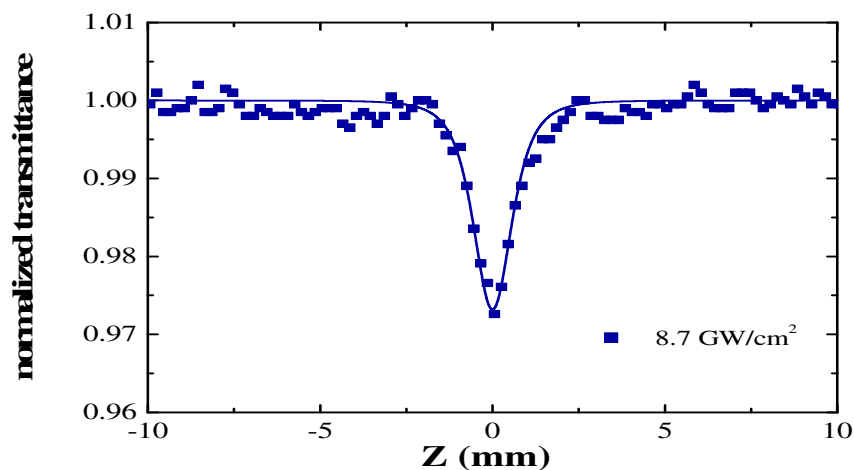


Fig. 6.13 Open aperture Z-scan results for **C10** at 800 nm. The data corresponding to the input intensity 8.7 GWcm^{-2} are fitted with equation (6.2), assuming 3PA.

Further, the effective absorption cross section of the two photon-induced excited state is a combination of both singlet–singlet and triplet–triplet ESA cross sections, which is laser pulse width dependent. Generally, in organic polyatomic molecules the transition of electrons from singlet (S) to triplet (T) states can take place and this singlet to triplet state intersystem crossing occurs on a nanosecond timescale (Couris et al. 1995). While Sutherland et al. (2005) proposed a one-step 3PA model to explain the 2PA-induced ESA observed on nanosecond timescale, Gu et al. (2008) have used a three-level two-step 3PA model to explain such a process observed in organic molecules in the fs regime, in which they combined singlet and triplet excited states to yield ST_n states. In the latter model, the system simultaneously absorbs two photons, promoting an electron from S_0 to ST_1 , whereby the electron can get excited to ST_2 by absorbing another single photon. In the present case, there can be contributions from both the singlet and the triplet excited states as the high repetition rate of laser pulses (80 MHz) can easily transfer the electron population from the first singlet to the low lying triplet state during the nonlinear

absorption process. The open aperture traces could be reproduced in the input intensity range involved in the experiments. The experiments were performed in non-resonant spectral regions; however, the cumulative thermal effects due to the high repetition rate of the laser pulses might also be playing their part in the nonlinear absorption process.

The investigation of nonlinear absorption was extended to a longer wavelength region. The nonlinear absorption trend of the sample at 1250 nm is shown in Fig. 6.14. A fit of data to equation (6.2) with 3PA yields the effective 3PA coefficient of $28 \text{ cm}^3 \text{ GW}^{-2}$. A direct comparison of this study with those of other organometallic or coordination compounds is rather hard because of different experimental conditions and reports on solutions. The $\chi^{(3)}$ value of the composite film is one order of magnitude larger than that of an organometallic polymer film measured near 1054 nm using picosecond pulses (Afanas'ev et al. 2002). An observation of 2PA and 3PA processes in the IR spectral region has been reported for solutions of fluorine-containing ferrocene derivatives in chloroform (Zheng et al. 2005). In another recent work, optical limiting of ns pulses based on RSA in Cu complexes, such as copper phthalocyanine/PMMA composite film coated on quartz substrates (Kurum et al. 2009) has been reported.

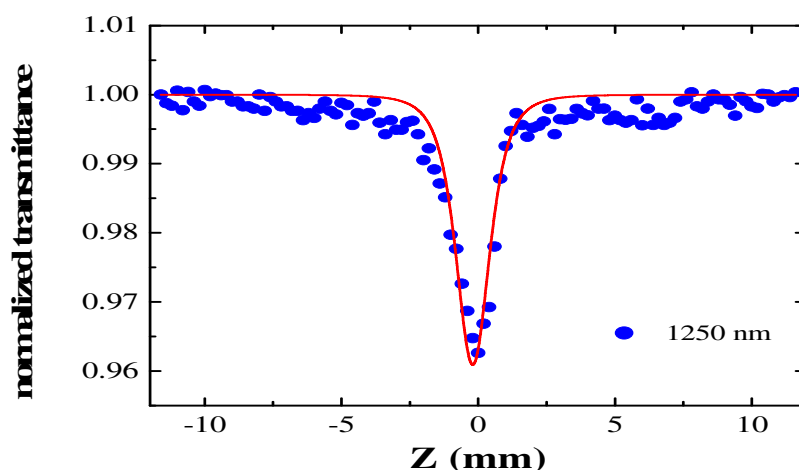


Fig. 6.14 3PA result for the compound in **C10** PMMA film at 1250 nm. The solid line is a theoretical data fit of the experimental.

—

6.5.2.3 Optical Kerr Gate measurement

The result of the DOKG experiment performed at 800 nm is depicted in Fig. 6.15. The solid line shows a fit to the experimental data. The optical Kerr effect (OKE) signal is symmetric about the zero time delay, indicating the nonlinear response time of the complex to be comparable to or faster than the laser pulse width (90 fs) used. Such an ultrafast response originates in this compound due to the conjugated π -electron system of ligands and is also influenced by metal–ligand interactions. CS₂ was used as the reference and its optical Kerr signal was recorded. CS₂ exhibited a biexponential nonlinear response curve (inset of Fig. 6.15) with response times of 0.2 and 1.8 ps, respectively. These values agree well with the previously reported values. The magnitude of $\chi^{(3)}$ for the sample can be estimated by comparing its OKE signal amplitude with that of CS₂ using the following equation 6.3 (Sutherland 2003).

$$\chi_s^{(3)} = \chi_r^{(3)} \left(\frac{I_s}{I_r} \right)^{1/2} \left(\frac{n_s}{n_r} \right)^2 \left(\frac{L_r}{L_s} \right) \times \frac{\alpha L_s}{\exp\left(-\frac{\alpha L_s}{2}\right) \cdot [1 - \exp(-\alpha L_s)]}, \quad \dots\dots\dots (6.3)$$

where the subscripts *s* and *r* represent the sample and the reference, *I* the absolute magnitude of the OKE signal, *n* the refractive index, *L* the thickness and α the linear absorption coefficient, respectively. The $\chi^{(3)}$ of CS₂ was taken as 1×10^{-13} esu (Sheik-Bahae 1990 and Minoshima 1991) and that of the composite film was derived to be 1.8×10^{-10} esu.

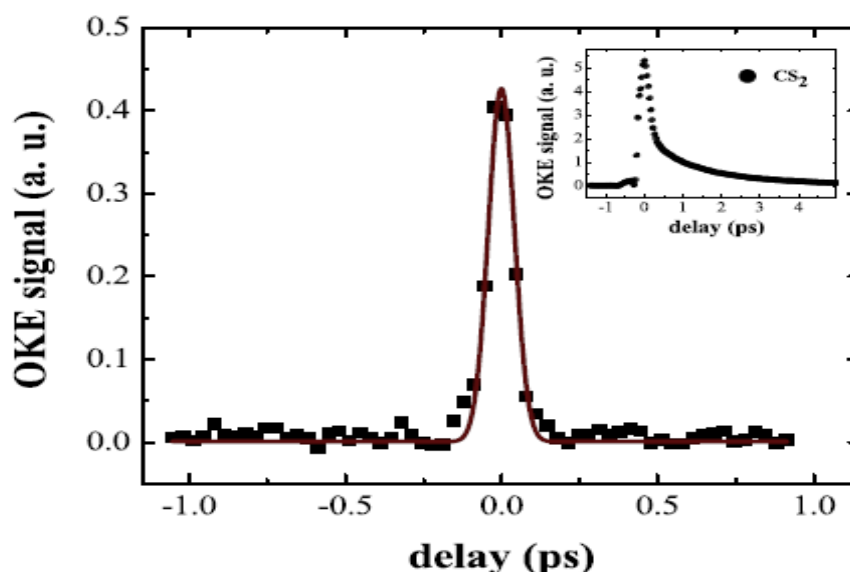


Fig. 6.15 Optical Kerr effect (OKE) signal from the C10 PMMA film at 800 nm. The nonlinear response is faster than or comparable to the laser pulse width (90 fs). The reference OKE signal of CS₂ is shown as an inset.

An ideal passive optical limiter based on a solid state NLO material should exhibit a low optical limiting threshold and a high speed response of the order of sub-ps and even shorter to efficiently limit potentially threatening ultrashort pulses (Tutt and Boggess 1993). The new metal complex that we developed seems to be very promising due to its remarkable nonlinear near-IR absorption and high transparency. The compound is thermally stable up to 250°C and exhibits no remarkable laser damage in the intensity range ($\sim 9 \text{ GW cm}^{-2}$) involved in the experiment. The design of this new metal complex demonstrates its significance in developing materials with large MPA coefficients. The NLO studies on a series of metal complexes derived from this compound will help us to understand metal–ligand charge transfer and identify ways to enhance the nonlinear absorption cross sections in these compounds. Present results

indicate the potential of this compound for applications demanding large MPA, such as optical power limiting, multi-photon microscopy and photodynamic therapy (Marder 2006).

CHAPTER 7

NONLINEAR OPTICAL STUDIES OF IONIC LIQUID TAGGED Ni(II) SCHIFF BASE COMPLEXES

Abstract

In the recent times, ionic liquids are beginning to be explored for their nonlinear optical responses. In this chapter, nonlinear optical behaviour of Schiff base Ni(II) complexes was studied by tagging with 1-methylimidazole ionic liquid. The ionic liquid tagged Schiff base ligand showed linear absorption in the UV region. The nonlinear optical studies were carried out at 532 nm using Z-scan technique. The complexes exhibited third order nonlinearity due to two photon absorption.

7.1 INTRODUCTION

Ionic liquids are organic salts that are in liquid state at room temperature. The important characteristics of ionic liquids are its low vapour pressure, thermal stability, high ionic conductivity, miscibility with other solvents and recyclable nature. Ionic liquids have a high utility in various applications like synthesis, catalysis, electrochemical and photo physical studies (Karmakar and Samanta 2002, Ingram et al. 2003, Chakrabarty et al. 2003, Paul et al. 2005). Ionic liquids are often described as “designer solvents”, as it is possible to design an ionic liquid with the desired properties using appropriate combinations of anionic and cationic constituents. Recently, ionic liquids are being explored for their optical properties. Some of these materials possess liquid crystal properties (Bowlas et al. 1996, Gordon et al. 1998), which indicate that these compounds may present large nonlinear optical responses. Organic materials with nonlinear optical responses have been used for the fabrication of opto-electronic devices such as optical

limiters, optical modulators and optofluidic lens (Calixto et al. 2009, Yin et al. 2007, Xu et al. 2005).

Among the coordinated complexes, metal complexes of Schiff base ligands have been extensively studied for their optical nonlinearity. Presence of extensive π -conjugation in the ligand environment adds on to the optical nonlinearity by increasing the hyperpolarizability. Also in the recent years, optical potential of room temperature ionic liquids based in imidazolium cations has been recognized. However, very few reports on its physicochemical and optical applications have been reported (Souza et al. 2008, Calixto et al. 2009). Hence in the present work, we aim to complement the nonlinear optical response of Schiff base metal complexes by tagging the ligands with imidazolium based ionic liquid. The nonlinear behaviour of the metal complexes thus synthesized has been elaborately discussed.

In this chapter, the synthesis, characterization and NLO measurements of ionic liquid tagged Ni(II) Schiff base complexes have been reported. To the best of our knowledge, we are reporting the NLO property of ionic liquid tagged Ni(II) Schiff base complexes for the first time.

7.2 EXPERIMENTAL

7.2.1 Materials

All the chemicals used were of analytical grade. Solvents were purified and dried according to standard procedure (Vogel 1989). $\text{Ni}(\text{OCOCH}_3)_2 \cdot 4\text{H}_2\text{O}$, 2,4-dihydroxybenzaldehyde, 1,3-dibromopropane and 1-methylimidazole were purchased from Sigma Aldrich.

7.2.2 Physical measurements

The C, H, N and S contents were determined by Thermoflash EA1112 series elemental analyzer. FT-IR spectra were recorded on a Thermo Nicolet Avatar FT-IR

spectrometer as KBr powder in the frequency range 400–4000 cm^{-1} . $^1\text{H-NMR}$ spectra were recorded in Bruker AV–400 instrument using TMS as internal standard. Electronic spectra of the complexes in the 200–800 nm range were measured on a GBC UV-Vis double beam spectrophotometer in N, N-dimethylformamide solution.

Open-aperture Z-scan measurements were performed to determine the nonlinear transmission of laser light through the samples. The Z-scan is a widely used technique developed by Sheik Bahae et al. (1990) to evaluate the NLO properties of a material. It is based on the transformation of phase distortion during beam propagation.

7.3 SYNTHESIS OF METAL COMPLEXES

The synthetic procedure followed for the preparation of ligand in the present work is similar to that carried out by Khungar and co-workers (2012).

7.3.1 Synthesis of ligand (L4)

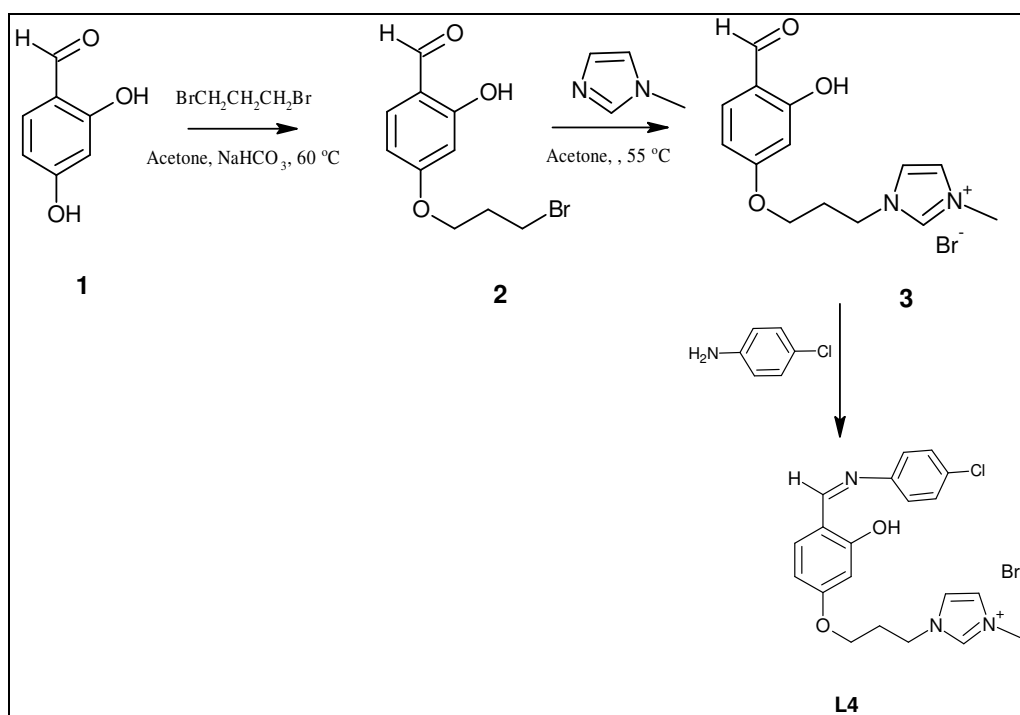
The mixture of 2,4-dihydroxybenzaldehyde (0.29g, 2.1 mmol), 1,3-dibromopropane (1.21g, 6.0 mmol) and sodium bicarbonate (0.41g, 3.0 mmol) were taken in 40 mL of acetone. The reaction mixture was heated at 60°C for 48 hours. After completion of reaction, the mixture was concentrated under vacuum and product was extracted with ethyl acetate. The crude product **2** (Scheme 7.1) was further purified by column.

The compound **3** was synthesized by reacting equimolar mixture of intermediate **2** (0.64g, 2.5 mmol) and 1-methylimidazole (0.20g, 2.5mmol) in acetone (40 mL) at 70°C for 24 hours. The viscous crude product was purified by washing with ethyl acetate to obtain ionic liquid tagged aldehyde.

The mixture of ionic liquid tagged aldehyde **3** (0.51g, 1.5 mmol) and 4-chloroaniline (0.19 g, 2.0mmol) in methanol was refluxed for 2 hours, and the solid

product **L4** formed was filtered and washed with ethanol. The synthetic procedure for the synthesis of ligand **L4** is given in Scheme 7.1.

Yield: 0.24g (52%). M.P: 155°C Anal. Calc. for $C_{20}H_{21}BrClN_3O_2$ (450.75), C: 53.28; H: 4.78; N: 9.35% Found: C: 53.29; H: 4.70; N: 9.32%. IR (KBr, cm^{-1}): 3394(O-H), 1611(C=N). 1H NMR (400 MHz, DMSO): 13.43 (s,1H)(OH), 9.16 (s,1H)(-C-N-), 8.89-6.48(m,11H)(Aromatic), 4.35(d,1H), 4.10(d,2H)(-CH₂), 3.85(s,3H)(-CH₃), 2.30(m,2H)(-CH₂). UV-Vis: λ_{max} (nm) intraligand interactions: 292,343

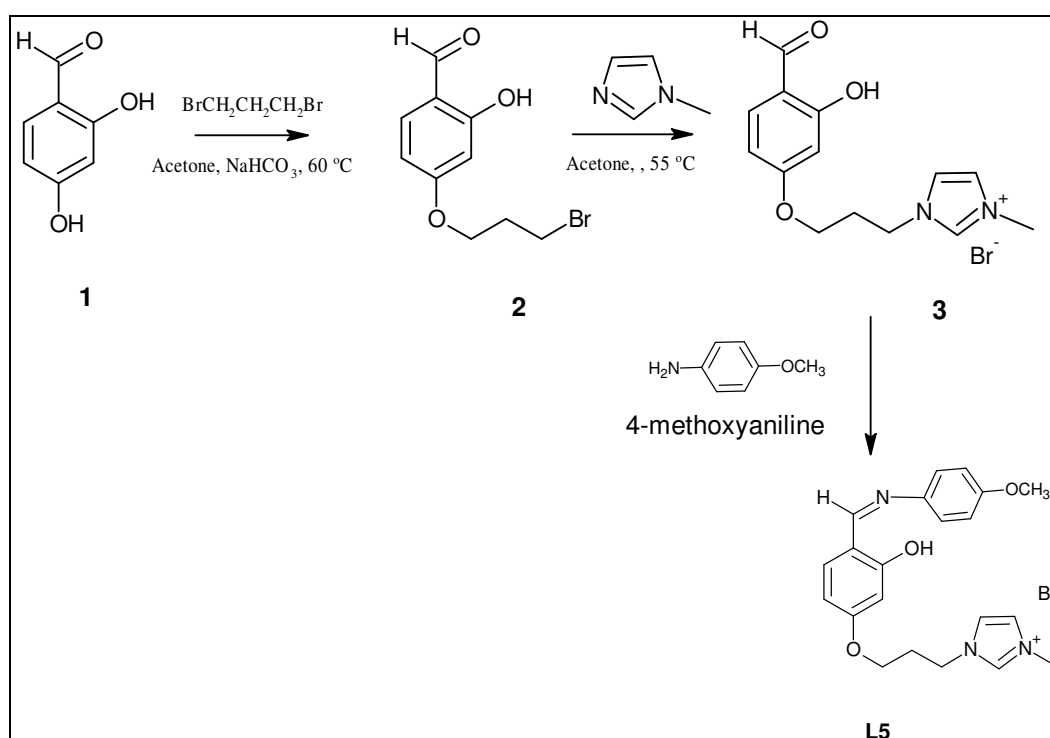


Scheme 7.1 Synthetic scheme for **L4**

7.3.2 Synthesis of ligand (L5)

The mixture of ionic liquid tagged aldehyde **3** (0.51g, 1.5mmol) and 4-methoxyaniline (0.19g, 1.5mmol) in methanol was refluxed for 2 hours, and the solid product **L5** formed was filtered and washed with ethanol. The synthetic procedure for the synthesis of ligand **L5** is given in Scheme 7.2.

Yield: 0.26g (56%). M.P: 145°C. Anal. Calc. for $C_{21}H_{24}BrN_3O_3$ (446.33): C: 56.58; H: 5.41; N: 9.51% Found: C: 56.51; H: 5.42; N: 9.41%. IR (KBr, cm^{-1}): 3353(O-H), 1617(C=N). 1H NMR (400 MHz, DMSO): 13.84(s,1H)(OH), 9.38(s,1H)(-C-N-), 6.43-8.69(m,8H)(aromatic), 4.11(d,2H)(-CH₂), 2.37(d,2H)(-CH₂), 3.82(s,3H)(-CH₃). UV-Vis: λ_{max} (nm) intraligand interactions: 285, 350

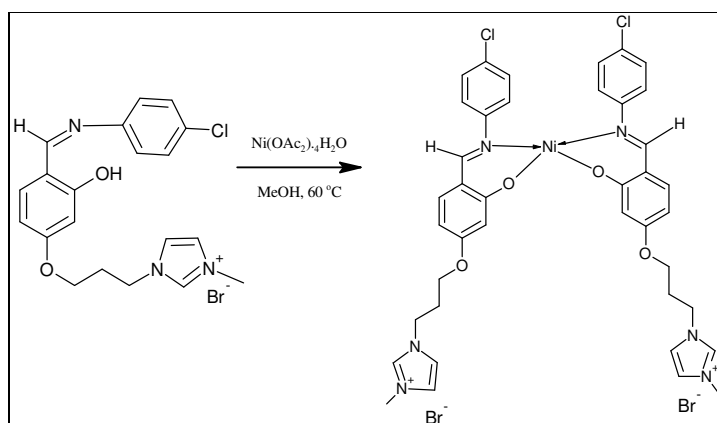


Scheme 7.2 Synthetic scheme for **L5**

7.3.3 Synthesis of complex (C13)

Ni(OCOCH₃)₂·4H₂O (0.273g, 1.1mmol) was added to the ligand (**L4**) (0.52g, 1.2mmol) taken in minimum quantity of methanol (15ml) solvent. The reaction mixture was refluxed at 80°C for 3 hours. The resulting precipitate was filtered, washed with methanol followed by ethanol and dried in *vacuo*. The synthetic method for metal complex **C13** is given in Scheme 7.3.

Yield: 0.31g (63%). M.P: > 330 °C. Anal. Calc. for C₄₀H₄₀Br₂Cl₂N₆NiO₄ (958.18) : C, 50.18; H, 4.18; N, 8.75% Found: C, 50.14; H, 4.21; N, 8.77%. IR (KBr, cm⁻¹): 1580(C=N), 570(N-M), 476(O-M). ¹H NMR (400 MHz, DMSO): 9.27(s, H)(-C-N-), 6.56-7.91(m,16H)(aromatic), 4.49, 4.10, 1.20(d,2H)(-CH₂), 3.90(s,3H)(-CH₃). UV-Vis: λ_{max} (nm) intraligand interactions: 258, 293, d→d forbidden transition: 378.

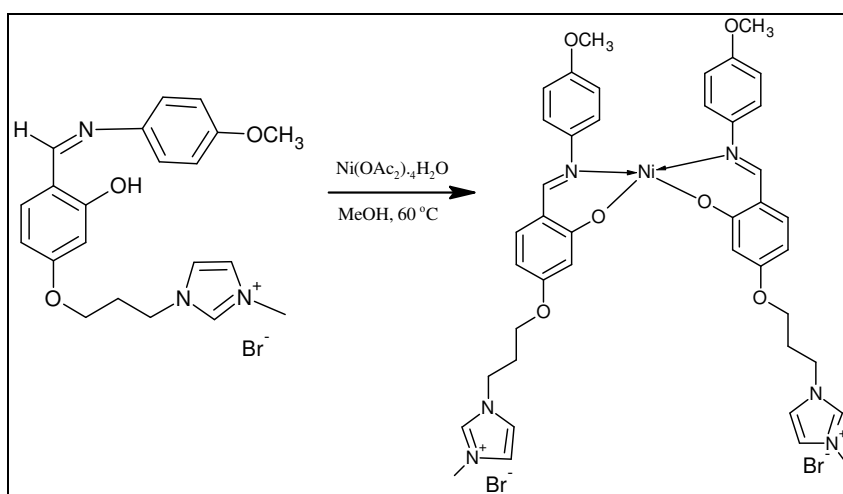


Scheme 7.3 Synthetic scheme for **C13**

7.3.4 Synthesis of complex (C14)

Ni(OCOCH₃)₂·4H₂O (0.273g, 1.1mmol) was added to the ligand (L5) (0.51g, 1.2mmol) taken in minimum quantity of methanol solvent. The reaction mixture was refluxed at 80°C for 2 hours. The resulting precipitate was filtered, washed with ethanol and dried in *vacuo*. The synthetic method for metal complex C14 is given in Scheme 7.4.

Yield: 0.33g (65%). M.P: > 330 °C. Anal. Calc. for C₄₂H₄₆Br₂N₆NiO₆ (949.35) : C, 53.14; H, 4.88; N, 8.85% Found: C, 52.89; H, 4.36; N, 8.97%. IR (KBr, cm⁻¹): 1569(C=N), 565(N-M), 448(O-M). ¹H NMR (400 MHz, DMSO): 9.27(s, H)(-C-N-), 6.56-7.91(m,16H)(aromatic), 4.49, 4.10, 1.20(d,2H)(-CH₂), 3.90(s,3H)(-CH₃). UV-Vis: λ_{max} (nm) intraligand interactions: 259, 295, d→d forbidden transition: 381.



Scheme 7.4 Synthetic scheme for C14

7.4 RESULTS AND DISCUSSION

The analytical data showed that the observed values are in good agreement with the theoretical values (Table 7.1).

Table 7.1 Analytical data of Schiff base complexes

Complex /Ligand	Decomp temp (°C)	% Found (Theoretical)			UV-vis Data, λ_{\max} (nm)	
		C	H	N	Intra ligand Transition	d-d Transition
L4	155	53.29 (53.28)	4.70 (4.78)	9.32 (9.35)	292, 343	-
L5	145	56.51 (56.58)	5.42 (5.41)	9.41 (9.51)	285, 350	
C13	>300	50.14 (50.18)	4.21 (4.18)	8.77 (8.75)	258, 293	378
C14	>300	52.89 (53.14)	4.36 (4.88)	8.97 (8.85)	259, 295	381

7.4.1 FT-IR Spectra

The characteristic stretching frequencies of ligand and complexes are shown in Table 7.2. The broad band in the IR spectra of the ligands in the range 3350–3495 cm^{-1} is assigned to O–H stretching vibrations. These bonds participate in intramolecular hydrogen bonding with azomethine group (O–H \cdots N=C) during complex formation. Therefore, these bands disappeared through complexation with the metal ions. IR absorption band due to $\nu(\text{C}=\text{N})$ of the free ligand appearing in the region 1620–1610 cm^{-1} , undergoes a negative shift by 5–25 cm^{-1} for complexes which indicates the coordination of azomethine nitrogen to the metal (Prabhakaran et al. 2005, Kovacic 1967). The band in the region 1250–1270 cm^{-1} is assigned to phenolic $\nu(\text{C}-\text{O})$. The

bands in the region $560\text{-}570\text{ cm}^{-1}$ and $450\text{-}480\text{ cm}^{-1}$ in the complexes are assigned to $\nu(\text{M-O})$ and $\nu(\text{M-N})$ respectively (Asadi et al. 2011). IR spectra of the synthesized ligands and complexes are shown in Fig. 7.1 to Fig. 7.4 respectively.

Table 7.2 Infrared spectral data (cm^{-1}) for ligands and complexes (**C13-C14**)

Ligand/Complex	$\nu(\text{O-H})$	$\nu(\text{C=N})$	$\nu(\text{M-O})$	$\nu(\text{M-N})$
L4	3394	1611	-	-
L5	3353	1617		
C13	-	1701	570	476
C14	-	1709	565	448

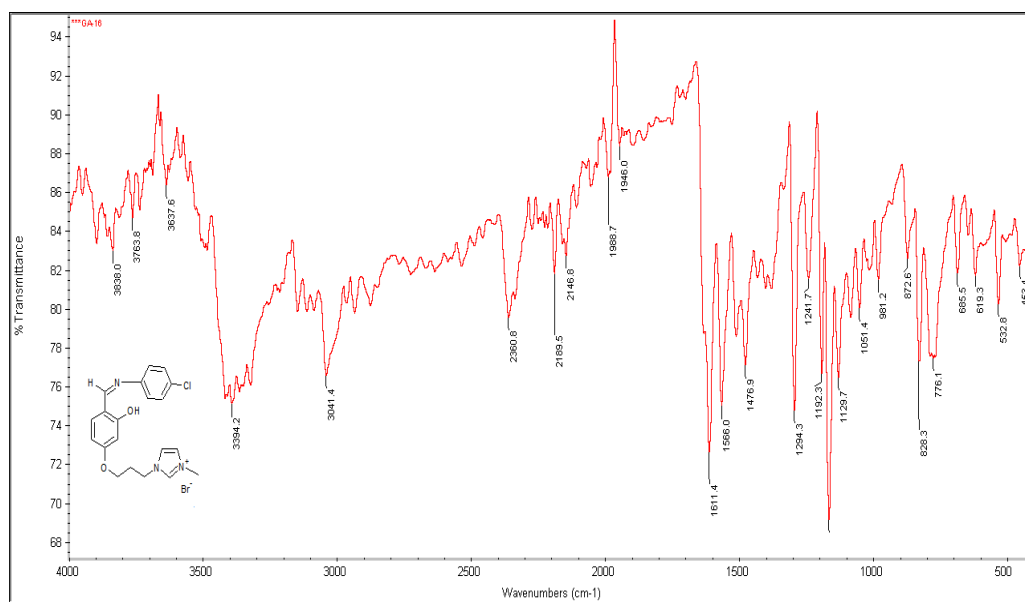


Fig. 7.1 IR spectrum of L4

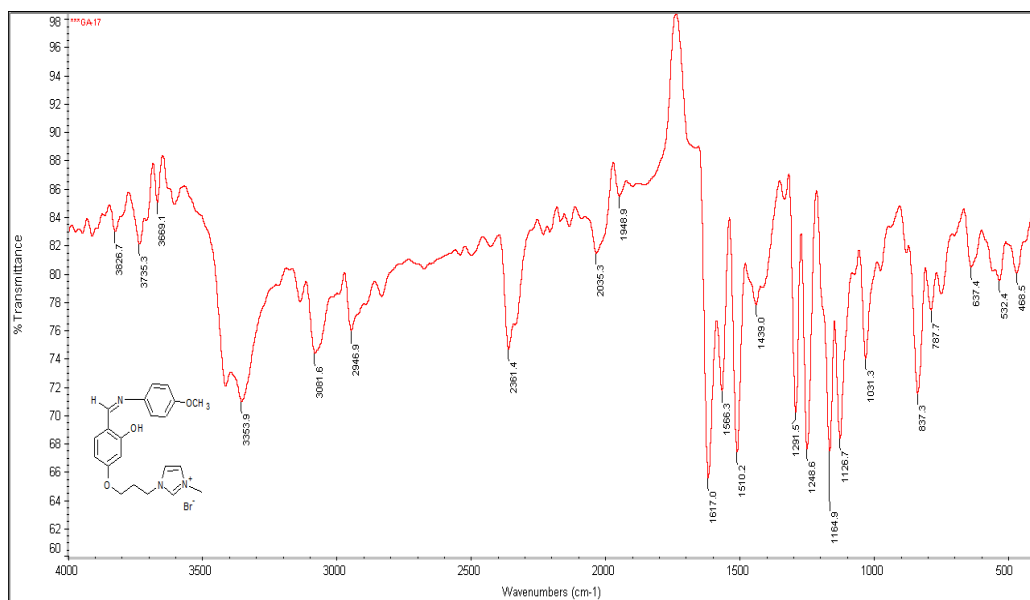


Fig. 7.2 IR spectrum of L5

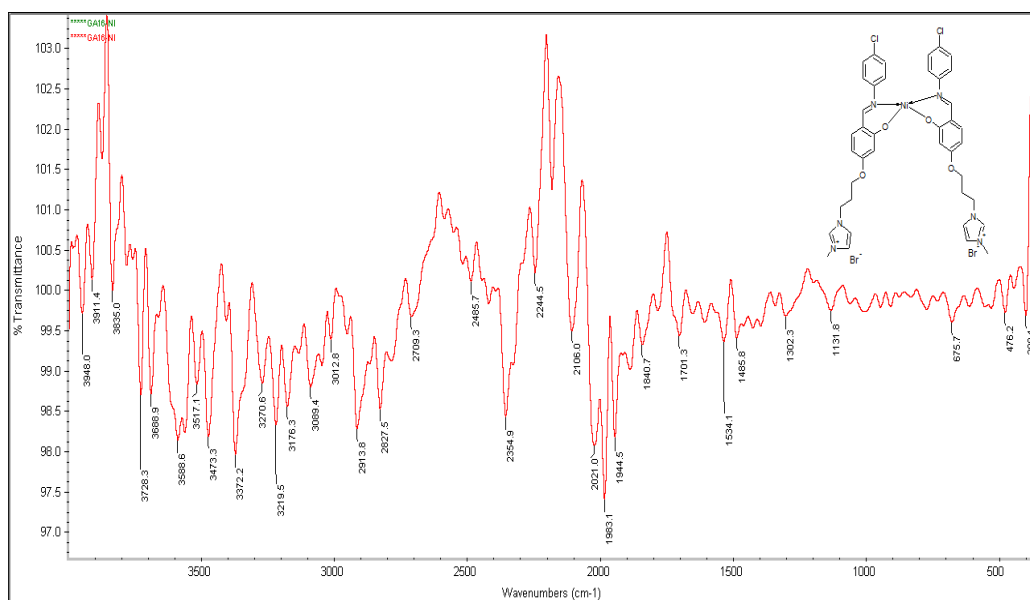


Fig. 7.3 IR spectrum of C13

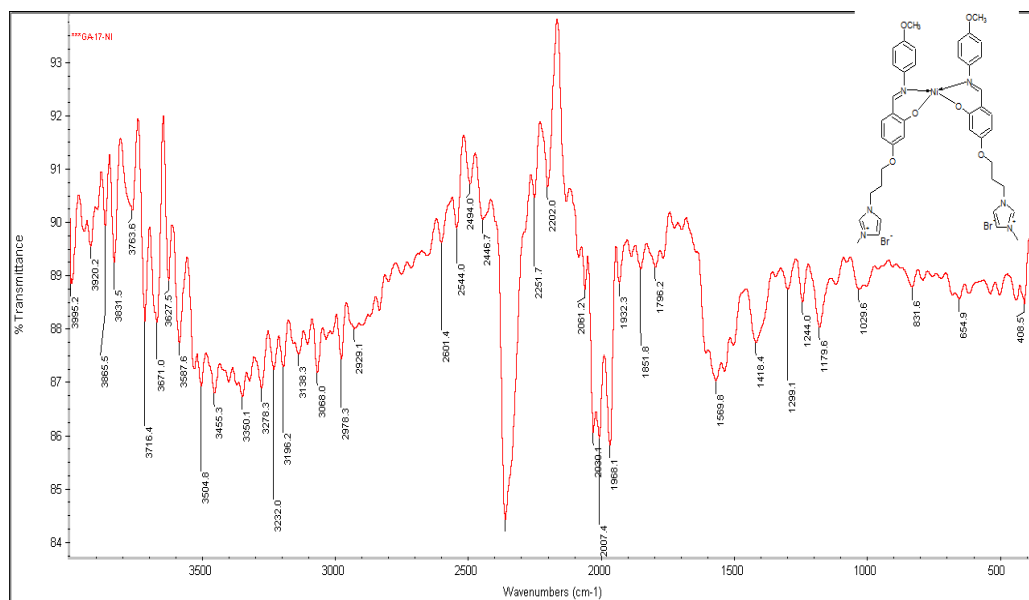


Fig. 7.4 IR spectrum of **C14**

7.4.2 $^1\text{H-NMR}$ Spectra

$^1\text{H-NMR}$ spectral data of the nickel (II) complexes exhibit a multiplet around 6.48-8.89 ppm which has been assigned to the protons of phenyl groups present in Schiff base ligand. A peak observed around 9.3-9.1 ppm in the complex has been assigned to azomethine proton ($-\text{C}=\text{N}-$) (Sorkau et al. 2005, Gnanasoundari and Natarajan 2005 and Balasubramanian et al. 2007). Further, a peak at 13.43 ppm (**L4**) and 13.84 ppm (**L5**) observed in the ligands were absent in the metal complex spectra. These two peaks are assigned to the hydroxyl group in the ligand, and the absence of a resonance due to these phenolic hydrogens in the metal complexes indicates the deprotonation of the Schiff base, to form the metal complex. The NMR spectra of ligands and complexes are given in Fig. 7.5 to Fig. 7.8.

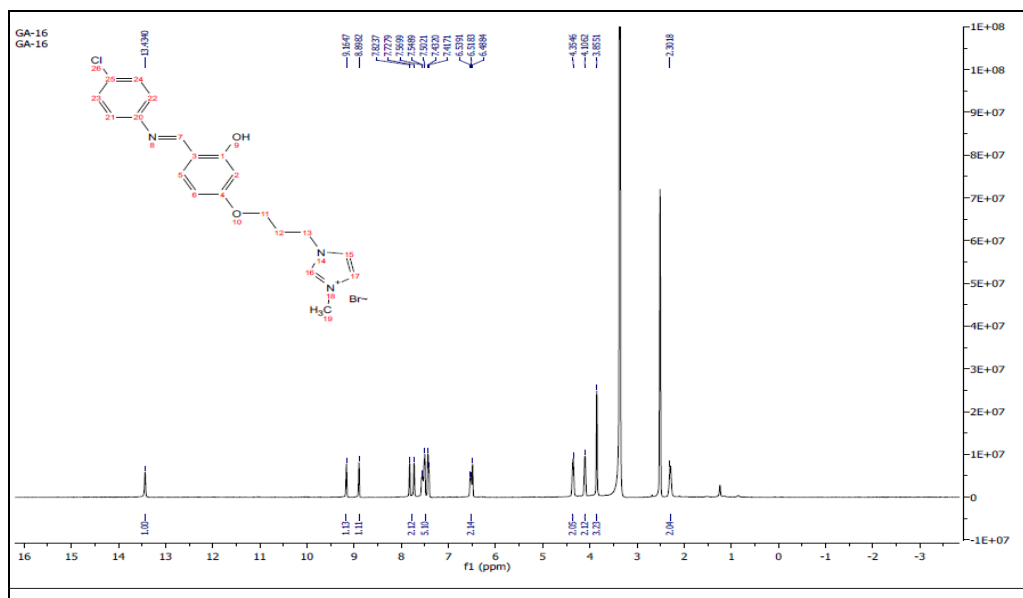


Fig. 7.5 ^1H NMR spectrum of L4

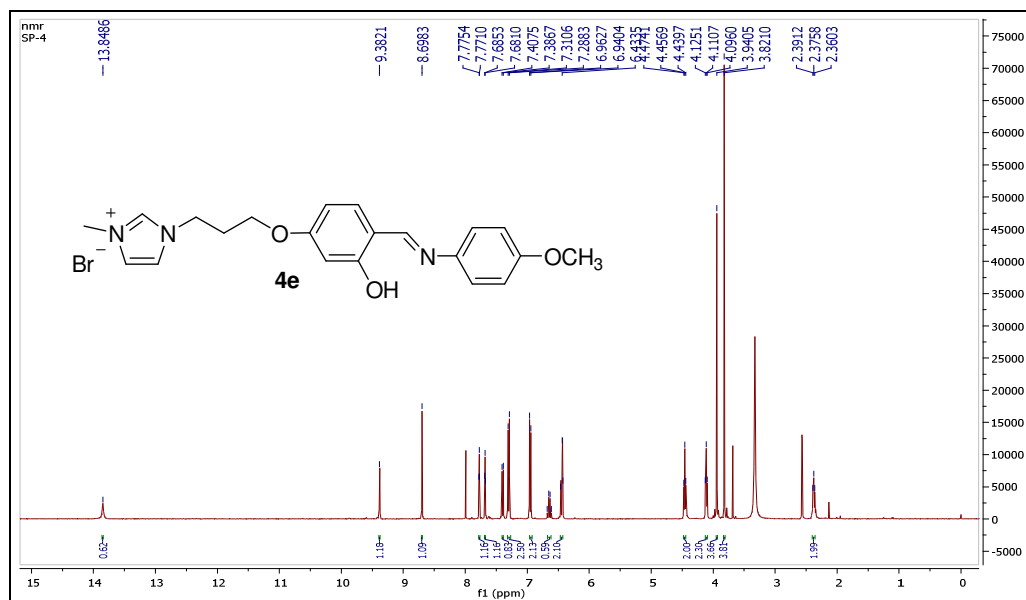


Fig. 7.6 ^1H NMR spectrum of L5

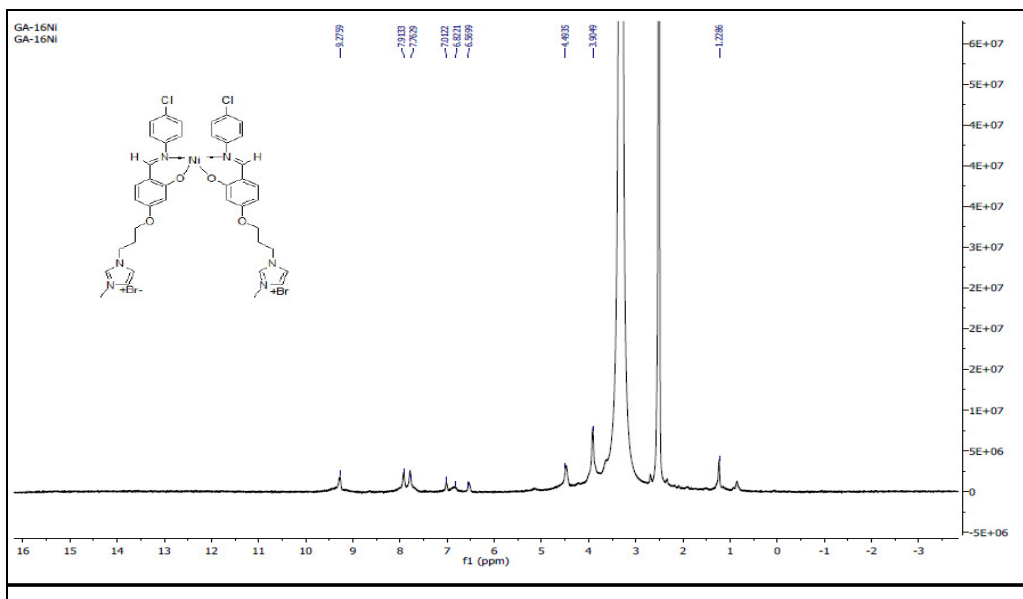


Fig. 7.7 ^1H NMR spectrum of C13

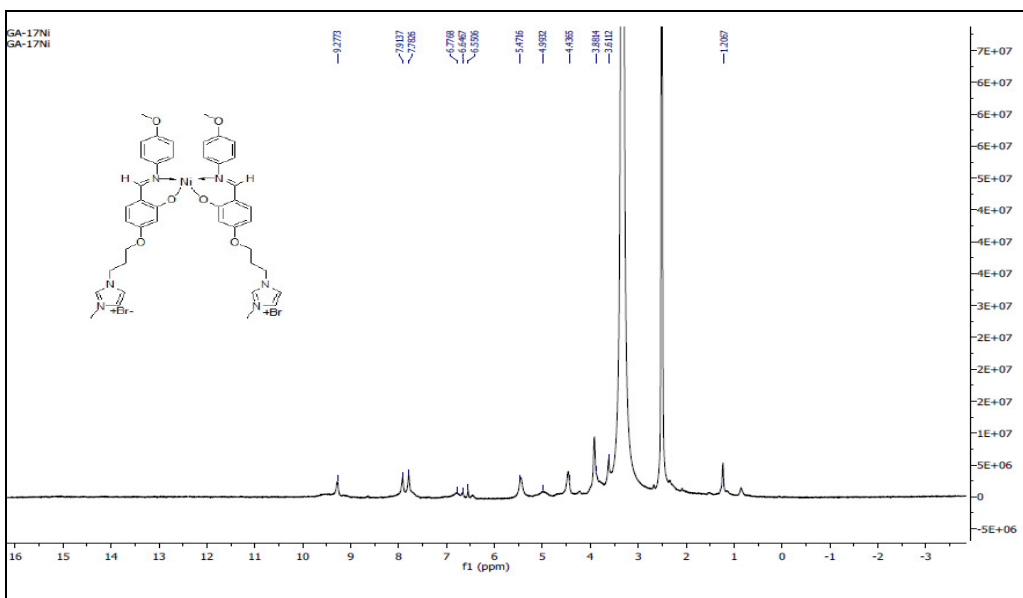


Fig. 7.8 ^1H NMR spectrum of C14

7.4.3 UV-Visible spectra

The UV–Vis spectral data of the ligand and complexes recorded in dry DMSO are depicted in Fig. 7.9. The values of the electronic spectra of ligands (**L4 - L5**) and complexes (**C13-C14**) are given in Table 7.1. Bands between 250 nm to 350 nm are mainly due to metal-to-ligand (MLCT) and ligand-to-metal charge transfer (LMCT) and intra-ligand transitions (ILCT). The spectra also show negligible single photon absorption at 532 nm wavelength. Therefore, the nonlinear optical measurements carried out in our experiments are under nonresonant excitation. Also, it can be seen that the complexes are transparent in the UV-vis region.

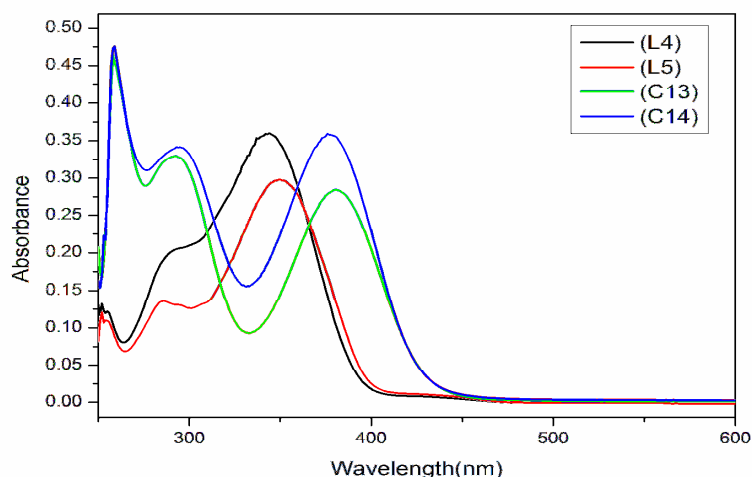


Fig. 7.9 Linear absorption spectra of ligands (**L4- L5**) and complexes (**C13-C14**)

7.5 NONLINEAR OPTICAL MEASUREMENT

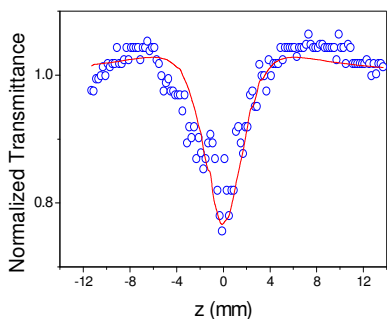
Among the range of organic materials used in optical applications, a class of molten salts called ionic liquids has recently gained attention due to their interesting physicochemical properties (Dupont et al. 2002, Antonietti et al. 2004, Cassol et al.

2006). These liquids have an ionic-covalent structure and present different molecular architectures (Dupont et al. 2002). The fact that some of these ionic liquids possess liquid crystal properties (Bowlas et al. 1996, Gordon et al. 1998), has encouraged the scientific community to explore their nonlinear optical responses. In the present work, ionic liquids were tagged to metal Schiff base complexes and their optical nonlinearity was studied using Z-scan technique. For this, the solutions required for the analysis were prepared by dissolving complexes in DMSO with concentration 1×10^{-3} mol/L and filtered off, prepared solutions to remove the any residue.

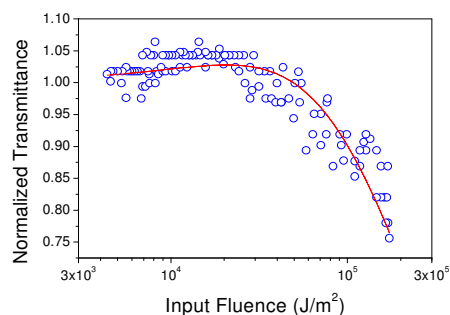
The open aperture Z-scan curves of the complexes are given in Fig 7.10 and Fig. 7.11. Curves shows an increase in absorption when the sample is nearing the beam focus, indicating reverse saturable absorption behaviour. Numerically, a 2PA type process described by the nonlinear transmission equation (7.1) (Sutherland et al. 1996) is given as follows.

$$T = \left(\frac{(1-R)^2 \exp(-\alpha L)}{\sqrt{\pi q_0}} \right) \int_{-\infty}^{\infty} \ln \left[\sqrt{1 + q_0 \exp(-t^2)} \right] dt \quad \dots\dots\dots (7.1)$$

The above equation was found to give the best fit to the data. Here T is the actual Z-dependent sample transmission (product of linear transmission and normalized transmittance) and L and R are the length and surface reflectivity of the sample respectively. α is the linear absorption coefficient. q_0 is given by $\beta(1-R)I_0L_{eff}$, where β is the 2PA coefficient, and I_0 is the on-axis peak intensity. L_{eff} is given by $1 - \exp^{-\alpha l}/\alpha$. The values of the two-photon absorption (2PA) coefficients β of the complexes are presented in the Table 7.3.

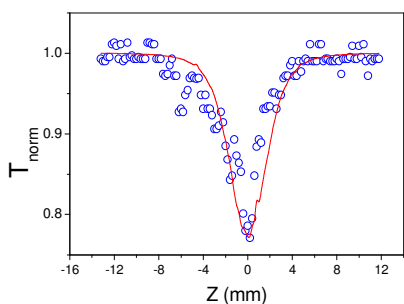


(a)

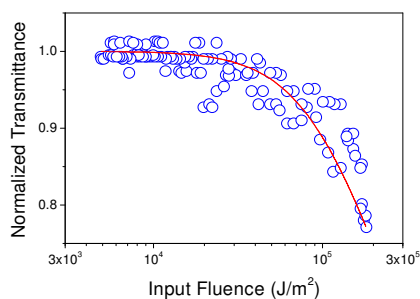


(b)

Fig. 7.10(a) Open aperture Z-scan curve for complex Linear transmission of the sample (corresponding to T (norm.) = 1) is 66%. Circles are data points while solid curves are numerical fits using equation 7.1. . (b) Nonlinear transmission curve of **C13**



(a)



(b)

Fig. 7.11 (a) Open aperture z-scan curve for complex. Linear transmission of the sample (corresponding to T (norm.) = 1) is 67%. Circles are data points while solid curves are numerical fits using equation 7.1. (b) Nonlinear transmission curve of **C14**

Nonlinear absorption is a phenomenon defined as a nonlinear change, either an increase or decrease, in absorption with increasing intensity. This can be of two types:

saturable absorption (SA) and reverse saturable absorption (RSA). With increasing intensity, if the excited states show saturation owing to their long life time, it is called as SA. However, if the excited state has strong absorption compared to that of the ground state, the transmission will show RSA characteristics. RSA is strongly dependent on the wavelength, intensity and excited state lifetime (Naga Srinivas et al. 2003). The most important application of RSA is in optical limiting devices, that protect sensitive optical components, including the human eye, from laser-induced damage (Tutt and Boggess 1993). RSA is observed as a result of ESA, 2PA or a combination of both.

Table 7.3 2PA coefficient β of Schiff base complexes

Complex	2PA coefficient β (mW^{-1})
C13	1.0×10^{-11}
C14	2.6×10^{-11}

The origin of this large nonlinearity can be discussed as follows. As known, ionic liquids are molecular structures with positive and negative charges. It is expected that molecules with positive and negative charges possess large electronic nonlinear optical responses (Sheikh-Bahae et al. 1990). This is because upon laser excitation, a large variation in the molecular dipole occurs, resulting in an optically induced transition of the molecule which leads to refractive and absorptive nonlinear optical response in the molecule. In the present case, we assume that synergic effect of the dipolar interaction in the ionic liquid along with the delocalization of π -electrons in the Schiff base is responsible for the observed optical nonlinearity.

CHAPTER 8

SUMMARY AND CONCLUSIONS

Abstract

In this chapter we summarize the work presented in the thesis along with the conclusions drawn in a chapter wise manner. Scope for further work has also been included.

8.1 SUMMARY AND CONCLUSIONS

In summary, the present research work mainly concentrates on the design and synthesis of ligands and transition metal complexes and consequently study on their nonlinear optical behavior. The selection of diaminobenzene, diaminobenzophenone and thiosemicarbazide as the amine component and 2-hydroxynaphthaldehyde and dimethylamino benzaldehyde as carbonyl component was based on the idea of developing ligands having D- π -A structure so that they can produce complexes with better NLO activity. The selection of 1,10-phenanthroline and triphenylphosphine was to introduce a π -conjugated environment. Due to their versatility, transition metal ions like Fe, Co, Ni, Cu and Zn were selected as the metal centers. The formation of the ligands and complexes was ascertained by elemental analysis, FT-IR spectroscopy, NMR spectroscopy and Single Crystal XRD. The linear absorption, measured by UV-Visible Spectrophotometer, provided light on the kind of charge transfer (metal-to-ligand, ligand-to-metal, d-d transition) prevailing in the system. Since the basic requirement for a complex to behave as an efficient NLO material is the presence of acceptor and donor groups with bridging π -conjugated system, the ligands and complexes were thus chosen and/or designed. For this, either Schiff base ligands were synthesized or ligands with large aromatic system were chosen. Transition metal ions like Fe(II), Co(II), Ni(II), Cu(I), Cu(II) and Zn(II) with d^6 to d^{10} configuration were utilized. Further, a novel

approach of tagging the complex system with ionic liquid has also been employed. The nonlinear optical studies (by Z-scan technique) of the synthesized complexes revealed encouraging results.

In the present context, it becomes significant to co-relate and summarize the results obtained. In brief, the thesis can be summarized as follows. The present research work was carried out to synthesize new metal complexes with large nonlinear response to be used as useful and processable materials for nonlinear applications. The thesis includes synthesis and characterization of five different series of transition metal complexes exhibiting good third-order nonlinearity with two and three photon absorption. The nonlinear optical studies were carried out using open aperture Z-scan technique. Three series of synthesized complexes viz., (1,2-diaminobenzene and 2-hydroxynaphthaldehyde) based Fe(II), Ni(II) and Zn(II) complexes; (3,4-diaminobenzene and 2-hydroxynaphthaldehyde) based Co(II), Ni(II) and Zn(II) complexes and ionic liquid tagged Schiff base Ni(II) complexes displayed two photon absorption. Furthermore, the other two series comprising of (dimethylamino benzaldehyde and thiosemicarbazide) based Ni(II), Cu(II) and Zn(II) complexes and (1,10-phenanthroline and triphenylphosphine) based Cu(I) complexes exhibited three photon absorption. The observed enhancement in the nonlinearity and absorption co-efficient values of the complexes can be assigned to the strong hyperpolarizability produced due to the electron asymmetry and extensive conjugation around the central metal ion. This draws attention to the important role played by polarizable molecular systems on nonlinear response.

The overall work in the thesis has been broadly divided into eight chapters. For an easy understanding, each working chapter has been divided into three major sections: the first and second section explaining the synthetic route and characterization respectively, whereas the final section dealing with nonlinear optical studies. Each chapter is briefly summarized and the conclusions drawn are provided below.

Chapter 1 speaks about the introduction on role of metal ions and various ligands in nonlinear optical behavior of metal complexes. The chapter also introduces the basics of nonlinear optics highlighting the theory of nonlinear optics, two photon and three photon absorption processes and the various methodologies prevalent in determining the nonlinear response.

Chapter 2 presents the survey of literature on the origin and contribution of metal complexes in nonlinear optics. The chapter concludes with an outline of the scope and objectives of the present work.

Chapter 3 gives a detailed study on the synthesis and characterization of ligand (1,2-diaminobenzene and 2-hydroxynaphthaldehyde) and its metal (Fe(II), Ni(II) and Zn(II)) complexes. The complexes displayed a two photon absorption with the Ni(II) complex showing the best NLO response ($5 \times 10^{-11} \text{ mW}^{-1}$).

In **Chapter 4**, 3,4-diaminobenzophenone was chosen as the amino substituent group for the synthesis of Schiff base ligand. This was mainly done to understand the impact of extended π -conjugation on the nonlinear response of its metal complexes with Co(II), Ni(II) and Zn(II) ions. These complexes too showed third-order nonlinearity with the β value going as high as $1.1 \times 10^{-10} \text{ mW}^{-1}$ (for Ni(II) complex). The enhancement of nonlinear response has been discussed.

Chapter 5 deals with the synthesis of Schiff base ligands of dimethylamino benzaldehyde and thiosemicarbazide. The ligand was complexed with Ni(II), Cu(II) and Zn(II) metal ions and well characterized. Here, thiosemicarbazide behaves as a monodentate ligand and forms a square planar complex with the metal ions. These complexes exhibited third-order nonlinearity with the highest three photon coefficient value of $8.5 \times 10^{-24} \text{ m}^3\text{W}^{-2}$ which is observed for Ni(II) complex.

Chapter 6 provides the synthesis of Cu(I) complex with large aromatic ligands like 1,10-phenanthroline and triphenylphosphine. A distorted square planar Cu(I) complex was formed. The structure was confirmed by single crystal XRD. Also, the

nonlinear optical studies were carried out in solution as well as thin film state. These complexes also exhibited three photon absorption. The observed third-order nonlinearity based on the structural feature and solid state packing of the complexes has been discussed.

In **Chapter 7**, an attempt has been made to study the effect of ionic liquid on optical nonlinearity of the Schiff base ligand and its nickel complex. The ionic liquid tagged Schiff base complexes displayed effective two photon absorption with good third-order nonlinear response.

The synthesized complexes proved to be a good third-order nonlinear optical materials exhibiting two photon or three photon absorption, thereby emphasizing the significant role these complexes can play in the field of nonlinear optics. The absorption coefficient values of the complexes suggest that these complexes can be used as optical limiters.

8.2 SCOPE FOR FUTURE WORK

The potential applications of transition metal complexes in information transmission, storage, extraction processing and display have led to a tremendous growth of these complexes as NLO materials. Transition metal complexes, such as those studied in the present thesis, are opening pathways for efficient functional materials. As per the requirement, the ligands and the metal ions can be chosen and tailored into NLO materials with exciting novel properties and functionalities. Keeping in view these factors, the scope of the present work can be extended but not limited to the following experiments.

- Design and synthesis of different ligands with good π -conjugated system to enhance the nonlinear optical response of the complex.

- Studies on the effect of employing metals like boron, tin, ruthenium, etc. on the optical nonlinearity.
- Extending the donor-acceptor system by employing two different metals (bimetallic complexes) and understanding their nature of nonlinear behavior.
- Studying the NLO response of complexes by tagging with different ionic liquids.

The field of nonlinear optics is incredibly large and since the quest for new novel materials is never ending, scope for the present work is bright

References

Afanas'ev, A.V., Zinovieva, A.P., Antipova, O.L., Bushukb, B.A., Bushukb, S.B., Rubinovb, A.N., Fominihc, J.Y., Klapshinac, L.G., Domrachevc, G.A. and Douglasd, W.E. (2002). "Picosecond z-scan measurements of nonlinear optical susceptibility of films and solutions of novel organometallic polymers." *Opt. Commun.*, 201, 207-215.

Akine, S. and Nabeshima, T. (2009). "Cyclic and acyclic oligo(N₂O₂) ligands for cooperative multi-metal complexation." *Dalton Trans.*, 47, 10395-10408.

Angela Sorkau, Christoph Wagner and Dirk Steinborn, (2005). "Ruthenium Catalyzed Reactions of Aldehydes: Molecular Structures of Ruthenium Complexes with Aldehyde Ligands." *Transit Metal Chem.*, 30, 691-695.

Anitha, C., Sheela, C.D., Tharmaraj, P and Sumathi, S. (2012). "Spectroscopic studies and biological evaluation of some transition metal complexes of azo Schiff-base ligand derived from (1-phenyl-2,3-diemthyl-4-aminopyrazol-5-one) and (5-((4-chlorophenyl)diazenyl)-2-hydroxybenzaldehyde)." *Spectrochim. Acta A*, 96, 493-500.

Antonietti, M., Kuang, D.B., Smarsly, B. and Yong, Z. (2004). "Ionic liquids for the convenient synthesis of functional nanoparticles and other inorganic nanostructures." *Angew. Chem. Int. Edn.*, 43, 4988-4992.

Asadi, M. and Khah, M.S. (2010). "Some New Unsymmetrical Diimino Tetradentate Schiff Base Derived from 3,4-Diaminobenzophenone: Synthesis, Characterization and the Formation Constant of Ni(II) and Cu(II) Complexes" *J. Iran. Chem. Soc.*, 7, 875-882.

Asadi, M., Hajar, S. and Khosro, M. (2011). "Tetradentate Schiff base ligands of 3,4-diaminobenzophenone: Synthesis, characterization and thermodynamics of complex formation with Ni(II), Cu(II) and Zn(II) metal ions." *J. Serb. Chem. Soc.*, 76, 63-74.

Averseng, F., Lacroix, P.G., Malfant, I., Lenoble, G., Cassoux, P., Nakatani, K., Maltey-Fanton, I., Delaire, J.A. and Aukaaloo, A. (1999). "Synthesis, crystal structure and second-order nonlinear optical properties of a new bis(salicylaldiminato) nickel (II) metal complex." *Chem. Mater.*, 11, 995-1002.

Balasubramanian, K.P., Karvembu, R., Prabhakaran, R., Chinnusamy, V., Natarajan. K. (2007). "Synthesis, spectral, catalytic and antimicrobial studies of PPh₃/AsPh₃ complexes of Ru(II) with dibasic tridentate O, N, S donor ligands." *Spectrochimica Acta Part A.*, 68, 50-54.

Bauer, D.J. (1972). Introduction to antiviral chemotherapy. In: Bauer D.J., editor. *Chemotherapy of virus diseases*. Vol. 1. Pergamon Press; Oxford, UK, 1-33.

Bhardwaj, C.N. and Singh, V.R. (1994). "Synthesis and characterization of thallium (I) complexes of biologically active benzothiazolines." *Indian J. Chem.*, 33A, 423-425.

Bharti K., Madharam, S.R., Kasiviswanadharaju, P., Pankaj, N., Naveen, J., Jitendra, P. and Anil, K. (2012). "Synthesis, characterization and microbial studies of novel ionic liquid tagged Schiff bases." *Comptes Rendus Chimie*, 15, 669-674.

Bhawalkar, J.D, He, G.S. and Prasad, P.N. (1996). "Nonlinear multiphoton processes in organic and polymeric materials." *Rep. Prog. Phys.*, 59, 1041-1046.

Bowlas, C.J., Bruce, D.W. and Seddon, K.R. (1996). "Liquid-crystalline ionic liquids." *Chem. Comm.*, 14, 1625-1626.

Bredas, J.L., Adant, C., Tackx, P., Persoons, A. and Pierce, B.M. (1994). "Third-Order Nonlinear Optical Response in Organic Materials: Theoretical and Experimental Aspects." *Chem. Rev.*, 94, 243-278.

Burland, D.M., Miller, R.D., and Walsh, C.A., (1994). "Second-order nonlinearity in poled-polymer systems." *Chem. Rev.*, 94, 31-75

Cai, Z., Zhou, M. and Xu, J. (2011). "Degenerate four-wave mixing determination of third-order optical nonlinearities of three mixed ligand nickel (II) complexes." *J. Mol. Struct.*, 1006, 282-287.

Calixto, S., Sanchez-Morales, M.E., Sanchez-Marin, F.J., Rosete-Aguilar, M., Martinez-Richa, A. and Barrere-Rivera, K.A. (2009). "Optofluidic variable focus lenses." *Appl. Opt.*, 48, 2308-2314.

Cambell, M.J.M. (1975). "Transition metal complexes of thiosemicarbazides and thiosemicarbazones." *Coord. Chem. Rev.*, 15, 279-319.

Cassano, T., Tommasi, R., Ferrara, M., Babudri, F., Cardone, A., Farinola, G.M. and Naso, F. (2001). "Substituent-dependence of the optical nonlinearities in poly(2,5-dialkoxy-p-phenylenevinylene) polymers investigated by the Z-scan technique." *Chem. Phys.*, 272, 111-118.

Cassol, C.C., Ebeling, G., Ferrera, B. and Dupont, J. (2006). "A simple and practical method for the preparation and purity determination of halide-free imidazolium ionic liquids." *Adv. Synth. Catal.*, 348, 243-248.

Chakrabarty, D., Hazra, P., Chakraborty, A., Seth, D. and Sarkar, N. (2003). "Dynamics of solvent relaxation in room temperature ionic liquids." *Chem. Phys. Lett.*, 381, 697-704.

Chakraborty, H., Paul, N. and Rahman, M.L. (1994). "Catalytic activities of Schiff base aquo complexes of Cu(II) towards hydrolysis of amino acid esters." *Trans. Met. Chem.*, 19, 524-526.

Chao, H., Li, R.H., Ye, B.H., Li, H., Feng, X.L., Cai, J.W., Zhou, J.Y. and Ji, L.N. (1999). "Synthesis, characterization and third-order nonlinear optical properties of ruthenium (II) complexes containing 2-phenylimidazo[4,5-*b*][1,10] phenanthroline derivatives." *J. Chem. Soc. Dalton Trans.*, 21, 3711-3717.

Chattopadhyay, D., Mazumdar, S.K., Banerjee, T. and Thomas, C.W. (1988). "Crystal and molecular structure of 4-(N,Ndimethylamino)benzaldehyde thiosemicarbazone." *J. Cryst. Spectrosc. Res.*, 18, 701-712.

Chemla, D.S. and Zyss, J. (1987). "Nonlinear optical properties of organic molecules and crystals." Academic, New York.

Chiang, W., Thompson, M.E. and VanEngen, D. (1991). "Synthesis and nonlinear optical properties of inorganic coordination polymers." *Organic Materials for Nonlinear Optics*, Hann, R.A. and Bloor, D (Eds.), Royal Chemical Society, London, 91, 210-217.

Chiang, W., Vanengen, D. and Thompson, M.E. (1996). "Second-order nonlinear optical properties of Fe(SALEN) complexes." *Polyhedron*, 14, 2369-2376.

Chohan, Z.H. and Sherazi, S.K.A. (1999). "Synthesis and characterization of some Co(II), Cu(II) and Ni(II) complexes with nicotinoylhydrazine derivatives and the biological role of metals and anions (SO_4^{2-} , NO_3^- , $\text{C}_2\text{O}_4^{2-}$ and CH_3CO_2^-) on the antibacterial properties." *Synth. React. Met. Org. Chem.*, 29, 105-118.

Cimernman, Z., Galic, N. and Bosner, B. (1997). "The Schiff bases of salicylaldehyde and aminopyridines as highly sensitive analytical reagents." *Anal. Chim. Acta.*, 343, 145-153.

Coe, B.J. (2004). *Comprehensive Coordination Chemistry II* (Eds.: J. A. McCleverty, T. J. Meyer), Elsevier Pergamon, Oxford, U. K., 9, 621-628.

Coe, B.J., Houbrechts, S., Asselberghs, I. and Persoons, A. (1999). "Efficient, reversible redox-switching of molecular first hyperpolarizabilities in ruthenium (II) complexes possessing large quadratic optical nonlinearities." *Angew. Chem. Int. Ed.*, 38, 366-369.

- Cohanoschi, I., Marisol, G., Carlos, T., Belfield, K.D. and Hernandez, F.E. (2006). "Three-photon absorption of a new series of halogenated fluorine derivatives." *Chem. Phys. Lett.*, 430, 133-138.
- Costes, J.P., Lamere, J.F., Lepetit, C., Lacroix, P.G., Dahan, F. and Nakatani, K. (2005). "Synthesis, crystal structures and nonlinear optical (NLO) properties of new Schiff-base nickel (II) complexes. Toward a new type of molecular switch?" *Inorg. Chem.*, 44, 1973-1982.
- Couris, S., Koudoumas, E., Ruth, A.A. and Leach, S. (1995). "Concentration and wavelength dependence of the effective third-order susceptibility and optical limiting of C60 in toluene solution." *J. Phys. B: At. Mol. Opt. Phys.*, 28, 4537-4543.
- Cymerman, J.C., Wills, D., Rubbo, S.D. and Edgar, J. (1955). "Mode of action of isoNicotinic hydrazide." *Nature*, 176, 34.
- Dalton, G.T., Cifuentes, M.P., Petrie, S., Stranger, R., Humphrey, M.G. and Samoc, M. (2007). "Independent switching of cubic nonlinear optical properties in a ruthenium alkynyl cruciform complex by employing protic and electrochemical stimuli." *J. Am. Chem. Soc.*, 129, 11882-11883.
- Dalton, L.R., Harper, A.W., Ghosn, R., Steir, W.H., Ziari, M., Fetterman, H., Shi, Y., Mustacich, R.V., Jen A.K.Y and Shea K.J.(1995)."Synthesis and Processing of Improved Organic Second-Order Nonlinear Optical Materials for Applications in Photonics." *Chem. Mater.*, 7, 1060-1081.
- Daneshvar, N., Entezami, A.A., Khandar, A.A. and Saghatforoush, L.A. (2003). "Synthesis and characterization of copper (II) complexes with dissymmetric tetradentate Schiff base ligands derived from aminothioether pyridine. Crystal structures of [Cu(pytlSal)]ClO₄·0.5CH₃OH and [Cu(pyAzosal)]ClO₄." *Polyhedron*, 22, 1437-1445.

Das G.P., Vaia, R., Yeates, A.T. and Dudis, D.S. (2001). "A theoretical model for excited state absorption." *Synth. Met.*, 116, 281-283.

Dhenaut, C., Ledoux, I., Samuel, I.D.W., Zyss, J., Bourgault, M. and Bozec, H.L. (1995). "Chiral metal complexes with large octupolar optical nonlinearities." *Nature*, 374, 339-341.

Dholakiya, P.P. and Patel, M.N. (2002). "Synthesis, spectroscopic studies and antimicrobial activity of Mn(II), Co(II), Ni(II), Cu(II) and Cd(II) complexes with bidentate Schiff bases and 2,2'-bipyridylamine." *Synth. React. Inorg. Met. Org. Chem.*, 32, 753-762.

Di Bella, S. (2001). "Second-order nonlinear optical properties of transition metal complexes." *Chem. Soc. Rev.*, 30, 355-366.

Di Bella, S. and Fragala I. (2000). "Synthesis and second-order nonlinear optical properties of bis(salicyldiaminato) M(II) metalloorganic complexes." *Synth. Metal.*, 115, 191-196.

Di Bella, S., Fragal, I., Guerri, A., Dapporto, P. and Nakatani, K. (2004). "Synthesis, crystal structure and second-order nonlinear optical properties of [N,N-(bis(1H-pyrrol-2-ylmethylene)-1,2-benzenediaminato]nickel(II) Schiff base complexes." *Inorg. Chim. Acta.*, 357, 1161-1167.

Di Bella, S., Fragala, I., Ledoux, I. and Marks, T.J. (1995). "Role of metal electronic properties in tuning the second-order nonlinear optical response of coordination complexes. A combined experimental and theoretical investigation of a homologous series of (N,N'-disalicylidene-1,2-phenylenediaminato)M(II) (M=Co, Ni, Cu) complexes." *J. Am. Chem. Soc.*, 117, 9481-9485.

Di Bella, S., Fragala, I., Ledoux, I., Diaz-Garcia, M.A. and Marks, T.J. (1997). "Synthesis, characterization, optical spectroscopic, electronic structure and second-order nonlinear optical (NLO) properties of a novel class of donor-acceptor bis(salicylaldiminato) nickel (II) Schiff base NLO chromophores." *J. Am. Chem. Soc.*, 119, 9550-9557.

Di Bella, S., Fragala, I., Ledoux, I., Diaz-Garcia, M.A., Lacroix, P.G. and Marks, T.J. (1994). "Sizable second-order nonlinear optical response of donor-acceptor bis(salicylaldiminato)nickel(II) Schiff base complexes." *Chem. Mater.*, 6, 881-883.

Di Bella, S., Oliveri, I.P., Colombo, A., Dragonetti, C., Righetto, S. and Roberto, D. (2012). "An unprecedented switching of the second-order nonlinear optical response in aggregate bis(salicylaldiminato) zinc (II) Schiff-base complexes." *Dalton Trans.*, 41, 7013-7016.

Dupont, J., de Souza, R.F. and Soares, P.A.Z. (2002). "Ionic liquid (molten salt) phase organometallic catalysts." *Chem. Rev.*, 102, 3667-3692.

Etthing, C. (1840). "Untersuchungen uber das atherische Oel der Spiraea Ulmaria und die salicylige Saure." *Ann. Chem. Pharm.*, 35, 241-276.

Farrugia, L.J.J. (1999). "WinGX suite for small-molecule single-crystal crystallography." *Appl. Cryst.*, 32, 837-838.

Freire, C. and de Castro, B. (1998). "Epr characterization of nickel (III) complexes with N₂O₂ Schiff base ligands derived from naphthaldehyde and their pyridine adducts." *Polyhedron*, 17, 4227-4235.

Fuks-Janczarek, I., Nunzi, B. Sahraoui, J.-M., Kityk, I.V., Berdowski, J., Caminade, A.M., Majoral, J.-P., Martineau, A.C., Frere, P., and Roncali, J. (2002). "Third-order

nonlinear optical properties and two-photon absorption in branched oligothiénylenevinylenes." *Optics Communications.*, 209, 461-466.

Gaudry J.P., Capes, L., Langot, P., Marcen. S., Kollmannsberger, M., Lavastre, O., Freysz, E., Letard, J.F. and Kahn, O. (2000). "Second-order nonlinear optical response of metallo-organic compounds towards switchable materials." *Chem. Phys. Lett.*, 324, 321-329.

Giuliano C. and Hess L., (1967). "Nonlinear absorption of light: Optical saturation of electronic transitions in organic molecules with high intensity laser radiation." *IEEE J. Quantum Electron.*, 3, 358-367.

Gnanasoundari, V.G. and Natarajan, K. (2005). "Synthesis, characterization and catalytic studies of iron (II), cobalt (II), nickel (II) and copper (II) complexes containing triphenylphosphine and β -diketones." *Transit. Metal Chem.*, 30, 433-438.

Gomez, S.L., Cuppo, F.L.S. and Neto, A.M.F. (2003). "Nonlinear optical properties of liquid crystals probed by Z-scan technique." *Braz. J. Phys.*, 33, 813-820.

Gordon, C.M, Holbrey, J.D., Kennedy, A.R. and Seddon, K.R. (1998). "Liquid crystals: hexafluorophosphate salts." *J. Mater. Chem.*, 8, 2627-2636.

Gradinaru, J., Forni, A., Druta, V., Tessore, F., Zecchin, S., Quici, S. and Garbalau, N. (2007). "Structural, spectral, electric-field-induced second harmonic, and theoretical study of Ni(II), Cu(II), Zn(II) and VO(II) complexes with [N₂O₂] unsymmetrical Schiff bases of S-methylisothiosemi carbazide derivatives." *Inorg. Chem.*, 46, 884-895.

Green, M.L.H., Marder, S.R., Thompson, M.E., Bandy, J.A., Bloor, D., Kolinsky, P.V., and Jones, R.J. (1987). "Synthesis and structure of (*cis*)-[1-ferrocenyl-2-(4-nitrophenyl)ethylene], an organotransition metal compound with a large second-order optical nonlinearity." *Nature*, 330, 360-362.

Gu, B., Ji, W., Patil, P.S., Dharmaparakash, S.M. and Wang, W.T. (2008). "Two-photon-induced excited-state absorption: Theory and experiment." *Appl. Phys. Lett.*, 92, 091118-091121.

Guo, W.F., Sun, X.B., Sun, J., Wang, X.Q., Zhang, G.H., Ren, Q. and Xu, D. (2007). "Nonlinear optical absorption of a metal dithiolene complex irradiated by different laser pulses at near-infrared wavelengths." *Chem. Phys. Lett.*, 435, 65-68.

Gupta, K.C., Sutar, A.K. and Lin, C.C. (2009). "Polymer-supported Schiff base complexes in oxidation reactions." *Coord. Chem. Rev.*, 253, 1926-1946.

Harilal, S.S., Bindhu, C.V., Nampoory, V.P.N. and Vallabhan, C.P.G. (1999). "Optical limiting and thermal lensing studies in C₆₀." *J. Appl. Phys.*, 86, 1388-1392.

He, G.S., Tan, L.S., Zheng, Q. and Prasad, P.N. (2008). "Multiphoton Absorbing Materials: Molecular Designs, Characterizations, and Applications." *Chem. Rev.*, 108, 1245-1330.

Holm, R.H., Everett, G.W. and Chakravorty, A. (1966). "Metal Complexes of Schiff Bases and β -Ketoamines." *Prog. Inorg. Chem.*, 7, 83-214.

Horst, K. and Vogler, A. (2002). "Electronic spectra of π -cyclopentadienyl(triethyl phosphine) copper(I). Ligand-to-ligand charge transfer." *Inorg Chem. Commun.*, 5, 112-114.

Hou, H., Li, G., Song, Y., Fan, Y., Zhu, Y. and Zhu L. (2003). "Synthesis, Crystal Structures and Third-Order Nonlinear Optical Properties of Two Novel Ferrocenyl Schiff-Base Complexes [Ag(L)₂](NO₃)·(MeOH)·(EtOH) and [HgI₂(L)] {L = 1,2-Bis[(ferrocen-1-ylmethylene)amino]ethane}." *Europ. J. Inorg. Chem.* 12, 2325-2332.

Hu, S., Chen, J.C., Tong, M.L., Wang, B., Yan, Y.X. and Batten, S.R. (2005). "Cu²⁺ Mediated Dehydrogenative Coupling and Hydroxylation of an N-Heterocyclic Ligand:

From Generation of a New Tetratopic Ligand to the Designed Assembly of Three-Dimensional Copper(I) Coordination Polymers.” *Angew. Chem. Int. Ed.*, 44, 5471-5475.

Qiong, Hua, Jin., Xia, Lan, Xin., Cheng-Jun, Dong and Hui, Ju, Zhu, (1998) “Iodo(1,10-phenanthroline-N,N')(triphenylphosphine)copper(I)” *Acta Cryst.*, C54, 1087-1089.

Huang, H. (Ed.), (1988). "Optical Nonlinearities and Instabilities in Semiconductors." Academic Press, Boston, MA, U.S.A.

Ingram, J.A., Moog, R.S, Ito, N., Biswas, R. and Maroncelli, M. (2003). “Solute rotation and solvent dynamics in a room-temperature ionic liquid.” *J. Phys. Chem. B*, 107, 5926-5932.

Jayabalakrishanan, C. and Natarajan, K. (2001). “Synthesis, characterization and biological activities of ruthenium (II) carbonyl complexes containing bifunctional tridentate Schiff bases.” *Synth. React. Met. Org. Chem.*, 31, 983-995.

Jeewoth, T., Wah, H.L.K., Bhowon, M.G., Ghoorohoo, D. and Babooram, K. (2000). “Synthesis and antibacterial/catalytic properties of Schiff bases and Schiff base metal complexes derived from 2,3-diaminopyridine.” *Synth. React. Met. Org. Chem.*, 30, 1023-1038.

Jin, Q.H., Xin, X.L. and Zhu, F.J. (1999). “Bromo(1,10-phenanthroline-N,N')(triphenylphosphine)copper(I).” *Acta Cryst.*, C55, IUC990010.

Jin, V.X., Tan, S.I. and Ranford, J.D. (2005). “Platinum(II) triammine antitumour complexes:structure-activity relationship with guanosine 5'-monophosphate {5'-GMP}.” *Inorg. Chim. Acta*, 358, 677-686.

Joffre, R., Gillon, D., Dardenne, P., Agneessens, R. and Biston, R. (1992). “The use of near-infrared reflectance spectroscopy in litter decomposition studies.” *Annales des Sciences Forestieres*, 49, 481-488.

Kalanithia, M., Kodimunthiric, D., Rajarajanb, M. and Tharmaraj, P. (2011). "Synthesis, characterization and biological activity of some new VO(IV), Co(II), Ni(II), Cu(II) and Zn(II) complexes of chromone based NNO Schiff base derived from 2-aminothiozole." *Spectrochim. Acta A*, 82, 290-298.

Kang, Y., Yao, Y.G., Qin, Y.Y., Zhang, J., Chen, Y.B., Zhao, J.L., Wen, Y.H., Cheng, J.K. and Hu, R.F. (2004). "A novel ligand-unsupported 3D framework polymer of trimeric copper(I) and its NLO property." *Chem. Commun.*, 1046–1047.

Karmakar, R. and Samanta, A. (2002). "Steady-state and time-resolved fluorescence behavior in C153 and PRODAN in room temperature ionic liquids." *J. Phys. Chem. A*, 106, 6670-6675.

Karthikeyan, B., Anija, M., Suchand Sandeep, C.S. and Muhammad Nadeer, T.M. (2008). "Optical and nonlinear optical properties of copper nanocomposite glasses annealed near the glass softening temperature." *Opt. Commun.*, 281, 2933-2937.

Karvembu, R., Hemalatha, S., Prabhakaran, R., Natarajan, K. (2003). "Synthesis, characterization and catalytic activities of ruthenium complexes containing triphenylphosphine/triphenylarsine and tetradentate Schiff bases." *Inorg. Chem. Commun.*, 6, 486-490.

Kiran, A.J., Lee, H.W., Sampath Kumar, H.C., Rudresha, B.J., Bhat, B.R., Yeom, D.I., Kim, K. and Rotermund, F. (2010). "The ultrafast nonlinear optical response and multiphoton absorption of a new metal complex in the near-infrared spectral range." *J. Opt.*, 12, 1-5.

Kovacic, J.E. (1967). "The C=N stretching frequency in the infrared spectra of Schiff's base complexes—I. Copper complexes of salicylidene anilines." *Spectrochim. Acta.*, 23A, 183-187.

Kurian, P., Vijayan, C., Sathiyamoorthy, K., Suchand, Sandeep, C.S. and Reji, P. (2007)

“Excitonic Transitions and Off-resonant Optical Limiting in CdS Quantum Dots Stabilized in a Synthetic Glue Matrix.” *Nano Res. Lett.*, 2, 561-568.

Kurtz, S.K. and Perry, T.T. (1968). “A powder technique for the evaluation of nonlinear optical materials.” *J. Appl. Phys.*, 39, 3798-37813.

Kurum, U., Ceyhan, T., Elmali, A. and Bekaroglu, O. (2009). “Optical limiting response by embedding copper phthalocyanine into polymer host.” *Opt. Commun.*, 282, 2426-2430.

Lacroix, P.G., Averseng, F., Malfant, I. and Nakatani, K. (2004). “Synthesis, crystal structures and molecular hyperpolarizabilities of a new Schiff base ligand, and its copper (II), nickel (II) and cobalt (II) complexes.” *Inorg. Chim. Acta.*, 357, 3825-3835.

Lacroix, P.G., Di. Bella, S. and Ledoux, I. (1996). “Synthesis and second-order nonlinear optical properties of new copper (II), nickel (II) and zinc (II) Schiff-base complexes. Toward a role of inorganic chromophores for second harmonic generation.” *Chem. Mater.*, 8, 541-545.

Lenoble, G., Lacroix, P.G., Daran, J.C., Di Bella, S. and Nakatani, K. (1998). “Synthesis, crystal structures and NLO properties of new chiral inorganic chromophores for second-harmonic generation.” *Inorg. Chem.*, 37, 2158-2165

Lever, A.B.P. (1968). *Inorganic Electronic Spectroscopy*; Elsevier publishing. Co. Ltd: New York, 105-106.

Liu, P., Shi, J.C., Tong, Q., Feng, Y., Huang, H. and Jia, L. (2009). “Synthesis and characterization of a chiral Schiff base containing α -D-altropyranoside unit and its Zinc (II) complex.” *Inorg. Chim. Acta*, 362, 229-232.

Liu, Y., Liu, C.G., Sun, S.L., Yang, G.C. and Qiu, Y.Q. (2012). "Redox-switching second-order nonlinear optical responses of N'N'N' Ruthenium complexes." *Comp. Theor. Chem.*, 979, 112-118.

Liu, Y.C., Li, C.I., Yeh, W.Y., Lee, G.H. and Peng, S.M. (2006). "Synthesis and structural characterization of dicopper(I) bis(diphenylphosphino)acetylene complexes containing tricyclic, cyclic and linear frameworks." *Inorg. Chim.Acta.*, 359, 2361-2368.

Long, N.J. (1995). "Organometallic Compounds for Nonlinear Optics—The Search for Enlightenment!" *Angew. Chem Int. Ed. Engl.*, 34, 21-35.

Lori, K.M., Langhoff, C., Ho, D.M. and Thompson, M.E. (1995). "Third order nonlinear optical properties of Group 4 metallocenes." *Polyhedron*, 14, 57-67.

Maiman, T.H. (1960). "Stimulated optical radiation in ruby." *Nature*, 187, 493.

Mao, Z., Chao, H.Y., Hui, Z., Che, C.M., Fu, W.F., Cheung, K.K. and Zhu, N. (2003). "3[(d^{x²-y²} d_{xy})(p_z)] Excited States of Binuclear Copper(I) Phosphine Complexes: Effect of Copper–Ligand and Copper–Copper Interactions on Excited State Properties and Photocatalytic Reductions of the 4,4'-Dimethyl-2,2'-bipyridinium Ion in Alcohols." *Chem. Eur. J.*, 9, 2885-2894.

Marder, S, R (2006) "Organic nonlinear optical materials: where we have been and where we are going" *Chem. Commun.* 2 131-134

Marder, S.R. (1995). In *Materials Chemistry, an Emerging Discipline*: L.V. Interrante, L.A Casper (Eds.), ACS:Washington, D.C., 189-210.

Marder, S.R., Sohn, J.E. and Stucky, G.D. (1991). "Materials for Nonlinear Optics – Chemical Perspectives." American Chemical Society., Washington, DC.

Marks, T.J. and Ratner, M.A. (1995). "Design, Synthesis, and Properties of Molecule-Based Assemblies with Large Second-Order Optical Nonlinearities." *Angew. Chem. Int. Ed. Engl.*, 34,155 -159.

McKay, T.J., Staromlynska, J., Davy, T.R. and Bolger, J.A. (2001). "Cross sections for excited-state absorption in a Pt: ethynyl complex." *J. Optical Soc. America B-Optical Phys.*, 18, 358-362.

McMillin, D.R. and McNett, K.M. (1998). "Photoprocesses of Copper Complexes That Bind to DNA." *Chem. Rev.*, 98, 1201-1220.

Miguel, A., Mendez-Rojas., Satish, G., Bodige, and William, H. (1999). "Structure and properties of potential nonlinear optical materials." *Watson J. of Chem. Cryst.*, 29, No. 12, 1225-1234.

Munoz, B.M., Santillan, R., Rodriguez, M., Mendez, J.M., Romero, M., Farfan, N., Lacroix, P.G., Nakatani, K., Ramos-Ortiz, G. and Maldonado, J.L. (2008). "Synthesis, crystal structure and nonlinear optical properties of boronates derivatives of salicylideneiminophenols." *J. Organomet. Chem.*, 693, 1321-1334.

Naga Srinivas, N.K.M., Rao, S.V. and Rao, D.N. (2003). "Saturable and reverse saturable absorption of rhodamine B in methanol and water." *J. Opt. Sci. Am. B*, 20, 2470-2479.

Nair, S.S., Thomas, J., Suchand Sandeep, C.S., Anantharaman, M.R. and Philip, R. (2008). "An optical limiter based on ferrofluids." *App. Phys. Lett.*, 92, 171908.

Nalwa, H.S. (1991). "Organometallic materials for nonlinear optics." *Appl. Organomet. Chem.* 5, 349-377.

Negm, N.A., Zaki, M.F. and Salem, M.A.I. (2010). "Cationic Schiff base amphiphiles and their metal complexes: Surface and biocidal activities against bacteria and fungi." *Colloids Surf. B*, 77, 96-103.

Nikolaev, A.V., Longvinenko, V.A. and Mychina, C. I. (1969). *Thermal Analysis*, Academic Press, New York.

Nishinaga, A., Yamada, T., Fujisawa, H., Ishizaki, K., Ihara, H. and Matsuura, T. (1988). "Catalysis of cobalt-Schiff complexes in the oxygenation of alkenes: on the mechanism of ketonization." *J. Mol. Catal. A*, 48, 249-264.

Olbrechts, G., Strobbe, R., Clays, K. and Persoons, A. (1998). "High frequency demodulation of multi-photon fluorescence in hyper-Rayleigh scattering." *Rev. Sci. Instrum.*, 69, 2233-2241.

Oudar, J.L. and Chemla, D.S. (1977). "Hyperpolarizabilities of the nitroanilines and their relations to the excited state dipole moment." *J. Chem. Phys.*, 66, 2664-2668.

Padhye, S. and Kaufman, G.B. (1985). "Transition metal complexes of semicarbazones and thiosemicarbazones." *Coord. Chem. Rev.*, 63, 127-160.

Paul, A., Mandal, P.K. and Samanta, A. (2005). "How transparent are the imidazolium ionic liquids? A case study with 1-methyl-3-butylimidazolium hexafluorophosphate, [bmin][PF₆]." *Chem. Phys. Lett.*, 402, 375-379.

Philip, R., Ravindrakumar, G., Sandhyarani, N. and Pradeep, T. (2000). "Picosecond optical nonlinearity in monolayer-protected gold, silver, and gold-silver alloy nanoparticles." *Phys. Rev. B*, 62, 13160-13166.

Philip, V., Suni, V., Kurup, M.R.P., Nethaji, M. (2004). "Structural and spectral studies of nickel(II) complexes of di-2-pyridyl ketone N⁴,N⁴-(butane-1,4-diyl) thiosemicarbazone." *Polyhedron*, 23, 1225-1233.

Pignatello, R., Panicol, A., Mazzone, P., Pinizzotto, M., Garozzo, A and Furneri, P. (1994). "Schiff bases of N-hydroxy-N'-aminoguanidines as antiviral, antibacterial and anticancer agents." *Eur. J. Med. Chem.*, 29, 781-785.

Poornesh, P., Hegde, P.K., Umesh, G., Manjunatha, M.G., Manjunatha, K.B. and Adhikari, A.V. (2010). "Nonlinear optical and optical power limiting studies on a new thiophene-based conjugated polymer in solution and solid PMMA matrix." *Opt. Laser Tech.*, 42, 230-236.

Powell, C. E. and Humphrey, M. G. (2004). "Nonlinear optical property of transition of metal acetylides and their derivatives." *Coord. Chem. Rev.*, 248, 725-756.

Powell, C.E., Morrall, J.P., Ward, S.A., Cifuentes, M.P., Notaras, E.G.A, Samoc, M. and Humphrey, M.G. (2004). "Dispersion of the third-order nonlinear optical properties of an organometallic dendrimer." *J. Am. Chem. Soc.*, 126, 12234-12235.

Prabhakaran, R., Karvembu, R., Hashimoto, T., Shimizu, K. and Natarajan, K. (2005). "Formation of structurally different solvated and non-solvated [Ni(PTSC)(PPh₃)] (PTSC = salicylaldehyde-N-phenylthiosemicarbazide anion) crystals from single pot." *Inorg. Chim. Acta.*, 358, 2093-2096.

Prasad, P.N. and Williams, D.J. (1991) "Introduction to Nonlinear optical effects in molecules and polymer." Wiley, New York.

Ramakrishna, D. and Bhat, B.R. (2010). "Cobalt complexes in [EMIM]Cl – A catalyst for oxidation of alcohols to carbonyls." *Inorg. Chem. Commun.*, 13, 195-198.

Ramesh, R. and Sivagamsundari, M. (2003). "Synthesis and antifungal activities of Ru(II) complexes." *Synth. React. Inorg. Met. Org. Chem.*, 33, 899-910.

Raptopoulou, C.P. Papadopoulos, A.N., Malamataris, D.A. Loannidis, E., Molsidis, G., Terzis, A. and Kessissoglou, D.P. (1998). "Ni(II) and Cu(II) schiff base complexes with an extended H-bond network." *Inorg. Chim. Acta.*, 272, 283-290.

Ray, D., Nag, A., Jana, A., Goswami, D. and Bharadwaj, P.K. (2010). "Coumarin derived chromophores in the donor-acceptor-donor format that gives fluorescence enhancement

and large two-photon activity in presence of specific metal ions.” *Inorg. Chim. Acta.*, 363, 2824-2832.

Reinhardt, B.A., Brott, L.L., Clarson, S.J., Dillard, A.G., Bhatt, J.C., Kannan, R., Yuan, L.X., He, G.S. and Prasad, P.N. (1998). “Highly active two-photon dyes: Design, synthesis, and characterization toward application.” *Chem. Mater.*, 10, 1863-1874.

Renouard, T., Bozec, H.L., Brasselet, S., Ledoux, I. and Zyss, J. (1999). “Tetrahedral bipyridyl copper(I) complexes: a new class of non-dipolar chromophore for nonlinear optics.” *Chem. Commun.*, 871–872.

Renx, Q., Sun, B., Wang, X. Q., Zhang, G.H., Yang, X.D., Zhang, F.J., Yang, H., Chow, Y.T. and Xu, D. (2008). "Short pulse Z -scan investigations of optical nonlinearities of a novel organometallic complex: [(C₂H₅)₄N]₂[Cu(dmit)₂] at 532 and 1064nm." *Appl. Phys. I.*, 90,685-688.

Reyes, H., Garcia, C., Farfan, N., Santillan, R., Lacroix, P.G., Lepetit, C. and Nakatani, K. (2004). “Synthesis, crystal structures and quadratic nonlinear optical properties in four “push-pull” diorganotin derivatives.” *J. Organomet. Chem.*, 689, 2303-2310.

Rodríguez, M., Maldonado, J.L., Ramos-Ortíz, G., Domínguez, O., Ochoa, M.E., Santillan, R., Farfán, N., Meneses-Nava, M.A. and García, O.B. (2012). “Synthesis, X-ray diffraction analysis and chemical-optical characterizations of boron complexes from bidentate ligands.” *Polyhedron*, 43, 194-200.

Rudresha, B.J., Bhat, B.R., Ramakrishna, D., Anthony, J.K., Lee, H.W. and Rotermund, F. (2012). “Nonlinear optical study of palladium Schiff base complex using femtosecond differential Optical Kerr gate and Z-scan techniques.” *Opt. Laser Tech.*, 44, 1180-1183.

Sagayaraj, P. and Selvakumar, S. (2009). "Studies on the growth and characterization of novel organometallic NLO crystal: $\text{Cd}(\text{HCOO})_2 \cdot 2\text{CS}(\text{NH}_2)_2$." *J Mater Sci: Mater. Electron.* 20, 299-302.

Sakaguchi, H., Nagamura, T. and Matsuo, T. (1991). "Quadratic nonlinear optical properties of ruthenium (II) – bipyridine complexes in crystalline powders." *App. Organomet. Chem.*, 5, 257-260.

Samadhiya, S. and Halve, A. (2001). "Synthetic utility of Schiff bases as potential herbicidal agents." *Orient. J. Chem.*, 17, 119

Santosh kumar S.R., Rao, S.V., Giribabu, L. and Rao, D.N. (2009). "Ultrafast nonlinear optical properties of alkyl phthalocyanines investigated using degenerate four-wave mixing technique." *Optical Mat.*, 31, 1042-1047.

Santosh Kumar, S.R., Rao, S.V., Giribabu, L. and Rao, D.N. (2007). "Femtosecond and nanosecond nonlinear optical properties of alkyl phthalocyanines studied using Z-scan technique." *Chem. Phys. Lett.*, 447, 274-278.

Sari, N., Gurkan, P. and Arslan, S. (2003). "Synthesis, potentiometric and antimicrobial activity studies on 2-pyridinylidene-DL-amino acids and their complexes." *Trans. Met. Chem.*, 28, 468-474.

Saxena, C.G. and Shrivastava, S.V. (1987). "Mn(II), Co(II), Ni(II) and Cu(II) complexes with p-toly-2-furylgloxalimine." *J. Ind. Chem. Soc.*, 64, 685-686.

Schiff, H. (1869). "Untersuchungen uber Salicinderivative." *Ann. Chem. Pharm.*, 150, 193-200.

Sheik-Bahae, M., Said, A.A., Wei, T.H., Hagan, D. J. and Van Stryland, E.W. (1990). "Sensitive measurement of optical nonlinearities using a single beam." *IEEE J. Quant. Electron.*, 26, 760-769.

Sheikhshoaie, I., Hossein, M., Mashhadizadeh, N. and Nia, S.S. (2004). "Synthesis, characterization and theoretical study of the structure and second-order nonlinear optical properties of two new monoazo Schiff base complexes." *J. Coord. Chem.*, 57, 417-423.

Sheldrick, G.M. (2008). "A short history of SHELX." *Acta Cryst.*, A64, 112-122.

Singh, K., Barwa, M.S. and Tyagi, P. (2006). "Synthesis, characterization and biological studies of Co(II), Ni(II) Cu(II) and Zn(II) complexes with bidentate Schiff bases derived by heterocyclic ketones." *Eur. J. Med. Chem.*, 41, 147-153.

Singh, N.K., Singh, N., Sodhi, A., Shrivastava, A., Prasad, G.C. (1996). "Synthesis, characterization and antitumour studies on N-salicyl-N'-thiobenzohydrazide and its copper(II) complex." *Trans. Met. Chem.*, 21, 556-559.

Singh, R.V., Gupta, N. and Fahmi, N. (1999). "Stereochemical, thermal and biochemical aspects of di-oxo molybdenum (VI) and manganese (II) complexes." *Indian J. Chem.*, 38A, 1150-1158.

Sivaramakrishnan S. (2007) "Nonlinear optical scattering and absorption in bismuth nanorod suspensions." *Appl. Phys. Lett.* 91, 093104- 093104-3.

Soliman, A.A., Mohamed, G.G. (2004). "Study of the ternary complexes of copper with salicylidene-2-aminothiophenol and some amino acids in the solid state." *Thermochim. Acta.*, 421,151-159.

Soltani, N., Behpour, M., Ghoreishi, S.M. and Naeimi, H. (2010). "Corrosion inhibition of mild steel in hydrochloric acid solution by some double Schiff bases." *Corros. Sci.*, 52, 1351-1361.

Sorkau, A., Wagner, C., Steinborn, D., Poetsch, E. and Wachtler, A.E.F. (2005). "Ruthenium catalysed reactions of aldehydes: molecular structures of ruthenium complexes with aldehydes ligands." *Transit. Metal Chem.*, 30, 691-695.

- Souza, R.F., Alencar M.A.R.C., Meneghetti, M.R., Dupont, J., and Hickmann, J.M. (2008). "Nonlocal optical nonlinearity of ionic liquids." *J. Phys.: Condens. Matter*, 20, 155102.
- Sudheesh, P. and Chandrasekharan, K. (2012). " $\chi^{(3)}$ measurements in Schiff base derivatives: Effect of metal nanoparticles." *Solid State Commun.*, 152, 268-272.
- Sun, X.X., Yang, G.C., Sun, S.L., Ma, N.N. and Qiu, Y.Q. (2011). "Effects of the substituting groups and proton abstraction on the nonlinear optical properties of heteroleptic bis-tridentate Ru(II) complexes." *J. Organomet. Chem.*, 696, 3384-3391.
- Sutherland, R.L. (1996). *Handbook of Nonlinear Optics*, Marcel Dekker (New York).
- Sutherland, R.L. (2003). *Handbook of Nonlinear Optics*. New York, Dekker.
- Sutherland, R.L., Brant, M.C., Heinrichs, J., Rogers, J.E., Slagle, J.E., MacLean, D.G. and Fleitz, P. (2005). "Excited-state characterization and effective three-photon absorption model of two-photon-induced excited-state absorption in organic push-pull charge-transfer chromophores." *J. Opt. Soc. Am. B.*, 22, 1939-1948.
- Sutton, D. (1968). "Electronic Spectra of Transition Metal Complexes." McGraw-Hill, London.
- Tang, G.D., Zhao, J.Y., Li, R.Q., Cao, Y. and Zhang, Z.C. (2011). "Synthesis, characteristic and theoretical investigation of the structure, electronic properties and second-order nonlinearity of salicylaldehyde Schiff base and their derivatives." *Spectrochim. Acta A.*, 78, 449-457.
- Tedim, J., Patricio, S., Bessada, R., Morais, R., Sousa, C., Marques, M.B. and Freire, C. (2006). "Third order nonlinear optical properties of DA-Salen-type Nickel (II) and Copper (II) complexes." *Eur. J. Inorg. Chem.*, 17, 3425-3433.

Terhune, R.W., Maker, P.D. and Savage, C.M. (1965). "Measurements of nonlinear light scattering." *Phys. Rev. Lett.*, 14, 681-684.

Thangadurai, T.D., Jeong, S., Yun, S., Kim, S., Kim, C. and Lee, Y. (2010). "Antibacterial and luminescent properties of new donor-acceptor ruthenium triphenylphosphine bipyridinium complexes." *Microchem. J.*, 95, 235-239.

Tian, Y.P., Yu, W.T., Zhao, C.Y., Jiang, M.H., Cai, Z.G. and Fun, H.K. (2002). "Structural characterization and second-order nonlinear optical properties of zinc halide thiosemicarbazone complexes." *Polyhedron*, 21, 1217-1222.

Tutt, L.W. and Boggess, T.F. (1993). "A review of optical limiting mechanisms and devices using organics, fullerenes, semi-conductors and other materials." *Prog. Quantum Electron.*, 17, 299-338.

Tykwinski, R.R., Gubler, U., Martin, R. E., Diederich, F., Bosshard, C. and Günter, P. (1998). "Structure-Property Relationships in Third-Order Nonlinear Optical Chromophores." *J. Phys. Chem. B.*, 102, 4451-4465.

Vettaikaranpudur, G., Gnanasoundari and Karuppanan Natarajan. (2005). "Synthesis, characterization and catalytic studies of iron(III), cobalt(II), nickel(II) and copper(II) complexes containing triphenylphosphine and β -diketones." *Transit Metal Chem.*, 30, 433-438.

Whittall, I.R., McDonagh, A.M., Humphrey, M.G. and Samoc, M. (1998). "Organometallic Complexes in Nonlinear Optics I: Second-Order Nonlinearities." *Adv. Organomet. Chem.*, 42, 291-362.

Xu, G., Liu, Z., Ma, J., Liu, B., Ho, S.T., Wang, L., Zhu, P., Marks, T., Luo, J. and Jen, A. (2005). "Organic electrooptic modulator using transparent conducting oxides as electrodes." *Opt. Express*, 13, 7380-7385.

Xue, Z.H., Tian, Y.P., Wang, D. and Jiang, M.H. (2003). "One and two photon excited dual fluorescence properties of zinc (II) and cadmium (II) complexes containing 4-dipropylaminobenzaldehyde thiosemicarbazone." *Dalton Trans.*, 7, 1373-1378.

Yam, V.W.W. and Lo, K.K.W. (1999). "Luminescent polynuclear d¹⁰ metal complexes." *Chem. Soc. Rev.*, 28, 323-334.

Yaoting, F., Gang, L., Zifeng, L., Hongwei, H. and Hai-rong, M. (2004). "Synthesis, Structure And third Order Nonlinear Optical Properties of 1,3,5-Triazine-Based Zn(II) Three Dimensional Supramolecule." *J. Mol. Struc.*, 693, 217-224.

Yim, S.H., Lee, D.R., Rhee, B.K. and Kim, D. (1998). "Nonlinear absorption of Cr⁴⁺:YAG studied with lasers of different pulse widths." *Appl. Phys. Lett.*, 73, 3193-3195.

Yin, S., Xu, H., Su, X., Wu, L., Song, Y. and Tang, B.Y. (2007). "Preparation and property of soluble azobenzenecontaining substituted poly(1-alkyne)s optical limiting materials." *Dyes and Pigments*, 75, 675-680.

Ying, S.M. (2012). "Synthesis, crystal structure and nonlinear optical property of a Zn(II) complex base on the reduced Schiff-base ligand." *Inorg. Chem. Commun.*, 22, 82-84.

Yu C., Michael, H., Werner, J. B., Danilo, D., Ying, L., Ying L., Jinrui, B., J. (2006). "Review Soluble axially substituted phthalocynes: Synthesis and nonlinear optical response." *J. Mat. Sci.*, 41, 2169-2185.

Zhang, F.J., Guo, W.F., Sun, X.B., Ren, Q., Gao, Y., Yang, H.L., Zhang, G.H., Chow, Y.T. and Xu, D. (2007). "Nonlinear optical absorption of [(C₂H₅)₄N]₂Cu(dmit)₂ irradiated by picosecond and nanosecond laser pulses." *Laser Phys. Lett.*, 3, 230-233.

Zhang, R., Ma, J., Wang, W., Wang, B. and Li, R. (2010). "Zeolite-encapsulated M(Co, Fe, Mn)(SALEN) complexes modified glassy carbon electrodes and their application in oxygen reduction." *J. Electroanal. Chem.*, 643, 31-38.

Zheng, Q., He, G.S., Lu, C. and Prasad, P.N. (2005) "Synthesis, two- and three-photon absorption, and optical limiting properties of fluorine-containing ferrocene derivatives." *J. Mat. Chem.*, 15, 3488-3493.

Zyss, J (Ed.), (1994.) "Molecular Nonlinear Optics." Academic Press, New York.

Zyss, J. and Ledoux, I. (1994). "Nonlinear optics in multipolar media: theory and experminets." *Chem. Rev.*, 94, 77-105.

LIST OF PUBLICATIONS

List of Research papers published in International Journals

1. **Sampath Kumar, H.C.**, Bhat, B.R., Rudresha, B.J., Ravindra, R. and Reji, P. (2010). "Synthesis, Characterization and Nonlinear optical studies of N, N'-bis(2-hydroxynaphthalidene)phenylene-1,2-diamine) of M (M= Ni(II), Zn(II) and Fe (II)) Schiff-Base Complexes." *Chem. Phys. Lett.*, 494, 95-99.
2. **Sampath Kumar, H.C.**, Rudresha, B.J., Bhat, B.R., Reji, P. and Guru, R.T.N. (2011). "Synthesis And Third-order Nonlinear Optical Studies Of Four-Coordinated Copper(I) Complexes." *AIP Conf. Proc.*, 1391, 671-673.
3. **Sampath Kumar, H.C.** and Bhat, R.B. (2013). "Third order Nonlinear optical properties of Co(II), Ni(II) and Zn(II) complexes with 3,4-Diaminobenzophenone Schiff base ligands." *Synth. Metals* (Under Review).
4. **Sampath Kumar, H.C.** and Bhat, R.B. (2013). "Third order Nonlinear optical properties of thiosemicarbazide complexes of Ni(II), Cu(II) and Zn(II) with Three photon absorption." Communicated to *Opt. Matt.*
5. **Sampath Kumar, H.C.** and Bhat, R.B. (2013). "Nonlinear optical studies of ionic liquid tagged Schiff base Ni(II) complexes." Communicated to *Chem. Phys. Lett.*
6. Rudresha B.J., Ramachandra Bhat B., **Sampath Kumar H.C.**, Shiva Kumar K.I., Safakath K and Reji Philip. (2011). "Synthesis, characterization and third-order nonlinear optical studies of copper complexes containing 1,10-phenanthroline-5,6-dione and triphenylphosphine ligands." *Synthetic Metals*. 161, 535-539.
7. Rudresha B.J., Sampath Kumar H.C., Reji Philip and Ramachandra Bhat B. (2013). "Synthesis, characterization and third-order nonlinear optical studies of binuclear boron Schiff base complexes." Communicated to 'Chem. Phys. Lett'.

8. Kiran, A.J., Lee, H.W., **Sampath Kumar, H.C.**, Rudresha, B.J., Bhat, B.R., Yeom, D.I., Kim, K. and Rotermund, F. (2010). "The ultrafast nonlinear optical response and multi-photon absorption of a new metal complex in the near-infrared spectral range." *J. Optics*, 12, 035211.
9. A. John Kiran, H.W. Lee, **H.C.S. Kumar**, B.J. Rudresha, B.R. Bhat, D.-I. Yeom and F. Rotermund. (2009). "Ultrafast optical response of a new metal organic complex-polymer composite film." *Conference Proceeding Lasers & Electro Optics & The Pacific Rim Conference on Lasers and Electro-Optics, 2009*. DOI: 10.1109/CLEOPR.2009.5292507

List of Research Papers presented in Conferences

1. **Sampath Kumar H.C.**, Rudresha B.J., Guru Row T.N. and Ramachandra Bhat B. "Synthesis, Characterization and X-Ray Crystal Structure of Chloro(1, 10-Phenanthroline-N,N') (Triphenylphosphine) Copper (I) Complex." 12th International Symposium on Inorganic Ring Systems (IRIS-12), Goa. 16-21 Aug 2009.
2. **Sampath Kumar H.C.**, Rudresha B.J., Guru Row T.N, Reji Philip and Ramachandra Bhat B. "Synthesis and Third-order Nonlinear Optical Studies of Four-Coordinated Copper(I) Complexes." OPTICS 11, National Institute of Technology Calicut, 23–25 May 2011.
3. **Sampath Kumar H.C.** and Ramachandra Bhat B. "Synthesis, Characterization and Nonlinear optical property of 3,4-Diaminobenzophenone Schiff base complexes of Co(II), Ni(II) and Zn(II)." ICRAMST-13, National Institute of Technology Surathkal, 17–19 Jan 2013.

CURRICULUM VITAE

Sampath Kumar H. C.

Research Scholar

Department of Chemistry

NITK-Surathkal

Mangalore-575025

India

E-mail: sampathkumarmrpl@gmail.com

Phone : +91-9901328586



Objectives

To attain a respectful position in an institution that values performance and commitment and provides a congenial atmosphere to exploit my potential.

Education

1. Ph.D. Thesis: “**Synthesis and characterization of transition metal complexes for nonlinear optical activity.**” Supervisor: Prof. B. Ramachandra Bhat
2. M.Sc. Chemistry, Mangalore University , 68.60 %, 2005, Karnataka, India.
3. B.Sc. Chemistry, Mangalore University, 78.60 %, 2003, Karnataka, India.

Work Experience

Presently working as Laboratory Officer at Mangalore Refinery and Petrochemicals Ltd. Quality Control Department, since August 2005. Here, I have been exposed to various petroleum testing instruments such Distillation, Density, Gas Chromatographs, Sulphur analyzers, Research Octane Number, AAS and others. I have also been actively involved in the implementation of Laboratory automation software LIMS (Laboratory Information and Management systems).

Instruments handled

- FT-IR spectrophotometer
- UV-Visible spectrophotometer
- Fluorescence spectrophotometer
- Buchi Rotary Evaporator
- All petroleum and water testing equipments

Research publications

List of Research papers published in International Journals

10. **Sampath Kumar, H.C.**, Bhat, B.R., Rudresha, B.J., Ravindra, R. and Reji, P. (2010). "Synthesis, Characterization and Nonlinear optical studies of N, N'-bis(2-hydroxynaphthalidene)phenylene-1,2-diamine) of M (M= Ni(II), Zn(II) and Fe (II)) Schiff-Base Complexes." *Chem. Phys. Lett.*, 494, 95-99.
11. **Sampath Kumar, H.C.**, Rudresha, B.J., Bhat, B.R., Reji, P. and Guru, R.T.N. (2011). "Synthesis And Third-order Nonlinear Optical Studies Of Four-Coordinated Copper(I) Complexes." *AIP Conf. Proc.*, 1391, 671-673.
12. **Sampath Kumar, H.C.** and Bhat, R.B. (2013). "Third order Nonlinear optical properties of Co(II), Ni(II) and Zn(II) complexes with 3,4-Diaminobenzophenone Schiff base ligands." *Synth. Metals* (Under Review).
13. **Sampath Kumar, H.C.** and Bhat, R.B. (2013). "Third order Nonlinear optical properties of thiosemicarbazide complexes of Ni(II), Cu(II) and Zn(II) with Three photon absorption." Communicated to *Opt. Matt.*
14. **Sampath Kumar, H.C.** and Bhat, R.B. (2013). "Nonlinear optical studies of ionic liquid tagged Schiff base Ni(II) complexes." Communicated to *Chem. Phys. Lett.*
15. Rudresha B.J., Ramachandra Bhat B., **Sampath Kumar H.C.**, Shiva Kumar K.I., Safakath K and Reji Philip. (2011). "Synthesis, characterization and third-order

- nonlinear optical studies of copper complexes containing 1,10-phenanthroline-5,6-dione and triphenylphosphine ligands.” *Synthetic Metals*. 161, 535-539.
16. Rudresha B.J., Sampath Kumar H.C., Reji Philip and Ramachandra Bhat B. (2013). “Synthesis, characterization and third-order nonlinear optical studies of binuclear boron Schiff base complexes.” Communicated to ‘*Chem. Phys. Lett*’.
17. Kiran, A.J., Lee, H.W., **Sampath Kumar, H.C.**, Rudresha, B.J., Bhat, B.R., Yeom, D.I., Kim, K. and Rotermund, F. (2010). “The ultrafast nonlinear optical response and multi-photon absorption of a new metal complex in the near-infrared spectral range.” *J. Optics*, 12, 035211.
18. A. John Kiran, H.W. Lee, **H.C.S. Kumar**, B.J. Rudresha, B.R. Bhat, D.-I. Yeom and F. Rotermund. (2009). “Ultrafast optical response of a new metal organic complex-polymer composite film.” *Conference Proceeding Lasers & Electro Optics & The Pacific Rim Conference on Lasers and Electro-Optics, 2009*. DOI: 10.1109/CLEOPR.2009.5292507

List of Research Papers presented in Conferences

4. **Sampath Kumar H.C.**, Rudresha B.J., Guru Row T.N. and Ramachandra Bhat B. “Synthesis, Characterization and X-Ray Crystal Structure of Chloro(1, 10-Phenanthroline-N,N’) (Triphenylphosphine) Copper (I) Complex.” 12th International Symposium on Inorganic Ring Systems (IRIS-12), Goa. 16-21 Aug 2009.
5. **Sampath Kumar H.C.**, Rudresha B.J., Guru Row T.N, Reji Philip and Ramachandra Bhat B. “Synthesis and Third-order Nonlinear Optical Studies of Four-Coordinated Copper(I) Complexes.” OPTICS 11, National Institute of Technology Calicut, 23–25 May 2011.
6. **Sampath Kumar H.C.** and Ramachandra Bhat B. “Synthesis, Characterization and Nonlinear optical property of 3,4-Diaminobenzophenone Schiff base complexes of

Co(II), Ni(II) and Zn(II).” ICRAMST-13, National Institute of Technology
Surathkal, 17–19 Jan 2013.

COMPETENCIES

Hardworking, Creative in thinking, Leadership qualities, Good communication skills,
Good laboratory practice.

COMPUTER KNOWLEDGE

Microsoft office, Basic SQL, Basic BO Xi (Reporting tool). Major role in
implementation of LIMS software for laboratory.

PERSONAL DETAILS

◆ Father's name	: Chandre Gowda .N.D
◆ Date of birth	: 3 rd September 1982
◆ Sex	: Male
◆ Nationality	: Indian
◆ Languages known	: English, Hindi, Kannada
◆ Permanent Address	: Hosakere village, Urubage PO, Mudigere, Chickamagalore, 577132

REFERENCE

Dr. B. Ramachandra Bhat

Professor

Department of Chemistry

National Institute of Technology Karnataka (NITK) Surathkal,

Srinivasnagar (PO), Mangalore Pin-575025

Karnataka, India.

Ph : +91-9449553759

Fax: + 91-824-2474033

Email: chandpoorna@yahoo.com

Dr. A. Chittaranjan Hegde

Professor and Head

Department of Chemistry

National Institute of Technology Karnataka (NITK) Surathkal,

Srinivasnagar (PO), Mangalore Pin-575025

Karnataka, India.

Mob: +91-9980360242

Email: hegdeac@rediffmail.com